Soluble Polyacetylenes by the Ring-Opening Metathesis Polymerization of Substituted Cyclooctatetraenes

Thesis by

Eric Jay Ginsburg

In Partial Fulfillment of the Requirements

For the Degree of

Doctor of Philosophy

California Institute of Technology

Pasadena, California

1991

(Submitted December 14, 1990)

To my grandparents and parents, and to Sandra.

Acknowledgements

My time at Caltech has, of course, had its share of low and high points, but on the whole I consider it to have been about as enjoyable as it's possible for graduate school to be. This is to the credit of those staff, faculty, and students who work to keep Caltech a special place, characterized by mutual respect. I can thank by name only a few who have contributed to my stay here.

The ability of my advisor, Bob Grubbs, to trust his students' ability to explore, while always being there to provide support and advice, has been a large part of my education at Caltech. I'm grateful to Steve Buchwald for pointing me towards Caltech and towards Bob's group in particular.

I consider myself extremely lucky to have had Tim Shepodd, Seth Marder, and Mike Sailor nearby to provide invaluable advice at certain points in my graduate career. They are good friends and mentors.

Also, Chris Gorman deserves a special mention. It's been an experience working with Chris, and I'm really going to miss the partnership. Through all of our arguments, he never hit me with the bat (and I never pulled his hair), and many of them ended with both of us learning something. Our projects have been extremely close, and sometimes overlapping, during the past two years, and it has only been through Chris's unselfishness that the whole thing has worked.

All eight classes or so of Grubbs group graduate students and post-docs that I've overlapped with have made the lab a stimulating (and endurable) place to be. I'm grateful to Dave Wheeler and Scott Virgil who patiently taught me a lot at the bench when I was starting out. Also, the insight and friendship of Dom McGrath and Lynda Johnson have been a great help during my time in the group. It's been fun working alongside Dom, my

fellow impatient American, and I'll thank Lynda in advance for forgiving me calling her the Tungsten Queen here.

Most recently, Lynda Johnson, Rick Fisher, Pui Tong (Joe) Ho, Chris Gorman, Mike Sailor, Elizabeth Burns, Rik Blumenthal, Zhe Wu, Dom McGrath, Marc Hillmyer, Tom Jozefiak, Mark McCleskey, Mike Rock and Dave Long have done me the favor of proofreading sections of my thesis and research proposals. Joe Ho has been especially helpful with publishing advice, in addition to having whiled away the hours with me searching for Elvis on one ten millionth of a square centimeter of graphite.

There have been a few unique aspects to my stay in Pasadena. First, I have my housemates in the Stucco Submarine to thank for introducing me to the joys of canine living, and our landlord, I guess, for not giving a damn. Further, I've appreciated the ease with which I could find someone willing to escape with me to the mountains or desert. Tim Shepodd, Dave Wheeler, Dave Long, Gail Ryba, Dom McGrath and Peter Green have been been willing to run, hike, climb, or bushwack to the middle of nowhere whenever I needed to get out. Some of them deserve credit for letting me know when that was.

For having constantly nurtured my curiosity, and thereby inspiring me to pursue science, I thank my parents. Both they and my grandparents have always been supportive.

Finally, I thank Sandie Gustafson for her steadfast friendship and love.

A research fellowship from the IBM Corporation is gratefully acknowledged.

Abstract

Ring-opening metathesis polymerization has been applied to the synthesis of substituted polyacetylenes. The set of Me_3M-substituted cyclooctatetraenes, where M = C, Si, Ge and Sn, have been polymerized using a well-defined tungsten alkylidene as an active metathesis catalyst. The resulting high molecular weight polyacetylenes have a substituent located at every eighth carbon atom, on the average. This substitution pattern allows substantial electronic delocalization along the main chain, in contrast to more highly substituted polyacetylenes which have been studied in the past.

The properties of the four polymers depend on the size of the side chain. As the substituent is varied from *t*-Bu to Me_3Si to Me_3Ge or Me_3Sn, the absorption maximum of the polymer decreases in energy. Also, whereas poly(*t*-butylcyclooctatetraene) and poly(trimethylsilylcyclooctatetraene) are soluble in organic solvents, including benzene, methylene chloride, and tetrahydrofuran, the trimethylgermyl- and trimethylstannyl-substituted polymers are not totally soluble.

As synthesized, the polymers contain a high percentage of cis double bonds. They may be isomerized to a form containing mostly trans double bonds either photochemically or thermally. The trans isomers absorb at lower energy than do the cis isomers, indicating that the trans polymers can assume a more conjugated conformation. A set of visible absorption spectra obtained over the course of a photochemical isomerization contain an isosbestic point, which indicates that a number of double bonds are isomerizing simultaneously, i.e., the isomerization does not proceed a bond at a time.

Molecular mechanics calculations have been used to explore the effect of the steric requirements of the side chain on the conformation of the polyene backbone. It is observed that those polyenes which are soluble are calculated to be significantly twisted because of nonbonded interactions between the substituent and the protons on adjacent carbon atoms. Substituted polyenes calculated to have a more planar conformation are found to be insoluble in the trans form.

trans-Poly(trimethylsilylcyclooctatetraene) films are greenish gold and appear metallic. After iodine doping, they have an electrical conductivity of $\sim 10^{-1}\ \Omega^{-1}\ cm^{-1}$. The doped polymer has been used to investigate the properties of conducting polymer/silicon Schottky-type solar cells in a collaborative effort with Drs. Michael Sailor and Nathan Lewis. It was found that the polymer/semiconductor interface is not subject to Fermi-level pinning, and that the efficiency of the device is limited by the properties of the silicon, not those of the interface, in contrast to devices made with conventional metals on silicon. The third-order nonlinear optical coefficient of the undoped polymer has been measured by Dr. Joseph Perry and was found to be $2\pm1 \times 10^{-11}$ esu.

Preliminary investigations of the polymers by scanning tunneling microscopy have been initiated in collaboration with Drs. Reginald Penner and Lewis. Some images which may represent individual polymer strands have been obtained, although interpretation of the data is complicated by the appearance of defects in the underlying graphite substrate.

Table of Contents

List of Tables

List of Figures

CHAPTER 1

INTRODUCTION

Conjugated Polymers.[1-4]

Both theoreticians and experimentalists have been intrigued by the distinctive properties of organic polymers with substantial electronic delocalization along their backbone.[5-7] These properties include their polarizable, low-energy π-systems, which lead to high, third-order, nonlinear optical coefficients,[8, 9] and the ability of these polymers to undergo a transformation into an electrically conductive state.[10, 11] The ability to oxidatively or reductively dope conjugated polymers to high electrical conductivities (>10 Ω^{-1} cm^{-1}) opens up the possibility of using them as "plastic metals."[12-14] Moreover, the mechanism of charge transport through these materials is of interest to both solid-state physicists and physical organic chemists.

Although a large number of different conjugated polymers have been synthesized,[5-7] two main obstacles have slowed advancement in the field. The first is the inherent instability of molecules with extended conjugation. In the undoped state, they are susceptible to crosslinking by free-radical processes, or in some cases, Diels-Alder reactions. When doped, the polymers typically have charges centered on carbon atoms, making them unstable in air. This obstacle has not yet been overcome, although proton-doped heteroatom-containing polymers such as polyaniline seem promising in this regard.[15]

Intractability is the second obstacle that frequently plagues scientists trying to examine conjugated polymers. Overcoming this problem is crucial if conducting polymers are to be widely used. The prospect of manipulating conjugated polymers in solution or in the melt is attractive, since this would facilitate the assembly of nonlinear optical waveguides[16, 17] and electronic devices such as solar cells.[18] In contrast to metals, which must be deposited electrochemically or evaporated into place, soluble polymers can be cast from

solution. Thus, the use of conducting polymers could result in devices that are more easily fabricated and lighter in weight than those made from conventional metals. Also, soluble materials are more amenable to characterization with the broad range of spectroscopic techniques employed by organic chemists.

An inherent contradiction is encountered, however, in attempting to design polymers that are both highly conjugated and soluble. Electronic delocalization through a π-system generally requires that adjacent monomer units along the backbone be coplanar. This enforced planarity tends to make the polymers inflexible. Since dissolution of a polymer is driven, in part, by the increase in entropy that results from the greater number of conformations available in solution than in the solid state, inflexible "rigid-rod" polymers are often insoluble. Synthetic modifications intended to make a conjugated chain more flexible can also result in a decrease in π-overlap along the polymer backbone with a concomitant loss of the interesting properties associated with electronic delocalization. An alternative view of solubilization that embodies the same contradiction states that the formation of the solid is driven by efficient molecular packing or crystallization. Since rigid-rod polymers pack well together, there is a large driving force for crystallization. Rigid polymer chains with random "kinks," or with randomly placed, large side groups, should thus be more soluble, because of the inability to pack the chains together.[19] In a given modified rigid-rod polymer, it is difficult to determine which of these two ideas, increased flexibility or poorer packing, is dominant, since the distinction depends in part on the time scale of the molecular motions. In either case, the contradiction inherent in solubilizing conjugated polymer chains necessitates compromise. For example, if the polymer is made more flexible by decreasing the tendency of the polymer backbone repeat units to be coplanar, the

perturbation should be enough to induce solubility, but not enough to interrupt conjugation fully.

The attachment of long, flexible alkyl side groups to a rigid chain can sometimes induce solubility without disrupting the main chain. The conformational mobility of the side chains, which act as "bound solvent,"[20] provides enough entropic driving force to carry the rigid polymer chain into solution. Certainly, the disruption of packing in the solid state may also help to solubilize such a polymer, although the issue is not so straightforward, since long, alkyl side chains can themselves crystallize.[21] A drawback of incorporating long, alkyl side chains is that the polymer backbone, which imparts the properties of interest, is being diluted by the side chains.

To varying extents, all of these factors — increasing main chain flexibility, disrupting packing in the solid state, and the attachment of "bound solvent" — are operative in a number of substituted rigid-rod polymers that have been solubilized by attaching side groups. Soluble derivatives have been described for almost every class of conjugated polymer. These include alkyl- and alkoxy-substituted polythiophenes,[22-24] polyanilines,[25, 26] poly(phenylene vinylenes)[27] and oligo(*para*-phenylenes).[28, 29] This dissertation describes the addition of a new class of polyacetylenes to this list of soluble conjugated polymers.

Polyacetylene, structurally the simplest extended π-system, has been the focus of a significant fraction of theoretical and experimental work on conjugated polymers. Films of the material are readily available via three routes (Figure 1): the gas-phase polymerization of acetylene with alkyl titanium catalysts (Shirakawa polyacetylene);[30] the retro-Diels Alder reaction of a polymer prepared by ring-opening metathesis polymerization[31, 32] (ROMP) of a tricyclic masked cyclobutadiene[33, 34] (the "Feast monomer") and the ROMP of cyclooctatetraene (COT).[35-37] In all cases, the polymer obtained is an intractable

solid. The latter two routes do proceed, though, via intermediate stages during which the material is somewhat tractable. A soluble precursor polymer is formed by the polymerization of the Feast monomer, and the polymerization of COT may be controlled so that the reaction mixture remains a viscous liquid for a short period of time before solidifying.[36]

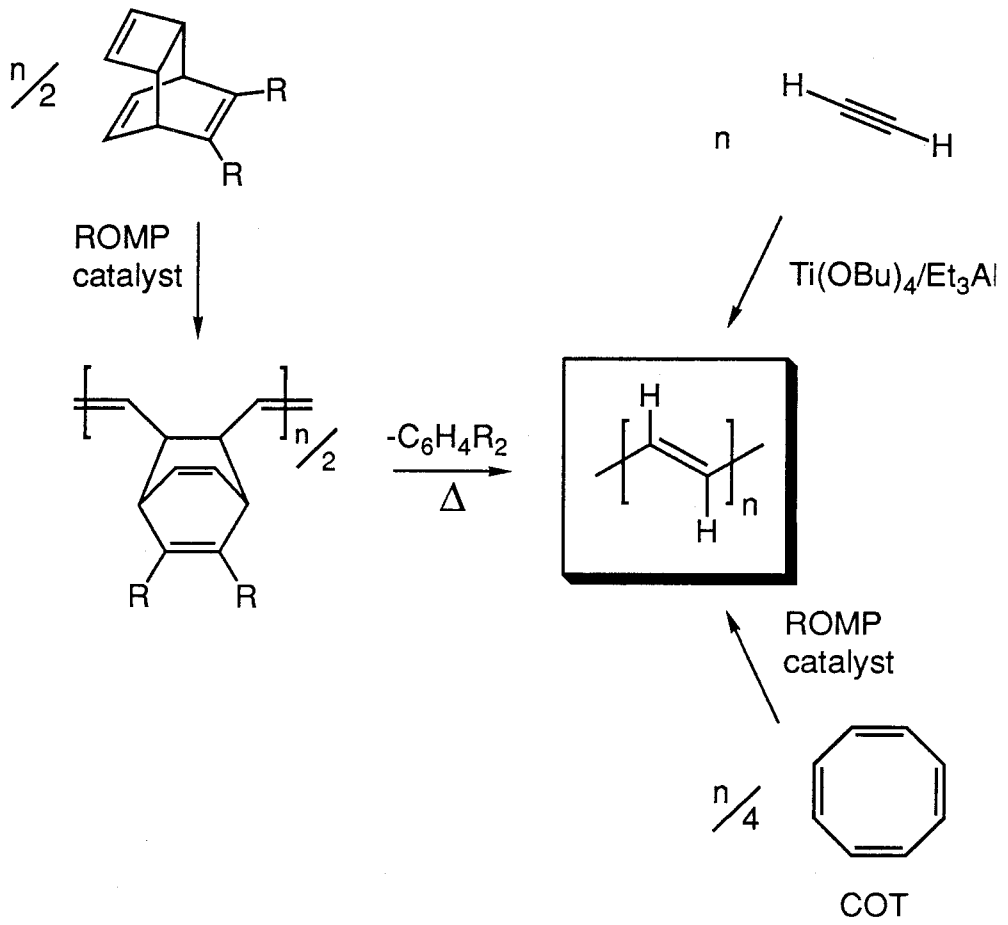

Figure 1. Three synthetic routes to polyacetylene.[10, 11, 33-37]

Researchers have investigated routes to soluble polyacetylenes for many years. Polyene chains have been grafted onto soluble nonconjugated polymers such as polybutadiene or polyisoprene.[38-43] The resulting copolymers have been used to obtain some spectroscopic information about the conjugated chains in

solution. Chemists have also synthesized a large number of highly substituted homopolymers from mono- or disubstituted alkynes using early transition metal catalysts.[44-52] The properties of these polyacetylenes are highly dependent on the substituent (Table 1). Polyphenylacetylene, for example, is somewhat conjugated and can be doped to moderate conductivities.[53] In contrast, the placement of bulky substituents, such as *t*-butyl or trimethylsilyl, at every other carbon atom of the backbone causes the polymer chain to twist severely (Figure 2). These twisted polymers are soluble, but adjacent double bonds are not in conjugation as indicated by the relatively high-energy absorption maxima of the polymers. Spacing the substituents farther apart along the main chain by copolymerizing acetylene with a substituted acetylene could potentially give a soluble, highly conjugated material, although Chien found that an acetylene/propyne copolymer containing only 15 percent acetylene was not soluble.[50] This tactic could be complicated by the formation of blocks, since the two monomers might have different rates of polymerization, and often one monomer is a gas and the other a liquid. The Feast route is not amenable to the synthesis of substituted polyacetylenes, since the olefin metathesis reaction is generally not facile with trisubstituted olefins, and finding synthetic routes to the required substituted monomers is not straightforward. In short, none of these approaches has yielded a polyacetylene comparable in utility to other known, solubilized, conjugated polymers.

Table 1. Properties of substituted polyacetylenes (poly-RC≡CH).

R	λ_{max} (nm)	solubility	reference
H	620	insoluble	54
Me	290	soluble	50
Me_3Si	292	soluble	49
Ph	325-350	soluble	53
o-(Me_3Si)Ph	550	soluble	55
CH[(Naphthyl)(Ph)-(Me)Si](*n*-C_5H_{11})	(yellow)	soluble	56

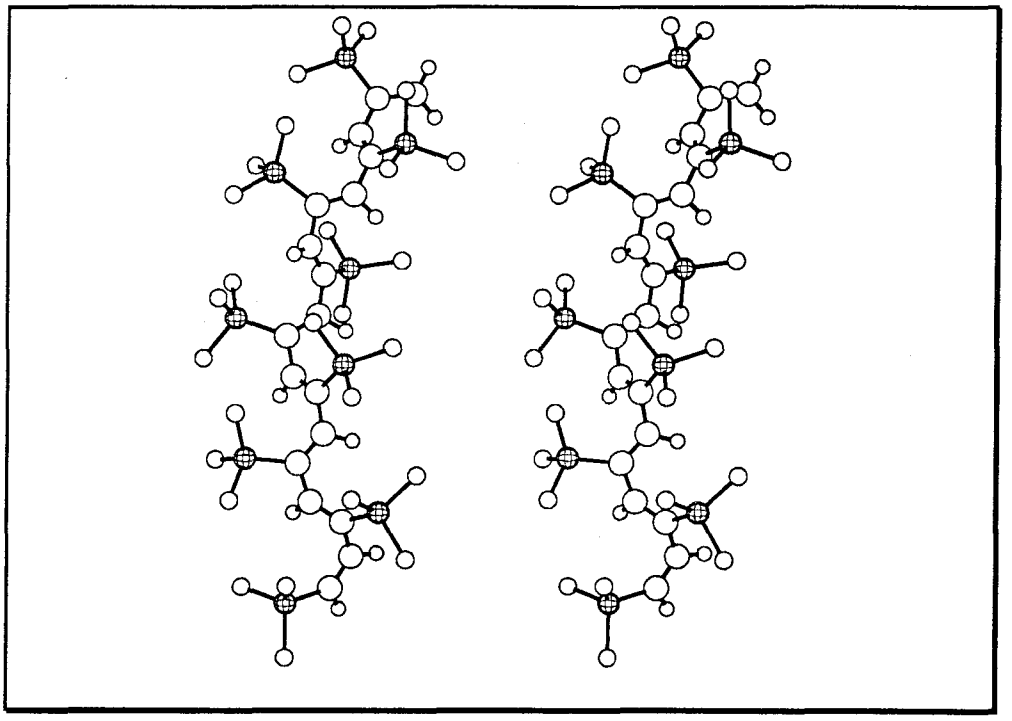

Figure 2. A stereo view of poly(trimethylsilylacetylene). The protons on the trimethylsilyl groups are omitted for clarity. Note the twisting along the main chain. (The structure shown is a calculated minimum found with the molecular mechanics program Batchmin. See Chapter 3.)

Ring-Opening Metathesis Polymerization.[32, 57, 58]

The polyacetylene chemistry described in this thesis is feasible because of recent improvements in olefin metathesis catalysts. Klavetter and Grubbs showed that the use of a well-defined tungsten alkylidene catalyst, developed by Schrock and coworkers,[59] enables the synthesis of polyacetylene with no detectable sp^3 defects or crosslinks. Moreover, since the alkylidene is preformed, the monomer-to-catalyst ratio may be controlled. In contrast, "classical" metathesis catalysts,[31] which are prepared in situ by mixing metal halides with alkylating agents, do not allow control of the stoichiometry of the polymerization and may react nonspecifically to form unwanted side products.

The mechanism of olefin metathesis is shown in Figure 3. The rate of the reaction depends upon the relative energies of the alkylidene and metallacyclobutane intermediates. If one is much more stable than the other, the reaction will proceed slowly, since there will be a large barrier to interconversion between the two.[60] The difference in stability of the two forms is a function of the metal and its ancillary ligands. The tungsten catalyst used in the present work is a relatively active metathesis catalyst,[59, 61] indicating that the carbene and metallacycles readily interconvert. An efficient catalyst is required for the polymerization of cyclooctatetraene, since the molecule is not highly strained (2.5 kcal/mole ring strain[62]). With highly strained monomers, such as norbornene, the catalytic cycle is driven by the release of ring strain upon cleavage of the metallacyclobutane. The reaction equilibrium is less favorable in the case of cyclooctatetraene. To drive the reaction towards polymerization and to prevent excessive "back-biting" to form benzene (See Figure 3 in Chapter 2), a high concentration of monomer is used. In fact, Klavetter and Grubbs optimized the polymerization by dissolving the catalyst in neat monomer.

Acyclic Olefins:

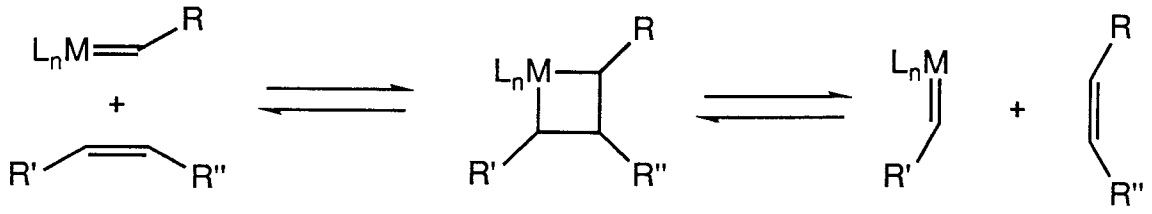

Cyclic Olefins:

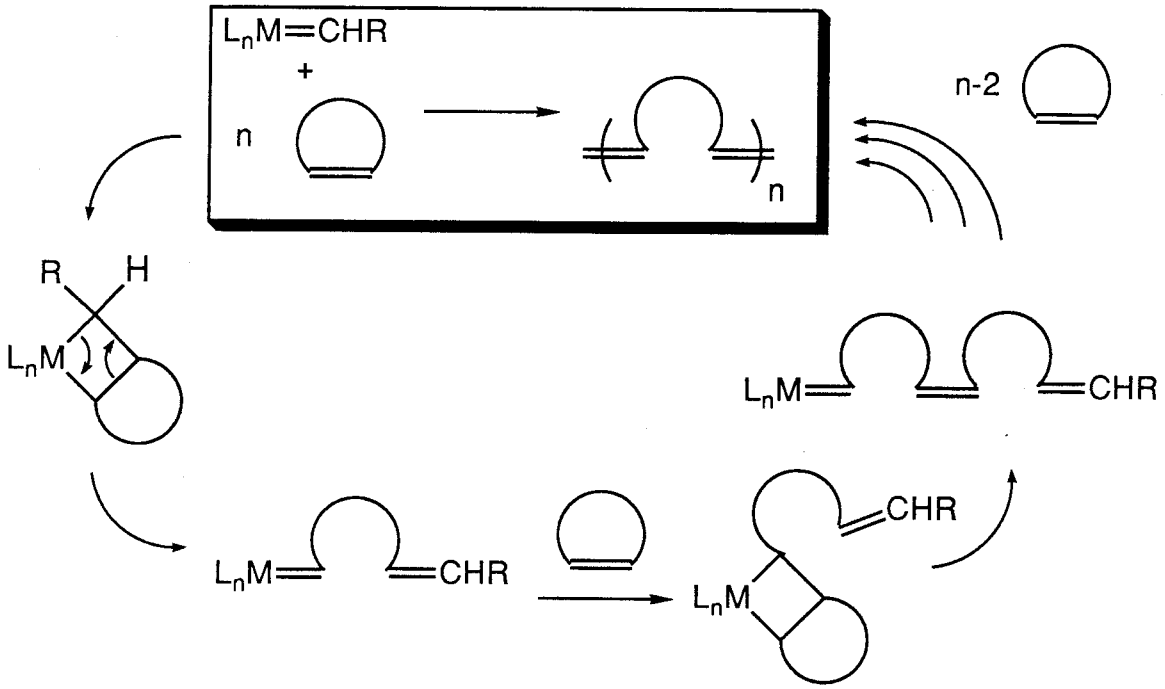

Figure 3. The mechanism of olefin metathesis. The arc in the lower reaction scheme represents any cyclic molecular structure. All the steps in the polymerization sequence are potentially reversible.

Summary.

The developments in metathesis chemistry described above have arrived at an opportune time to aid the pursuit of soluble conjugated polymers. The following chapters discuss a route into a class of substituted polyacetylenes that could not be obtained by methods used in the past. The controlled reactivity of the new ROMP catalysts allows the synthesis of well-defined polymers. In the context of polycyclooctatetraene chemistry, these catalysts permit the placement

of side groups in a more regular fashion than has been possible, allowing an optimum balance to be struck between decreasing conjugation length and increasing solubility.

References and Notes

(1) More background information on both conjugated polymers and ROMP may be found in a variety of sources, including a number of dissertations of past Grubbs group members. See References 2-4.

(2) Gilliom, L. R.; Ph. D. Dissertation; California Institute of Technology: 1986.

(3) Swager, T. M.; Ph. D. Dissertation; California Institute of Technology: 1988.

(4) Novak, B. M.; Ph. D. Dissertation; California Institute of Technology: 1989.

(5) *Handbook of Conducting Polymers, Vol.1;* Skotheim, T. A., Ed.; Marcel Dekker: New York, 1986.

(6) *Handbook of Conducting Polymers, Vol. 2;* Skotheim, T. A., Ed.; Marcel Dekker: New York, 1986.

(7) *Electroresponsive Molecular and Polymeric Systems;* Skotheim, T. A., Ed.; Marcel Dekker: New York, 1988.

(8) Kajzar, F.; Etemad, S.; Baker, G. L.; Messier, J. *Synth. Met.* **1987**, *17*, 563-567.

(9) Beratan, D. N.; Onuchic, J. N.; Perry, J. W. *J. Phys. Chem.* **1987**, *91*, 2696-2698.

(10) Shirakawa, H.; Louis, E. J.; MacDiarmid, A. G.; Chiang, C. K.; Heeger, A. J. *J. Chem. Soc. Chem. Comm.* **1977**, 578-580.

(11) Chiang, C. K.; Fincher, C. R., Jr.; Park, Y. W.; Heeger, A. J.; Shirakawa, H.; Louis, E. J.; Gau, S. C.; MacDiarmid, A. G. *Phys. Rev. Lett.* **1977**, *39*, 1098-1101.

(12) Brandstetter, F. *ECN Speciality Chemicals Supp.* **1988**, *Jan..*, 32-36.

(13) Freundlich, N. *Business Week* **1989**, *Dec. 11*, 114-115.

(14) Frommer, J. E.; Chance, R. R. in *Encyclopedia of Polymer Science and Engineering*; Kroschwitz, J. I., Ed.; Wiley & Sons: New York, 1986; pp 462-507.

(15) MacDiarmid, A. G.; Chiang, J.; Halpern, M.; Huang, W. S.; Krawczyk, J. R.; Mammone, R. J.; Mu, S. L.; Somasiri, N. L. D.; Wu, W. *Polym. Prepr.* **1984**, *25*, 248-249.

(16) *Nonlinear Optical Properties of Organic Materials and Crystals, Vol. 2*; Chemla, D. S.; Zyss, J., Eds.; Academic: Orlando, FL, 1987.

(17) Wilson, J.; Hawkes, J. F. B. *Optoelectronics: An introduction, 2nd ed.*; Prentice Hall: New York, 1989.

(18) Sailor, M. J.; Ginsburg, E. J.; Gorman, C. B.; Kumar, A.; Grubbs, R. H.; Lewis, N. S. *Science* **1990**, *249*, 1146-1149.

(19) G. L. Baker, personal communication.

(20) Ballauff, M. *Angew. Chem. Int. Ed. Engl.* **1989**, *28*, 253-267.

(21) Rabolt, J. F.; Hofer, D.; Fickes, G. N.; Miller, R. D. *Macromolecules* **1986**, *19*, 611-616.

(22) Hotta, S.; Rughooputh, S. D. D. V.; Heeger, A. J.; Wudl, F. *Macromolecules* **1987**, *20*, 212-215.

(23) Rughooputh, S. D. D. V.; Hotta, S.; Nowak, M.; Heeger, A. J.; Wudl, F. *Synth. Met.* **1987**, *21*, 41-50.

(24) Jen, K. Y.; Oboodi, R. L.; Elsenbaumer, R. L. *Polym. Mat. Sci. Eng.* **1985**, *53*, 79-83.

(25) Leclerc, M.; Guay, J.; Dao, L. H. *Macromolecules* **1989**, *22*, 649-653.

(26) MacIness, D., Jr.; Funt, B. L. *Synth. Met.* **1988**, *25*, 235-242.

(27) Elsenbaumer, R. L.; Jen, K.; Miller, G. G.; Eckhardt, H.; Shacklette, L. W.; Jow, R. in *Electronic Properties of Conjugated Polymers.*; Kuzmany, H.; Mehring, M. Roth, S., Eds.; Springer-Verlag: Berlin, 1987; pp 400-406.

(28) Rehahn, M.; Schlüter, A. D.; Wegner, G.; Feast, W. J. *Polymer* **1989**, *30*, 1060-1062.

(29) Rehahn, M.; Schlüter, A. D.; Wegner, G.; Feast, W. J. *Polymer* **1989**, *30*, 1054-1059.

(30) Ito, T.; Shirakawa, H.; Ikeda, S. *J. Polym. Sci.: Polym. Chem. Ed.* **1974**, *12*, 11-20.

(31) Ivin, K. J. *Olefin Metathesis*; Academic: London, 1983.

(32) Grubbs, R. H. in *Comprehensive Organometallic Chemistry*; Wilkinson, G., Ed.; Pergamon: New York, 1982; pp 499-551.

(33) Edwards, J. H.; Feast, W. J. *Polymer* **1980**, *21*, 595-596.

(34) Bott, D. C.; Brown, C. S.; Chai, C. K.; Walker, N. S.; Feast, W. J.; Foot, P. J. S.; Calvert, P. D.; Billingham, N. C.; Friend, R. H. *Synth. Met.* **1986**, *14*, 245-269.

(35) Korshak, Y. V.; Korshak, V. V.; Kanischka, G.; Höcker, H. *Makromol. Chem., Rapid Commun.* **1985**, *6*, 685-692.

(36) Klavetter, F. L.; Grubbs, R. H. *J. Am. Chem. Soc.* **1988**, *110*, 7807-7813.

(37) Tlenkopachev, M. A.; Korshak, Y. V.; Orlov, A. V.; Korshak, V. V. *Doklad. Akad. Nauk, Eng. Transl.* **1987**, *291*, 1036-1040 (Original Russian article: pp. 409-413, 1986).

(38) Armes, S. P.; Vincent, B.; White, J. W. *J. Chem. Soc. Chem. Commun.* **1986**, 1525-1527.

(39) Baker, G. L.; Bates, F. S. *Macromolecules* **1984**, *17*, 2619-2626.

(40) Dorsinville, R.; Tubino, R.; Krimchansky, S.; Alfano, R. R.; Birman, J. L.; Bolognesi, A.; Destri, S.; Catellani, M.; Porzio, W. *Phys. Rev. B* **1985**, *32*, 3377-3380.

(41) Stowell, J. A.; Amass, A. J.; Beevers, M. S.; Farren, T. R. *Makromol. Chem.* **1987**, *188*, 1635-1639.

(42) Tubino, R.; Dorsinville, R.; Lam, W.; Alfano, R. R.; Birman, J. L.; Bolognesi, A.; Destri, S.; Catellani, M.; Porzio, W. *Phys. Rev. B* **1984**, *30*, 6601-6605.

(43) Stowell, J. A.; Amass, A. J.; Beevers, M. S.; Farren, T. R. *Polymer* **1989**, *30*, 195-201.

(44) Masuda, T.; Higashimura, T. *Adv. Polym. Sci.* **1986**, *81*, 121-165.

(45) Gibson, H. W. in Reference 5, pp 405-439.

(46) Masuda, T.; Higashimura, T. *Adv. Polym. Sci.* **1987**, *81*, 121-165.

(47) Zeigler, J. M. *U.S. Patent Appl. US 760 433 AO, 21 November, 1986;* **1986**, *Chem. Abstr.* **1986**, *20*, 157042.

(48) Okano, Y.; Masuda, T.; Higashimura, T. *J. Polym. Sci.: Polym. Chem. Ed.* **1984**, *22*, 1603-1610.

(49) Zeigler, J. M. *Polym. Prepr.* **1984**, *25*, 223-224.

(50) Chien, J. C. W.; Wnek, G. E.; Karasz, F. E.; Hirsch, J. A. *Macromolecules* **1981**, *14*, 479-485.

(51) Ciardelli, F.; Lanzillo, S.; Pieroni, O. *Macromolecules* **1974**, 174-179.

(52) Leclerc, M.; Prud'homme, R. E.; Soum, A.; Fontanille, M. *J. Polym. Sci.: Polym. Phys. Ed.* **1985**, 2031-2041.

(53) Ehrlich, P.; Anderson, W. A. in Reference 5, pp 441-488.

(54) Chien, J. C. W. *Polyacetylene: Chemistry, Physics, and Material Science*; Academic: Orlando, FL, 1984.

(55) Masuda, T.; Higashimura, T. *Adv. Chem. Ser.* **1990**, *224*, 641-661.

(56) Tang, B.-Z.; Kotera, N. *Macromolecules* **1989**, *22*, 4388-4390.

(57) Grubbs, R. H.; Tumas, W. *Science* **1989**, *243*, 907-915.

(58) Schrock, R. R. *Acc. Chem. Res.* **1990**, *23*, 158-165.

(59) Schrock, R. R.; DePue, R. T.; Feldman, J.; Schaverien, C. J.; Dewan, J. C.; Liu, A. H. *J. Am. Chem. Soc.* **1988**, *110*, 1423-1435.

(60) Collman, J. P.; Hegedus, L. S.; Norton, J. R.; Finke, R. G. *Principles and Applications of Organotransition Metal Chemistry*; University Science Books: Mill Valley, CA, 1987.

(61) Schrock, R. R.; Feldman, J.; Cannizzo, L. F.; Grubbs, R. H. *Macromolecules* **1987**, *20*, 1169-1172.

(62) Schleyer, P. v. R.; Williams, J. E.; Blanchard, K. R. *J. Am. Chem. Soc.* **1970**, *92*, 2377-2386.

CHAPTER 2

SYNTHESIS AND PROPERTIES OF SUBSTITUTED POLYCYCLOOCTATETRAENES

Abstract.

This chapter and the next describe substituted polyacetylenes produced by the ring-opening metathesis polymerization (ROMP) of substituted cyclooctatetraenes.[1-3] A variety of polymers have been synthesized, enabling predictive modeling of structure/property relationships. The focus will be on polymers substituted with Me_3M, where M = C, Si, Ge, and Sn, with an emphasis on the trimethylsilyl derivative, although other substituted polyacetylenes, prepared by Christopher B. Gorman in this laboratory, will be discussed as well. This chapter describes the synthesis and characterization of the polymers. Also, evidence for a cis to trans photoisomerization of the polymer is presented.

Introduction

Several synthetic routes to substituted polyacetylenes were described in the introductory chapter. In general, these syntheses lead either to materials that are too highly substituted to be conjugated, such as poly(trimethylsilylacetylene),[4] or to ones that have poorly defined structures, such as poly(acetylene-*co*-propyne).[5] The successful ring-opening metathesis polymerization of cyclooctatetraene to form polyacetylene[6-8] offered the opportunity to synthesize substituted polyacetylenes in which side groups were placed widely apart in a more regular manner. This may be thought of as an alternative method for the preparation of a copolymer of acetylene and a substituted acetylene. The method is versatile, given the variety of substituted cyclooctatetraenes that are synthetically accessible,[9, 10] offering the possibility of tuning the properties of the polymer by perturbing the polyene chain in a controlled fashion.

A few requirements guide the selection of substituted cyclooctatetraenes to be polymerized. Catalyst compatibility is the most stringent. The highly active catalyst used for these studies[11, 12] is sensitive to many protic, electrophilic

and nucleophilic functionalities. In addition, the characterization of a polymer is much easier if the polymer, and therefore the monomer, can be readily synthesized on a large scale. Thus, monomers requiring lengthy multistep syntheses have been avoided. The Me_3M-cyclooctatetraene series was chosen for its relative inertness and synthetic accessibility, as well as the variation in steric and electronic properties of the congeners.[13]

Results

Monomer synthesis. Trimethylsilylcyclooctatetraene (TMSCOT), trimethylgermylcyclooctatetraene (Me_3GeCOT), and trimethylstannylcyclooctatetraene (Me_3SnCOT) were prepared from bromocyclooctatetraene (BrCOT)[14, 15] by lithium-halide exchange followed by nucleophilic addition to Me_3MCl, as reported in the literature.[16] *t*-Butylcyclooctatetraene[17, 18] was prepared by a coupling reaction between a *t*-butyl cuprate and BrCOT. (See Figure 1.) The four monomers are yellow oils at room temperature and were stored in an inert atmosphere below room temperature to prevent decomposition via Diels-Alder reactions or free-radical processes.

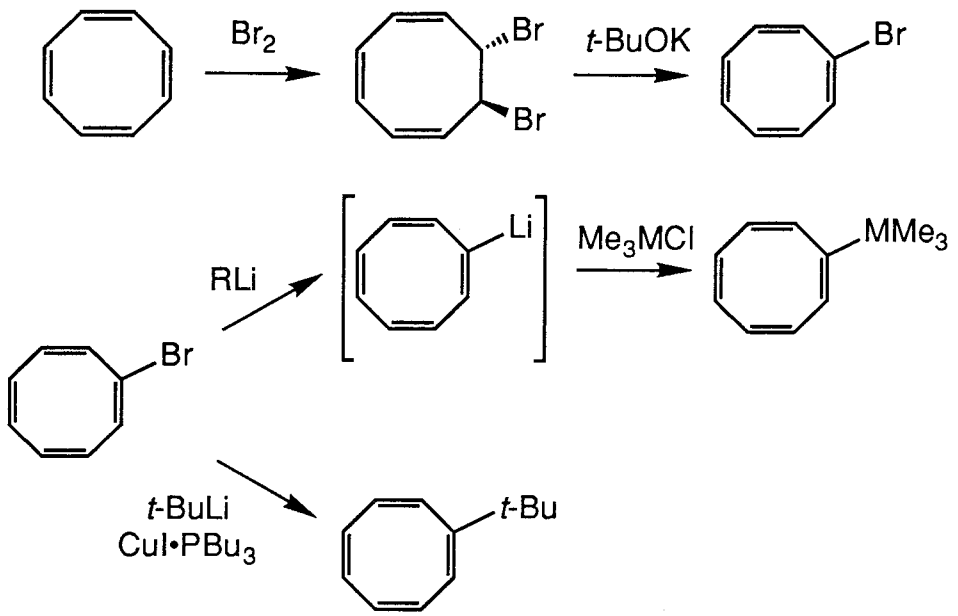

Figure 1. Syntheses of substituted cyclooctatetraenes.

Polymer Synthesis. The polymers were prepared under a nitrogen atmosphere by dissolving the catalyst, W(CH(*t*-Bu))(N(2,6-(*i*-Pr)$_2$C$_6$H$_3$)-(OCMe(CF$_3$)$_2$)$_2$,[12] in a minimum amount of a hydrocarbon solvent, typically pentane, and adding the yellow catalyst solution and a small amount of tetrahydrofuran (THF) (typically [THF]:[Catalyst] is ca. 10:1) to the monomer (Figure 2). THF was added to decrease the rate of polymerization by reversibly complexing the catalyst.[6, 19, 20] This procedure allowed sufficient time to mix the polymerization solution to ensure homogeneity and to transfer the polymer before it solidified. The solution was placed on the desired substrate and allowed to stand. As the polymerization proceeded, the solution darkened to red or blue. The time required before the reaction mixture solidified depended on the amount of THF added.[21] Typically, the polymer could be removed from the substrate as a free-standing film after times ranging from 15 minutes to three hours.

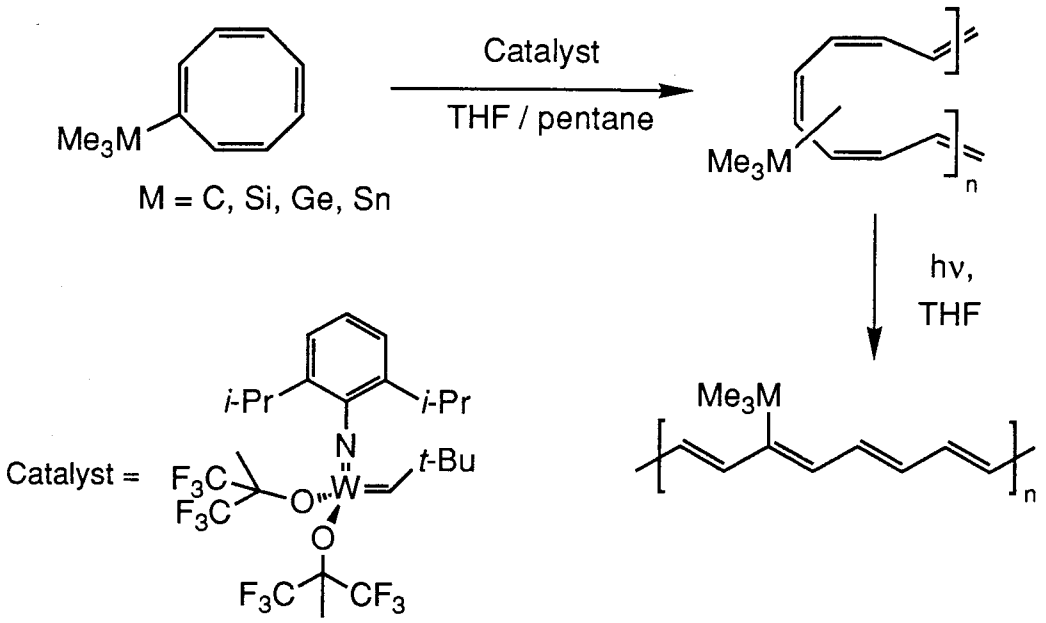

Figure 2. The synthesis of substituted polyacetylene via the ring-opening metathesis polymerization of substituted cyclooctatetraenes, followed by photoisomerization of the polymer to a trans structure.

The bulk polymerizations did not give a quantitative yield of polymer, as indicated by ^{1}H NMR spectroscopy. (See Figure 9 below.) Unreacted monomer and substituted benzenes produced by "back-biting" reactions[6] (Figure 3) remained after the reaction mixture solidified. Presumably the rate of diffusion in the polymer matrix decreases over the course of the polymerization and some monomer molecules are trapped indefinitely without access to propagating alkylidene, effectively stopping the reaction.

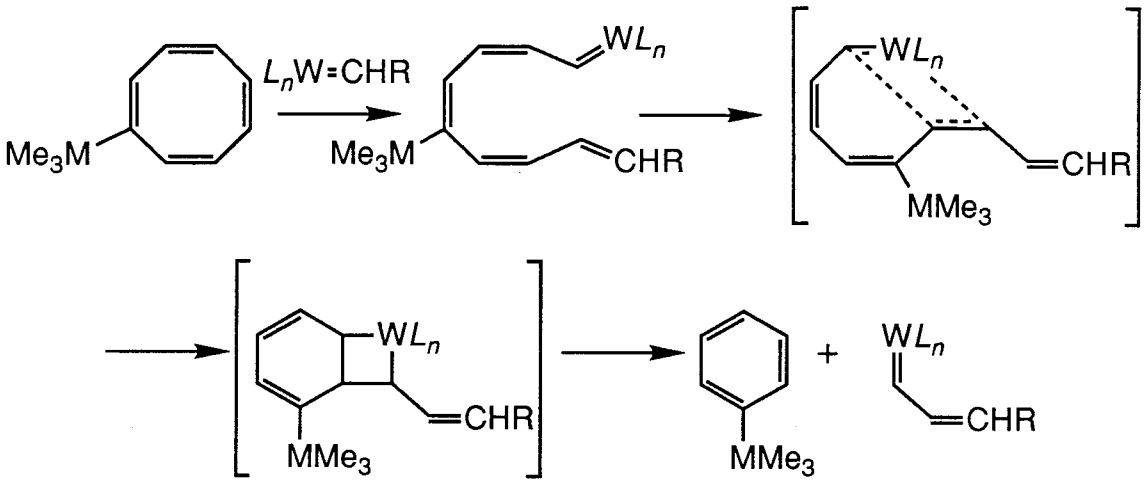

Figure 3. Chain-transfer by back-biting, yielding substituted benzene derivatives.

The polymers were treated as moderately air-sensitive materials. Films decomposed within days in air, becoming brittle and yellow. Solutions that were exposed to air became colorless with time. After exposure of a 20- to 30-μm-thick poly(TMSCOT) film to air for two hours, approximately 20% of the material was no longer soluble in tetrahydrofuran, as determined by ^{1}H NMR integration versus an internal standard by assuming that any insoluble solid was NMR-silent. The sensitivity of the polymers is presumably due to oxygen-promoted crosslinking reactions. It is well known that shorter polyenes and unsubstituted polyacetylene degrade in air.[22, 23]

Polymer Characterization. The four Me_3M-substituted polymers differ in solubility and appearance. Poly(*t*-BuCOT) and poly(TMSCOT) are soluble in organic solvents, including benzene, THF, and methylene chloride, and remain so indefinitely if stored in an inert atmosphere. Poly(Me_3GeCOT) and poly(Me_3SnCOT) are soluble if dissolved immediately after polymerization, but become less so over time. This change in solubility is discussed below.

Poly(TMSCOT) has been investigated in the most detail because it is both tractable and highly conjugated.

UV/Visible spectra of the four polymers dissolved immediately after polymerization are shown in Figure 4. The spectra are characterized by a strong absorption ($\varepsilon \approx 10^4$ L/cm·moles of repeat unit) at approximately 400 nm and a slightly weaker one between 450 and 550 nm. The *t*-butyl-substituted polymer is orange/red in the solid state or in solution, while poly(Me_3SnCOT) is a blue/black solid, which forms greenish-gray solutions if dissolved immediately after synthesis. Both as-synthesized (nascent) poly(TMSCOT) and poly-(Me_3GeCOT) are red in the solid state and in solution.

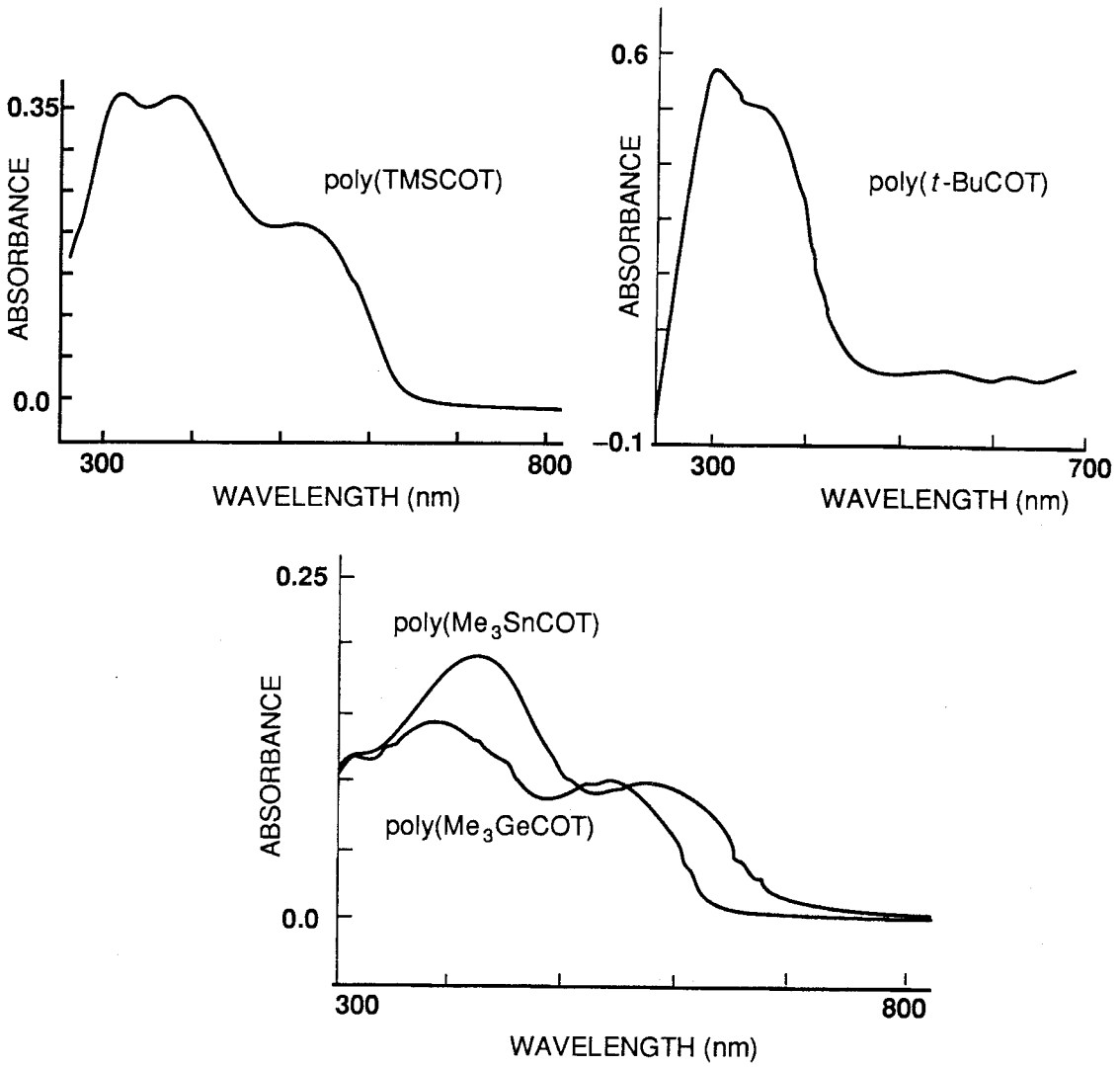

Figure 4. UV/Visible absorption spectra of poly(Me_3MCOT), M = C, Si, Ge, Sn.

Molecular Weight Determination. Although the yield of polymer is less than quantitative, high molecular weights were obtained. Static light-scattering data gave M_w=20,000 for a poly-*t*-BuCOT solution. Unfortunately, light-scattering data could not be obtained for the other polymers, because their absorption coefficients are too high at the lowest energy laser line (632.8 nm) that is feasible to use in these experiments. Gel permeation chromatography (GPC) versus polystyrene standards typically indicated molecular weights of 10^4 to 10^5 for different samples of poly(TMSCOT). The poly(*t*-BuCOT) solution used for

the light-scattering experiment had relative molecular weights of M_n=25,000 and M_w=42,000 by GPC.

Vibrational Spectroscopy. Resonance Raman spectra of the polymers are qualitatively similar to spectra of *trans*-polyacetylene (Figure 5).[24, 25] On the basis of the polyacetylene spectra, the band at ca. 1100 cm^{-1} is assigned to an A_g C-C stretch and the band at ca. 1500 cm^{-1} to an A_g C=C stretch. Both the optical absorbance and Raman data are summarized in Table 1.

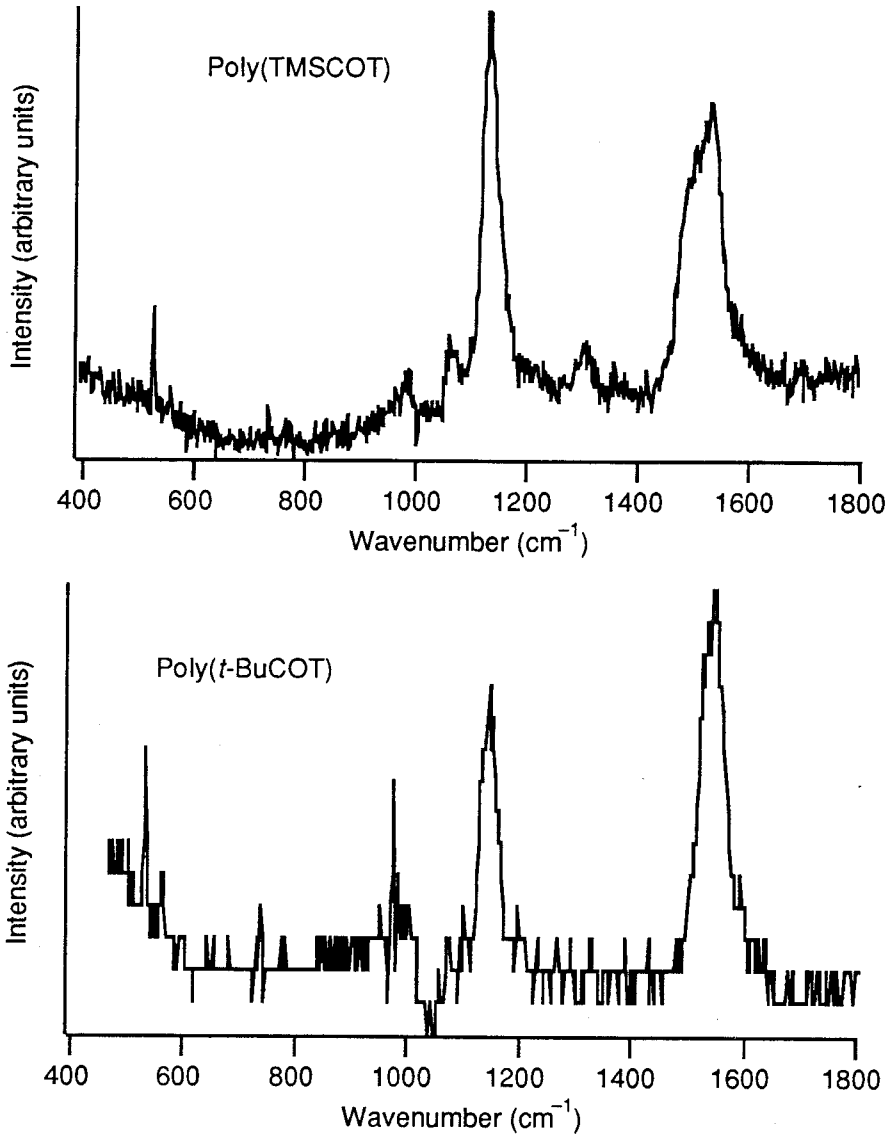

Figure 5. Resonance Raman spectra of poly(trimethylsilylcyclooctatetraene) and poly(*t*-butylcyclooctatetraene). ($\lambda_{excitation}$ = 488 nm.)

Table 1. Visible absorption (of the trans polymer (*vide infra*)) and resonance Raman spectroscopic data on poly(RCOT).

R	λ_{max} (nm)*	Resonance Raman peaks (cm^{-1}) (488 nm excitation)	
		A_g C–C	A_g C=C
H	650[26]	1113	1491[6]
Me_3C	430	1147	1539-1547
Me_3Si	540[27]	1132	1532
Me_3Ge	550	–	–
Me_3Sn	578	1140	1550

* All values are for polymers in solution, except for R = H.

Infrared spectra of these polymers are not readily interpreted by analogy to the spectrum of unsubstituted polyacetylene,[28] since they are dominated by absorptions of the side group. The infrared spectrum of poly(TMSCOT) is shown in Figure 6. The strong absorptions at 840 cm^{-1} and 1248 cm^{-1} are attributed to a trimethylsilyl group stretch and bend, respectively.[29]

Some vibrational information may be gleaned from the fine structure in the low-temperature visible absorption spectrum of *trans*-poly(TMSCOT) (Figure 7). The spacing between the lowest energy peaks, about 1700 cm^{-1}, is of the same magnitude as the A_g C=C stretching vibrations observed in the Raman spectra, suggesting that the structure is vibronic in origin. Simpson et al. have observed that the most prominent vibronic structure in the absorption spectrum of all-*trans*-2,4,6,8,10,12,14-hexadecaheptaene is due to combinations of symmetric C=C stretching vibrations.[30] The appearance of fine structure in the poly(TMSCOT) absorption spectrum at low temperatures is evidence that the polymer chain is assuming a more rigid, conjugated conformation as the temperature decreases. The vibronic coupling is resolved because fewer conformational states are populated at the lower temperatures. The red shift (30-50 nm) and increase in

absorption coefficient are consistent with solvent and temperature effects observed in shorter polyenes[31] and *cis*-polyacetylene.[32]

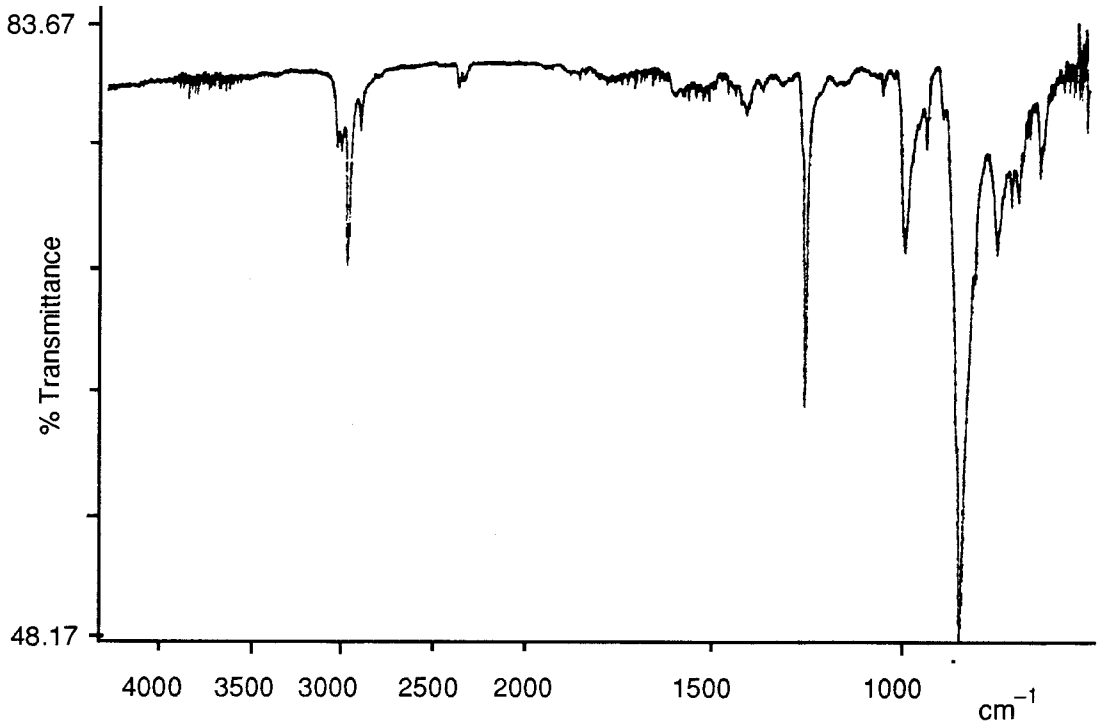

Figure 6. Infrared spectrum of poly(TMSCOT).

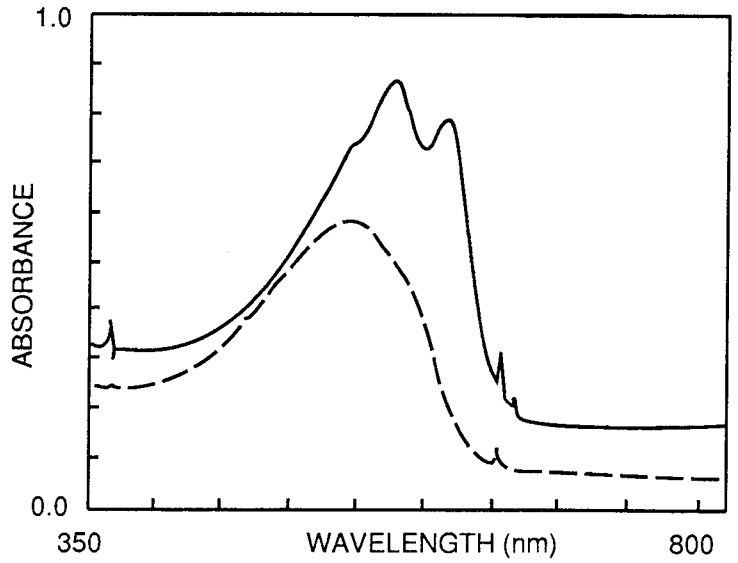

Figure 7. Visible absorption of *trans*-poly(TMSCOT) dissolved in THF at room temperature (dashed) and –78 °C (solid).

Isomerization. A number of observations are consistent with these polymers undergoing a thermal or photochemical cis-trans isomerization. If exposed to ambient light, the absorption maxima of dilute (transparent) solutions of the nascent polymers was red-shifted within a few hours. A series of absorption spectra obtained over the course of a photolysis of a poly(TMSCOT) solution using a medium pressure mercury lamp is shown in Figure 8. The transformation was considered to be complete when no additional changes in the spectra were seen with further irradiation. The quantum yield of the reaction has not been determined. The final spectrum is characterized by a strong absorption ($\varepsilon = 4 \times 10^4$ l/cm·moles of repeat unit) at the same energy as the lower energy absorbance of the nascent material. This photoreaction occurred at both room temperature and –78 °C and in a number of solvents, including carbon tetrachloride, tetrahydrofuran, and benzene. In contrast to the red, dull nascent poly(TMSCOT) films, the polymer cast from a photolyzed solution forms shiny films, which are green/gold in reflection and purple in transmission. The isomerization could also be carried out by heating a THF solution of the polymer to 80 °C for two hours.

Attempts to photolyze poly(TMSCOT) films led to their decomposition, presumably because the samples were not adequately cooled. One half of a silyl film that was exposed to ambient light for many weeks developed a sheen, indicative of the photoisomerization, while the other half, which was kept covered, did not. The NMR (see below) and absorption spectra of solutions of both halves, however, were identical to those of the nascent polymer. This indicates that the photoinduced transformation occurred only at a thin layer at the surface. The reaction may be autoinhibited in the solid state, since the photolyzed polymer is more reflective than the unphotolyzed polymer.

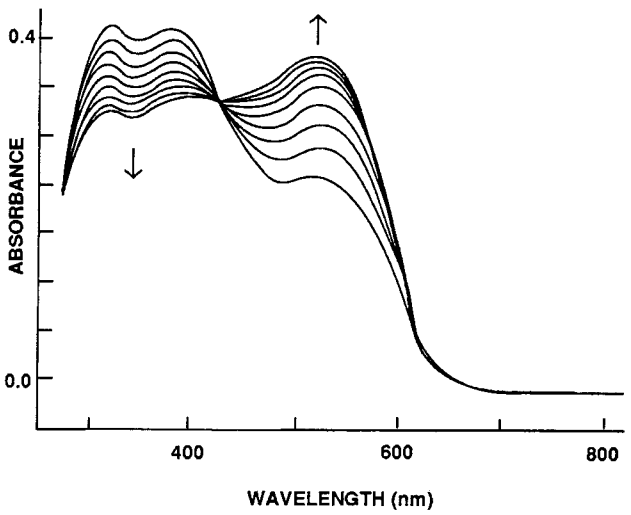

Figure 8. UV/Visible spectra of poly(TMSCOT) in carbon tetrachloride (10^{-6} M) obtained between eight periods of photolysis (10 s each) with a 350 watt mercury lamp.

In addition to optical spectroscopy, the isomerization was monitored by NMR spectroscopy and differential scanning calorimetry (DSC). The trimethylsilyl region of the ^{1}H NMR spectra of poly(TMSCOT) solutions obtained over the course of a photolysis is shown in Figure 9. A broad peak at 0.14 ppm assigned to the methyl protons decreased in intensity as the polymer was photolyzed, while a peak at 0.23 ppm increased in intensity. Changes were also observed in the olefinic region of the spectrum. Similar changes upon photolysis were observed in the ^{1}H NMR spectra of the other polymers (See the Experimental Section). DSC thermograms of poly(TMSCOT) before and after photolysis are shown in Figure 10. The thermogram of the nascent polymer contains two exotherms. The first is at 120 to 160 °C and the second at 160 to 220 °C. Neither exotherm is associated with a loss of material, as thermogravimetric analysis (Figure 11) showed negligible weight loss below 260 °C. The lower temperature exotherm is assigned to thermal cis-trans isomerization, since the DSC thermogram of the photolyzed polymer does not display the exotherm at

120-160 °C. Furthermore, unsubstituted polyacetylene samples are known to isomerize between 115 °C[33] and 145 °C,[34] depending on the degree of crystallinity.

The exotherm at 160-220 °C observed in the first DSC scan of the photolyzed polymer is not present in a second scan. This exotherm is proposed to result from an irreversible crosslinking reaction, since a sample of the trans polymer remained mostly soluble in THF after being heated to 165 °C and then cooled to room temperature, but a sample that was heated to 250 °C only swelled in THF.

Figure 9. The CH_3Si region of ^1H NMR spectra of poly(TMSCOT) in THF obtained over the course of a photolysis. Tic marks are at 0.1 ppm intervals. The spectra were obtained after (from left to right) approximately 0, 12, 18, 36, and 60 hours of photolysis. (The polymer is unwashed and therefore contains some residual monomer and other low molecular weight impurities such as trimethylsilylbenzene.)

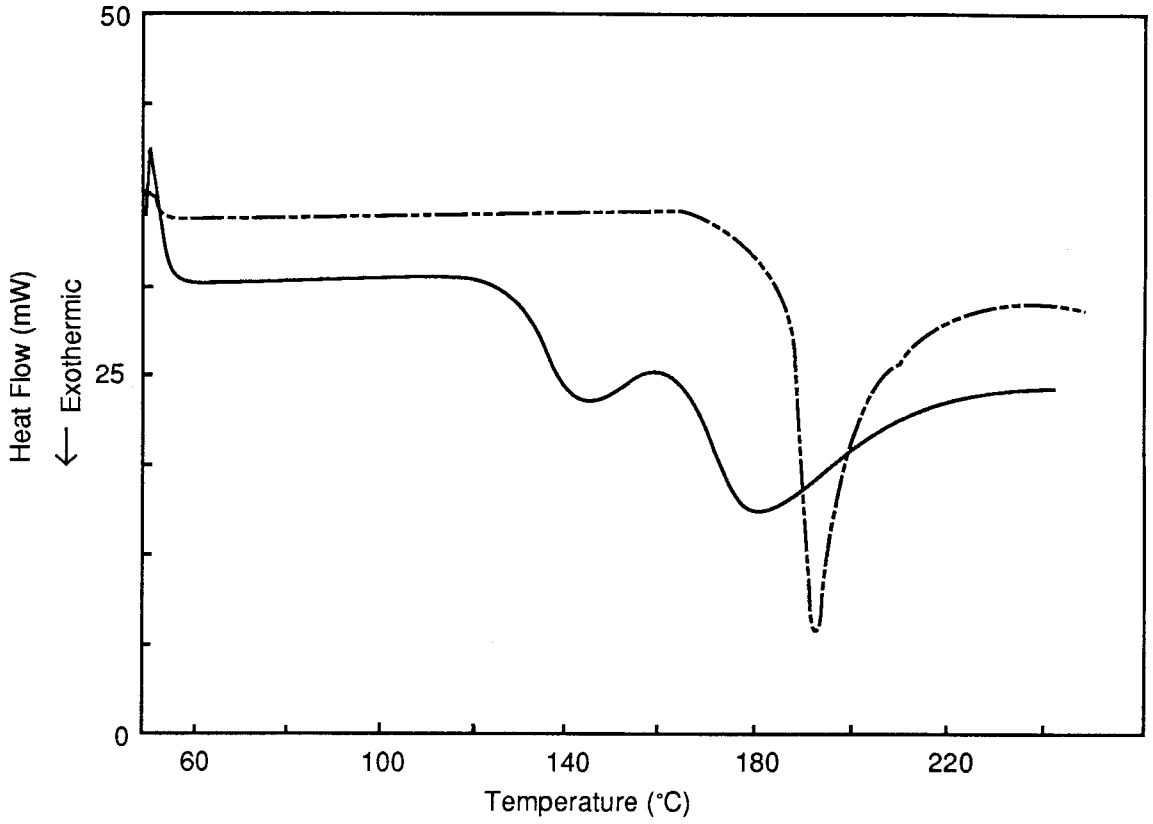

Figure 10. Differential scanning calorimetry thermograms (20 °C/min) of poly(TMSCOT) before (solid) and after (dashed) photolysis.

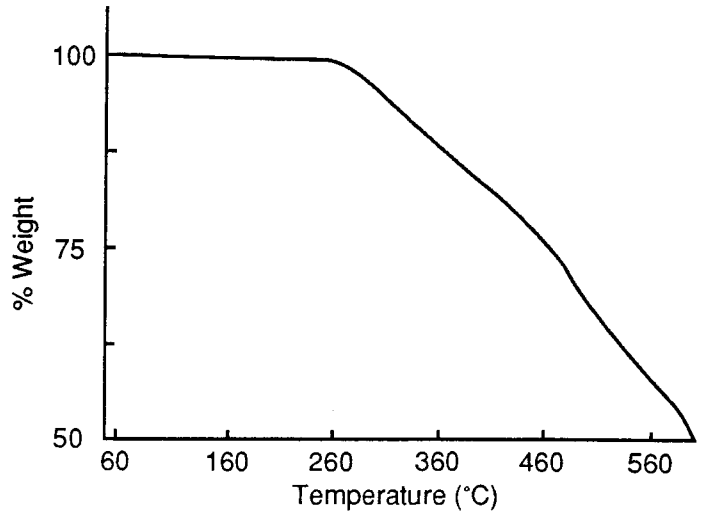

Figure 11. Thermogravimetric analysis of poly(TMSCOT). (The sample was washed to extract volatiles and not photolyzed).

The properties of the other three polymers after isomerization differ from those of poly(TMSCOT) in several respects. Spectra of these polymers before and after photolysis are shown in Figures 12 and 13. All of the spectra of the photolyzed polymers exhibit an absorption maximum at a lower energy than before photolysis. Poly(*t*-BuCOT) was found to be soluble before and after the photolysis, but unlike poly(TMSCOT), films cast from a *trans*-poly(*t*-BuCOT) solution had a dull finish. In contrast, films of *trans*-poly(Me_3GeCOT) were highly reflective and greenish gold. The polymer is similar in many ways to *trans*-poly(TMSCOT), except that solutions of poly(Me_3GeCOT) sometimes contained insoluble material after being photoisomerized. Poly(Me_3SnCOT) is less tractable than the other three polymers. Films of nascent poly(Me_3SnCOT) were soluble only if dissolved immediately after the polymerization. This behavior is similar to that observed for other highly conjugated poly(RCOT)s ($\lambda_{max} \approx 600$ nm), which become insoluble upon standing in the solid state at room temperature.[2] Dilute solutions (e.g., ~10^{-4} M) of *cis*-poly(Me_3SnCOT) remained in solution after photoisomerization, but the polymer precipitated or gelled upon standing as a concentrated solution.

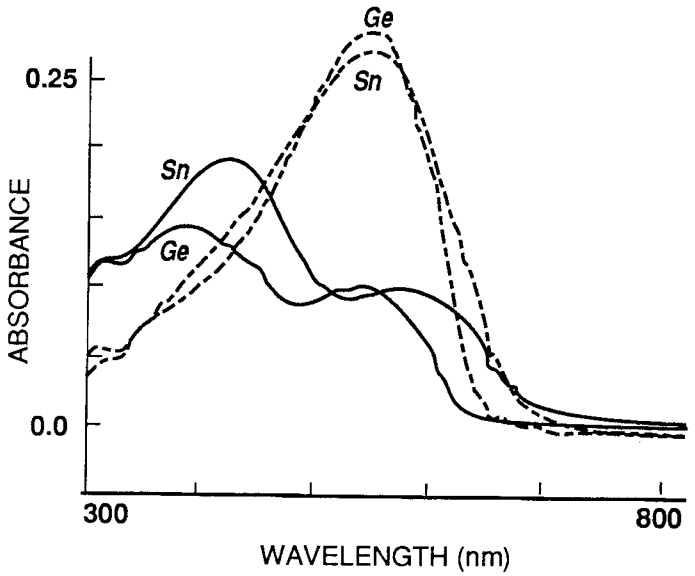

Figure 12. UV/Visible spectra of poly(Me_3GeCOT) and poly(Me_3SnCOT) in tetrahydrofuran before (solid) and after (dashed) photolysis (400 s) with a 350 watt mercury lamp.

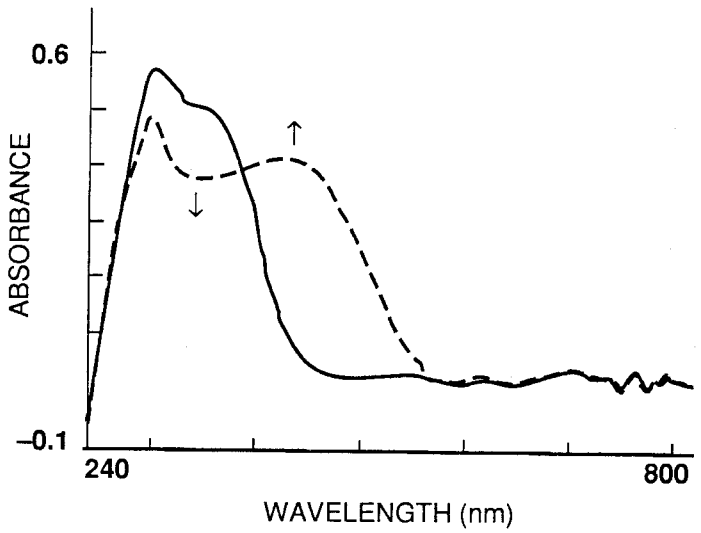

Figure 13. UV/Visible spectra of poly(*t*-BuCOT) in THF before (solid) and after (dashed) photolysis (280 s) with a 350 watt mercury lamp.

Discussion

Polymer Structure. Because of the distribution of the side groups along the chain, it is likely that the microstructure of the poly(RCOT) polymers is

complex. Assuming no back-biting, the polymer contains one side group for every eight carbon atoms. Formally, the monomer may be ring-opened in eight different ways, i.e., with the tungsten atom binding to any one of the eight atoms of the ring. It is reasonable to assume, however, that the trisubstituted double bonds are not ring-opened. (Trisubstituted double bonds are known to be much less reactive towards olefin metathesis catalysts, presumably because of unfavorable steric interactions.[35, 36]) If this is the case, the monomer may be ring-opened in six different ways, and the polymer side chains may end up anywhere from four to fourteen carbon atoms apart, with nine carbon atoms being the most probable separation. The resulting structural variation along the chain, in addition to the slow tumbling rate of the macromolecules,[37] is probably responsible for the ^{1}H and ^{13}C NMR resonances' being very broad.

Cis-Trans Isomerization. The UV-Visible, DSC, and NMR data presented above are consistent with the polymers undergoing a thermal or photochemical cis-trans isomerization. (See Figure 14.) Since the cyclooctatetraene monomers contain four cis double bonds and only one double bond of the molecule reacts during the polymerization, neglecting secondary acyclic metathesis, it is expected that the majority of the double bonds of the nascent polymer are cis in configuration. Because the backbone of unsubstituted *cis*-polyacetylene is twisted to avoid unfavorable steric interactions, it absorbs at higher energy than *trans*-polyacetylene.[22] The thermal cis-trans isomerization of unsubstituted polyacetylene has been studied in detail.[28, 34] It has been shown that Shirakawa polyacetylene contains predominantly cis double bonds if prepared at low temperatures, and this cis form isomerizes to the thermodynamically more stable, predominantly trans isomer at 145 °C. The isomers may be distinguished by their absorption, low-temperature Raman, IR, and CPMAS NMR spectra. The photoisomerization of unsubstituted polyacetylene has not been reported,

however cis-trans photoisomerizations of shorter polyenes are well known,[38, 39] the most prominent example being the isomerization of a double bond of retinal in photoreceptor cells of the eye.[40]

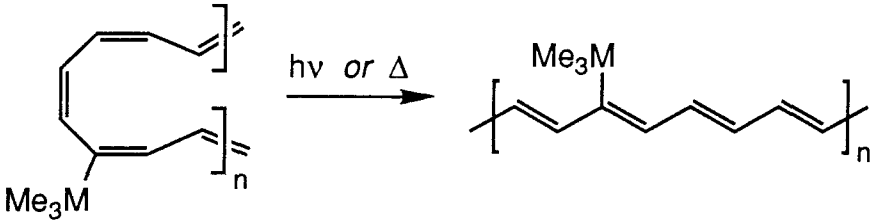

Figure 14. Thermal or photochemical cis-trans isomerization.

The resonance Raman spectra of poly(TMSCOT) are the same before and after photolysis. Unsubstituted *cis*- and *trans*-polyacetylene have very different Raman spectra,[24] however. Apparently, *cis*-poly(RCOT) films or solutions are isomerized by the laser during data accumulation. Equipment adequate for cooling the sample, as was used by Lichtmann to obtain spectra of unsubstituted *cis*-polyacetylene,[24] has not been available. Attempts to obtain spectra from cis-poly(RCOT) solutions that were held in a spinning sample holder in order to minimize exposure to the laser also gave spectra consistent with a trans structure. This result might indicate that the trans segments present in the "cis" samples were more strongly resonance-enhanced by the 488 nm light than were the cis segments, causing them to be overrepresented in the spectra.

The series of absorption spectra in Figure 7 contains an isosbestic point at 425 nm. Isosbestic points in sets of absorption spectra occur when all species (or ensembles of species) present in a mixture have identical absorption coefficients at a single wavelength. Since the probability of three species' having the same (nonzero) absorption coefficient at a given wavelength is generally very low, the presence of an isosbestic point is an indication that a reaction is proceeding directly from reactants to products, without detectable amounts of intermediates

being formed. Either a single reactant is forming a single product, or a set of reactants is being converted to a product or set of products at a single rate. It might be expected that the isomerization of a polyene from a predominantly cis form to a predominantly trans form with a different absorption maximum would proceed one double bond at a time, with the formation of discrete intermediates, each having different absorption maxima. If the photoisomerization did occur in this manner, however, the resulting series of spectra obtained over the course of the reaction would not display an isosbestic point (Figure 15).

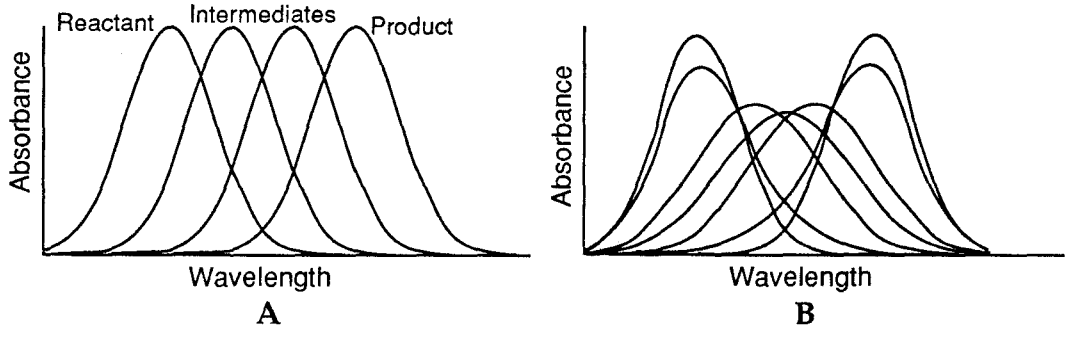

Figure 15. Absorption spectra of a hypothetical reaction that proceeds through two intermediates and thus does not lead to an isosbestic point. **(A)** Superimposed spectra of a reactant, two intermediates, and a product. **(B)** Spectra that would arise from various reaction mixtures of these species, assuming no mass is lost. These spectra are sums of various proportions of the individual spectra shown in **A**.

The absorbance maximum of *trans*-poly(TMSCOT)[41] (ca. 540 nm) is lower in energy than the absorption maximum of a polyene containing 15 unsubstituted double bonds (~500 nm), which was prepared by Schrock and coworkers.[42, 43] This implies an effective conjugation length of approximately 16 or 17 double bonds, if one makes the simplistic assumption that each double bond adds 30 nm to the absorption maximum.[44] The "effective conjugation length" of a given polyene is defined as the length of an unsubstituted trans-transoid polyene that has the same absorption maximum. Thus, although the

degree of polymerization indicates that each polymer contains hundreds of double bonds, the effective conjugation length is much shorter.

The polymer consists of chromophores of varying effective conjugation lengths. The dispersion in the length of these chromophores is determined, in part, by the irregular substitution pattern along the chain. Evidently, during the cis-trans photoisomerization, the double bonds within a chromophore act as a unit, isomerizing together. The isosbestic point indicates that a set of "cis" chromophores are converted to a set of "trans" chromophores without intermediates. Further investigations of the photophysics of this process are justified, since although cis-trans photoisomerizations involving two double bonds are well known,[40, 45] there is no precedent for a photoisomerization involving larger numbers of double bonds.

In summary, the ROMP of substituted cyclooctatetraenes provides high molecular weight, substituted polyacetylenes. Visible absorption and resonance Raman spectra of the polymers are consistent with extensive electronic delocalization along the backbone. The properties of the Me_3M-substituted polymers vary from the orange, highly soluble poly(*t*-BuCOT) to the blue, insoluble poly(Me_3SnCOT). The factors responsible for these differences will be discussed in the next chapter.

Experimental Section

General Procedures. The syntheses and purification of air- and/or moisture-sensitive compounds were performed under argon using standard high-vacuum or Schlenk-line techniques. Argon was purified by passage through columns of BASF RS-11 (Chemalog) and Linde 4Å molecular sieves. Manipulation of air-sensitive compounds was carried out inside a nitrogen-filled Vacuum Atmospheres drybox equipped with a –20 °C refrigerator and a dry-cool

recirculator. Proton and carbon NMR spectra were recorded on a JEOL FX-90Q NMR (89.9 MHz ^{1}H, 22.5 MHz ^{13}C) and a JEOL GX-400 NMR (399.65 MHz ^{1}H, 100.67 MHz ^{13}C). Proton chemical shifts are referenced to internal residual solvent protons. Carbon chemical shifts are referenced to the carbon signal of the deuterated solvents. UV-Visible spectroscopy was performed with a Hewlett-Packard 8154A diode array spectrophotometer. Typically, quartz cuvettes with a 1 cm pathlength were used. Low-temperature optical spectra were obtained by placing a solution in an NMR tube into the window of a clear quartz finger dewar filled with a dry ice/acetone slurry. Most of the absorption spectra presented here are traces of the actual spectra. The spectra were scanned into a computer, then traced using Adobe Illustrator 88 (Adobe Systems), resulting in some smoothing. Gas chromatography analyses (VPC) were performed on a Shimadzu GC-Mini-2 flame-ionization instrument with a 50 m capillary column and a Hewlett-Packard model 339A integrator. Low-resolution mass spectra were obtained on a Hewlett-Packard Series 5970 mass selective detector in conjunction with a Series 5890 GC equipped with a 15 m SE-30 capillary column. Preparative VPC was performed on a Varian 920 Aerograph with a thermal conductivity detector equipped with a Hewlett Packard 7127A strip recorder. Thin-layer chromatography (TLC) was performed on precoated TLC plates (silica gel 60 F-254, EM Reagents). Flash chromatography was by the method of Still et al.,[46] using silica gel 60 (230-400 mesh ATM, EM Reagents). Prior to obtaining thermograms, elemental analyses, and gel permeation chromatograms, the polymer films were rinsed repeatedly with dry pentane and methanol under argon in order to remove soluble components such as residual monomer, catalyst-decomposition products, and trimethylsilylbenzene produced by back-biting during the polymerization. Elemental analysis was determined at the analytical facilities of the California Institute of Technology. Gel permeation

chromatography was performed on one of two instruments: a homemade instrument employing three Shodex size exclusion columns, model numbers KF-803, KF-804, and KF-805 (70,000, 400,000, and 4,000,000 MW polystyrene exclusion limit, respectively), an Altex model 110A pump and a Knauer differential refractometer, with CH_2Cl_2 as an eluant at a flow rate of 1.5 mL/min, or a Waters GPC-120C with THF as an eluant. GPC samples (0.5 wt%) were filtered through a 0.5 μm filter prior to injection. Static light-scattering data were obtained by Glen Heffner and Dale Pearson (UC Santa Barbara). Resonance Raman spectra were obtained using 488 nm excitation from an argon ion laser source. Scans were taken with a power source of 300-330 mW, and each sample was referenced to the known absorption frequencies of a CCl_4 or silicon sample. Samples were polymer films enveloped between two thin glass plates (biological cover slips). No attempt was made to cool the sample during analysis. Thermal analysis was performed under a nitrogen purge on a Perkin Elmer DSC-7, a TGS-2 thermogravimetric analyzer, and a 3600 data station. Infrared spectra of polymer films coated onto NaCl plates were obtained in air on a Perkin-Elmer 1600 Series FTIR.

Materials. For air-sensitive manipulations, the solvents were purified as follows: toluene, benzene, tetrahydrofuran, and diethyl ether were distilled from sodium benzophenone ketyl into solvent flasks equipped with Teflon screw-type valves. Methylene chloride, chloroform, and carbon tetrachloride were distilled from phosphorous pentoxide at atmospheric pressure and subsequently freeze-pump-thaw degassed. Trimethylsilylcyclooctatetraene, trimethylgermylcyclo-octatetraene, and trimethylstannylcyclooctatetraene were prepared as described in the literature.[16] The trimethylstannylcyclooctatetraene was purified to remove bromocyclooctatetraene by preparative vapor-phase chromatography at 120 °C on a 4' x 1/2" column packed with 15% SE-30 on Chromasorb. The tungsten

metathesis catalyst, $W(CH(t\text{-}Bu))(N(2,6\text{-}(i\text{-}Pr)_2C_6H_3)(OCMe(CF_3)_2)_2$, was prepared by literature methods.[12] Scott C. Virgil is gratefully acknowledged for the preparation of catalyst precursors.

***t*-Butylcyclooctatetraene.**[17, 18] $CuI{\cdot}PBu_3$[47] (prepared by Bruce Tiemann) (70.6 g, 0.18 mol) was placed in a 1 L Schlenk flask in an N_2 drybox. Then, under argon, the solid was dissolved in Et_2O (250 mL) and cooled to –40 °C. *t*-BuLi (260 mL, 1.4 M in pentane, 0.36 mol) was then added to the stirred solution via a cannula over ~15 minutes. After stirring at –40 to –30 °C for 75 minutes, BrCOT[14] (8.3 g, 0.045 mol) in Et_2O (100 mL) was added to the purple solution and the resulting mixture was allowed to stir for 7 hours at –50 to –20 °C. At –78 °C, oxygen was bubbled through the black mixture with a long needle for 5 minutes. The mixture was then diluted with Et_2O and hydrolyzed with saturated aqueous NH_4Cl. The aqueous layer was back-extracted with Et_2O twice and the combined organic phases were washed with water, then twice with brine, then again with water. The yellow organic solution was dried over $MgSO_4$, filtered and concentrated on a rotary evaporator. The residue was purified by a crude distillation followed by flash chromatography (pet. ether). One chromatography fraction (1.2 g), determined to be product by GCMS, was subjected to three freeze-pump-thaw degassing cycles and stored under nitrogen in a –20 °C freezer. An earlier fraction containing *t*-butylcyclooctatriene and product was dissolved in benzene containing dichlorodicyanoquinone (~200 mg). The solution was allowed to stir for 20 minutes at room temperature and was then applied to the top of a silica pad on a fritted funnel and washed with petroleum ether (~250 mL). A red band remained on the silica. The eluant was concentrated to a yellow oil (0.8 g), which was determined to be pure product by GCMS. It was degassed by freeze-pump-thawing and stored in a –20 °C nitrogen drybox freezer. The total yield was 27%.

Polymerizations. In a typical polymerization, in a nitrogen-filled drybox, the catalyst W(CH(*t*-Bu))(N(2,6-(*i*-Pr)$_2$C$_6$H$_3$)(OCMe(CF$_3$)$_2$)$_2$[12] (2.5 mg, 3 μmol) was weighed into a vial and dissolved in a minimum amount of THF (~5 μL, ~70 μmol). The monomer (e.g., 83 mg, 470 μmol for poly(TMSCOT)) was weighed into a vial and was then transferred by pipette into the vial containing catalyst. (Pentane (~100 μL) was sometimes added to the solution to give thinner films.) The yellow mixture was agitated with a pipette, and once homogeneous, was coated onto the desired substrate (usually a glass slide.). The solution became darker with time and hardened to a film, which could be removed from the substrate.

NMR data for *cis*-poly(TMSCOT) and poly(Me$_3$GeCOT) were obtained from samples containing both isomers of the polymer. A representative ^{1}H NMR spectrum of *trans*-poly(TMSCOT) is shown in Figure 16. *cis*-poly(TMSCOT): ^{1}H NMR (THF-d_8, 400 MHz) δ 0.14 (s) C*H*$_3$Si, 5.8-7.1 (br m) olefinic protons. *trans*-Poly(TMSCOT): ^{1}H NMR (THF-d_8) δ 0.23 (s, 9H) C*H*$_3$Si, 6.5 (br s, 5H) and 7.0 (br m, 2H) olefinic protons; ^{13}C{^{1}H} NMR (CD_2Cl_2) δ -0.25 (s) CH_3Si, 128-145 (m); IR (film cast on NaCl) 3028 w, 2993 w, 2960 m, 2892 w, 1406 w, 1248 s, 989 m, 836 s, 749 m, 707 w 690 w, 635 w cm^{-1}; elemental analysis, calculated for $(C_{11}H_{16}Si)_n$: C, 74.93; H, 9.14. Found: C, 74.2; H, 8.9. Poly(Me$_3$GeCOT): ^{1}H NMR (THF-d_8, 400 MHz) *trans:* 0.36 (br s); *cis* 0.26-0.29 (br m) C*H*$_3$Ge; *cis* and *trans:* 6-7.2 (br m) olefinic protons; IR (film cast on NaCl) 3027 w, 2970 m, 2907 w, 2801 w, 1410 w, 1235 m, 990 m, 823 s, 746.5 m, 594 s cm^{-1}. Poly(*t*-BuCOT) (both isomers): ^{1}H NMR (C_6D_6, 400 MHz) 1.02-1.09 (br s) C*H*$_3$Si, 6.0-7.0 (br m) olefinic protons. Poly(Me$_3$SnCOT) (both isomers): ^{1}H NMR (C_6D_6, 400 MHz) δ 0.16-0.19 (br unresolved peaks) C*H*$_3$Sn, 6-6.8 (br m) olefinic protons; IR (film cast on NaCl) 2980 m, 2918 m, 2363 m, 1595 w, 991 m, 765 s, 710 m cm^{-1}.

Photoisomerizations.[27] Pyrex- and water-filtered light from a 350 watt, medium pressure, Hanovia mercury lamp was used for most photolyses. Concentrated solutions were cooled either in a clear Pyrex dewar filled with dry ice/isopropanol or a chilled water bath maintained at less than 30 °C. The light from an ELH 250 watt projector bulb was also used for some applications.

Thermal isomerization. In a nitrogen-filled drybox, *cis*-poly(TMSCOT) (3 mg) was dissolved in 6 mL of THF in a flask equipped with a Kontes teflon valve and an attached cuvette (1 mm pathlength) into which an aliquot of the solution could be poured and then diluted by vacuum-transferring solvent from one section of the flask to the other. The solution was then degassed by freeze-pump-thawing, and the solution heated at 80 °C. The reaction mixture was periodically monitored by UV/Visible spectroscopy and was completely isomerized within 2 hours.

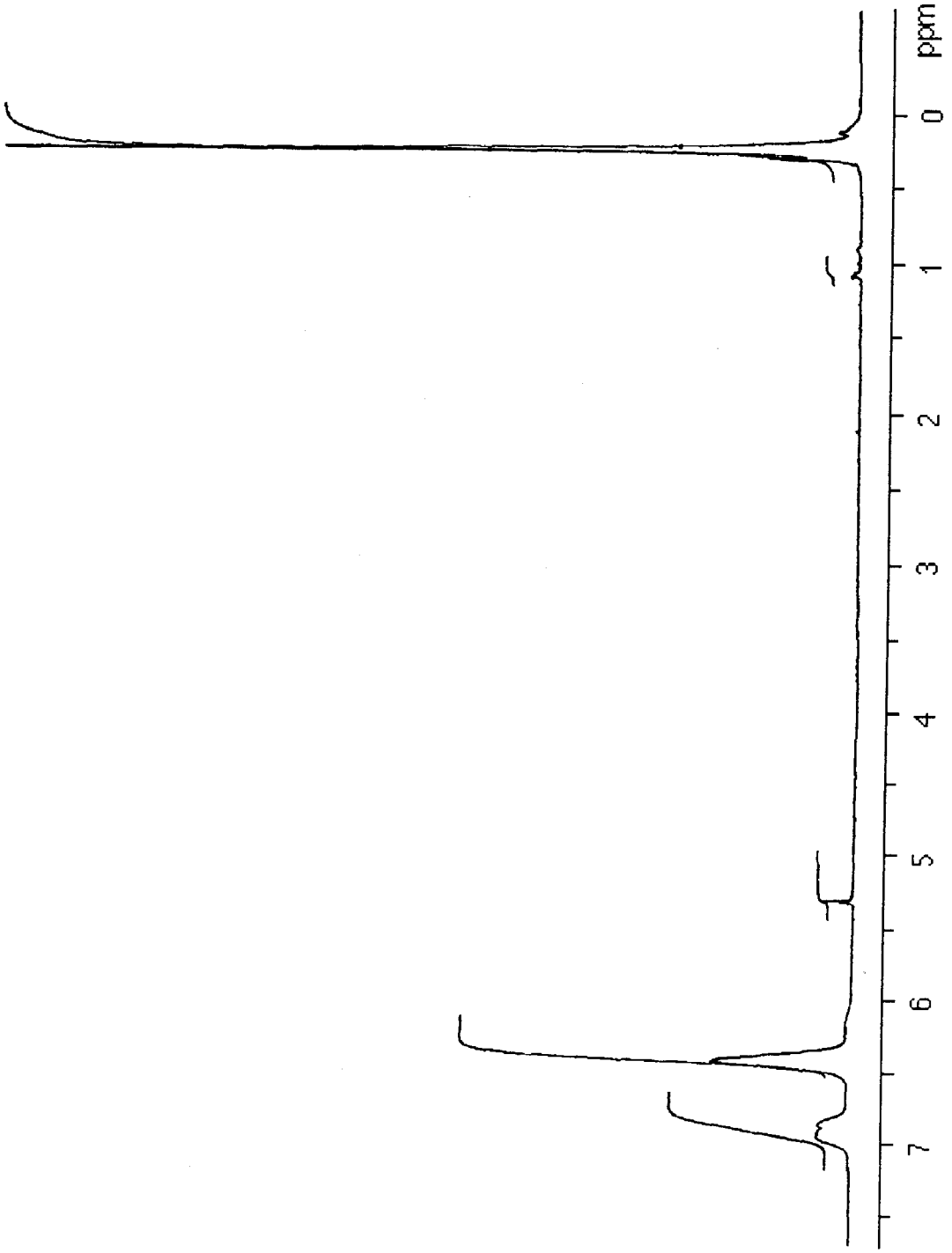

Figure 16. ^1H NMR spectrum (400 MHz) of washed *trans*-poly(TMSCOT) dissolved in CD_2Cl_2.

References and Notes

(1) Ginsburg, E. J.; Gorman, C. B.; Marder, S. R.; Grubbs, R. H. *J. Am. Chem. Soc.* **1989**, *111*, 7621-7622.

(2) Gorman, C. B.; Ginsburg, E. J.; Marder, S. R.; Grubbs, R. H. *Angew. Chem. Adv. Mater.* **1989**, *101*, 1603-1606.

(3) Ginsburg, E. J.; Gorman, C. B.; Grubbs, R. H.; Klavetter, F. L.; Lewis, N. S.; Marder, S. R.; Perry, J. W.; Sailor, M. J. in *Opportunities in Electronics, Optoelectronics, and Molecular Electronics.*; Brédas, J. L., Chance, R. R., Eds.; Kluwer: Dordrecht, the Netherlands, 1990; pp 65-81.

(4) Zeigler, J. M. *Polym. Prepr.* **1984**, *25*, 223-224.

(5) Chien, J. C. W.; Wnek, G. E.; Karasz, F. E.; Hirsch, J. A. *Macromolecules* **1981**, *14*, 479-485.

(6) Klavetter, F. L.; Grubbs, R. H. *J. Am. Chem. Soc.* **1988**, *110*, 7807-7813.

(7) Tlenkopachev, M. A.; Korshak, Y. V.; Orlov, A. V.; Korshak, V. V. *Doklad. Akad. Nauk, Eng. Transl.* **1987**, *291*, 1036-1040 (Original Russian article: pp. 409-413, 1986).

(8) Korshak, Y. V.; Korshak, V. V.; Kanischka, G.; Höcker, H. *Makromol. Chem., Rapid Commun.* **1985**, *6*, 685-692.

(9) Fray, G. I.; Saxton, R. G. *The Chemistry of Cyclo-octatetraene and its Derivatives*; Cambridge University: Cambridge, 1978.

(10) Schroder, G. *Cyclooctatetraen*; Verlag Chemie: Weinheim, 1965.

(11) Schrock, R. R.; Feldman, J.; Cannizzo, L. F.; Grubbs, R. H. *Macromolecules* **1987**, *20*, 1169-1172.

(12) Schrock, R. R.; DePue, R. T.; Feldman, J.; Schaverien, C. J.; Dewan, J. C.; Liu, A. H. *J. Am. Chem. Soc.* **1988**, *110*, 1423-1435.

(13) Paquette, L. A.; Wright III, C. D.; Traynor, S. G.; Taggart, D. L.; Ewing, G. D. *Tetrahedron* **1976**, *32*, 1885-1891 and references therein.

(14) Gasteiger, J.; Gream, G.; Huisgen, R.; Konz, W.; Schnegg, U. *Chem. Ber.* **1971**, *104*, 2412-2419.

(15) BrCOT was polymerized by Klavetter and Grubbs to produce a polyacetylene that is insoluble, but which swells in THF more than does unsubstituted polyacetylene. See Reference 6.

(16) Cooke, M.; Russ, C. R.; Stone, F. G. A. *J. C. Dalton* **1975**, 256-259.

(17) Miller, J. T.; Dekock, C. W.; Brault, M. A. *J. Org. Chem.* **1979**, *44*, 3508-3510.

(18) Miller, M. J.; Lyttle, M. H.; Streitwieser, A., Jr. *J. Org. Chem.* **1981**, *46*, 1977-1984.

(19) Schlund, R.; Schrock, R. R.; Crowe, W. R. *J. Am. Chem. Soc.* **1989**, *111*, 8004-8006.

(20) Wu, Z.; Grubbs, R. H., manuscript in preparation.

(21) Other factors, such as the purity of the monomer, may be responsible for variations in the rate of reaction, which have sometimes been observed. It is hypothesized that when a cold vial containing the monomer is opened in the drybox, small amounts of volatile impurities, such as THF, that are present in the drybox atmosphere, may condense into the vial.

(22) Rao, B. K.; Darsey, J. A.; Kestner, N. R. *Phys Rev. B* **1985**, *31*, 1187-1190.

(23) Spangler, C. W.; Rathunde, R. A. *J. Chem. Soc. Chem. Commun.* **1989**, 26-27.

(24) Lichtmann, L. S.; Ph. D. Dissertation; Cornell University: 1981.

(25) Reference 22, pp. 211-225 and references therein.

(26) Patil, A. O.; Heeger, A. J.; Wudl, F. *Chem. Rev.* **1988**, *88*, 183-200.

(27) In Reference 1, the optical absorption maximum of *trans*-poly(TMSCOT) was reported as 515 nm. This is the value obtained when a 350 watt mercury lamp is used for the photoisomerization (See Figure 7). When white light (either ambient or from a projector lamp) was used, or when a solution was thermally isomerized, the value was found to be ~540 nm.

The reasons for this discrepancy are still not clear. A similar phenomenon has been observed with the other poly(RCOT)s.

(28) Shirakawa, H.; Ikeda, S. *Polymer* **1971**, *21*, 595-596.

(29) Gordon, A. J.; Ford, R. A. *The Chemist's Companion*; Wiley & Sons: New York, 1972; pp 187-211.

(30) Simpson, J. H.; McLaughlin, L.; Smith, D. S.; Christensen, R. L. *J. Chem. Phys.* **1987**, *87*, 3360-3365.

(31) Sklar, L. A.; Hudson, B. S.; Petersen, M.; Diamond, J. *Biochemistry* **1977**, *16*, 813-819 and references therein.

(32) Norris, J.; White, J. W. *Chem. Phys. Lett.* **1983**, *102*, 534-536.

(33) Bott, D. C.; Brown, C. S.; Chai, C. K.; Walker, N. S.; Feast, W. J.; Foot, P. J. S.; Calvert, P. D.; Billingham, N. C.; Friend, R. H. *Synth. Met.* **1986**, *14*, 245-269.

(34) Ito, T.; Shirakawa, H.; Ikeda, S. *J. Polym. Sci. Polym. Chem. Ed.* **1975**, *13*, 1943-1950.

(35) Grubbs, R. H. in *Comprehensive Organometallic Chemistry*; Wilkinson, G., Ed.; Pergamon: New York, 1982; pp 499-551.

(36) Ivin, K. J. *Olefin Metathesis*; Academic: London, 1983.

(37) Sanders, J. K. M.; Hunter, B. K. *Modern NMR Spectroscopy*; Oxford University: New York, 1987; pp 165-167.

(38) Turro, N. J. *Modern Molecular Photochemistry*; Benjamin/Cummings: Menlo Park, CA, 1978; Chapter 12.

(39) Kohler, B. E.; Mitra, P.; West, P. *J. Chem. Phys.* **1986**, *85*, 4436-4440.

(40) Becker, R. S. *Photochem. Photobiol.* **1988**, *48*, 369-399.

(41) The photolyzed polymer is referred to as "trans"; however, it is not assured that this isomer is actually all-trans. Preliminary molecular modeling calculations (Ginsburg, E. J.; Gorman, C. B.; Grubbs, R. H.,

unpublished results) indicate that for the polyenes substituted with large substituents, the trisubstituted double bond might be more stable in the cis configuration. The "trans" polymers might therefore be 75% trans. Ongoing work by Gorman and Grubbs using substituents with better resolved NMR signals, such as *sec*-butyl, is under way to explore this issue more deeply. The preliminary calculations on polyenes containing a cis trisubstituted double bond indicate that the results discussed in Chapter 3 should not be qualitatively different if the polyenes are not all-trans.

(42) Schrock, R. R.; Krouse, S. A.; Knoll, K.; Feldman, J.; Murdzek, J. S.; Yang, D. C. *J. Mol. Cat.* **1988**, *46*, 243-253.

(43) Knoll, K.; Krouse, S. A.; Schrock, R. R. *J. Am. Chem. Soc.* **1988**, *110*, 4424-4425.

(44) Pasto, D. J.; Johnson, C. R. *Laboratory Text for Organic Chemistry*; Prentice-Hall: Englewood Cliffs, NJ, 1979; Chapter 4.

(45) Liu, R. S. H.; Browne, D. T. *Acc. Chem. Res.* **1986**, *19*, 42-48.

(46) Still, W. C.; Kahn, M.; Mitra, A. L. *J. Org. Chem.* **1978**, *43*, 2923-2925.

(47) Kauffman, G. B.; Teter, L. A. *Inorg. Syn.* **1963**, 9-12.

CHAPTER 3

COMPUTATIONAL MODELING OF SUBSTITUTED POLYACETYLENE OLIGOMERS

Introduction[1]

As the results of computational chemistry become more sophisticated, the use of computers to model chemical structures and reactions is becoming an independent discipline of chemistry. A variety of computational programs are now readily available. These programs are being used to obtain geometric, thermodynamic, and electronic information on molecules, both real and hypothetical.[2-8] These data are, in some cases, more accurate than experimental data. Advances in the field are associated with increases in computing speed, since the more sophisticated a chemical computation, the smaller the molecule it can handle in a given amount of computer time. With currently available computer hardware, this makes ab initio routines, the most rigorous calculations in general use, prohibitively slow, or expensive, for molecules as large as those discussed here. This situation will change, but slowly, since advances in computing power are typically arithmetic, while the number of individual calculations required for a molecular simulation increases geometrically with the size of the molecule. Therefore, molecular mechanics programs,[6] the simplest type of molecular simulation, are typically used for large molecules. In 1990, a "large" molecule is one that contains tens of heavy (nonhydrogen) atoms.

Molecular mechanics programs model atoms and bonds as complex balls and springs. Experimental data are used to provide stretching, bending, and twisting force constants and bond lengths for each type of bond; van der Waals radii are specified for each element. These parameters are used in equations that determine the thermodynamic energy of a molecule for any given conformation. For example, various trigonometric functions are used to model torsional potentials of bonds. An example with relevance to modeling polycyclooctatetraenes is the torsional potential used in MM2[9] for a single bond between two double bonds, shown in Figure 1. Other chemical forces, such as

hydrogen bonding and coulombic interactions, are accounted for similarly. The programs are empirical; the parameters are adjusted until the program provides reasonable results for a set of compounds chosen to be representative. Obviously, the choice of compounds used for this optimization process will determine the range of molecules that the program can adequately model.

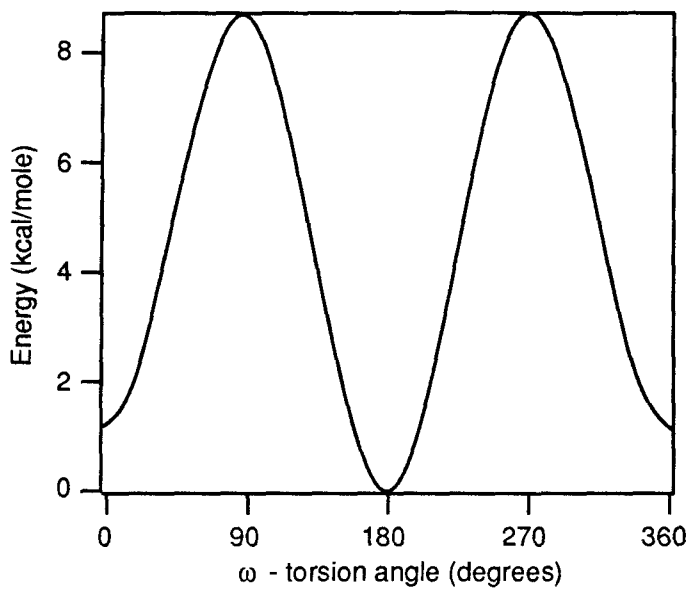

Figure 1. MM2 torsional potential for a single bond between two double bonds ($C(sp^2)=C(sp^2)-C(sp^2)=C(sp^2)$) described by Equation 1.[10] Note that the *total* twisting potential for this bond contains steric factors which are included through separate equations that describe nonbonded interactions.

To find molecular conformations of lowest energy, the program uses one of a few available search routines to explore conformational space. The energy is calculated for each new conformation that is generated, and the program aims for the conformation at the bottom of a potential well. The simplification of treating a molecule as a purely mechanical object allows reasonable approximations to the conformational minima and heats of formation of large molecules to be found in a feasible amount of processing time. The accuracy of the technique

is quite good within certain limits and is improving as new experimental data is parameterized.[7, 11, 12]

$$E = [0.625(1 + \cos\omega) + 4(1 - \cos 2\omega)] \quad (1)$$

In contrast to molecular mechanics, ab initio and semiempirical routines calculate the energies and shapes of molecular orbitals explicitly. These programs yield electronic as well as geometric and thermodynamic information. Semiempirical programs (those developed by Dewar are used most extensively[8, 13]) are faster than ab initio methods because they consider only valence electrons, use a simpler (unvaried) basis set of orbitals, and neglect a number of calculation-intensive overlap integrals. Just as in molecular mechanics, the accuracy of semiempirical programs is improved by adjusting parameters (sizes of atomic orbitals and values of specific overlap or resonance integrals) to best fit the program's results to a certain body of experimental data. Although potentially more accurate and more informative than molecular mechanics, semiempirical and (especially) ab initio programs are much slower. With currently available hardware, molecular mechanics calculations on a molecule with 200 atoms may be completed in approximately an hour of processor time, whereas semiempirical calculations can take about an order of magnitude longer and ab initio programs are slower still.

Other researchers have reported molecular calculations on substituted conductive polymers.[14-16] Thémans et al. examined 3-alkyl derivatives of oligothiophenes using MNDO.[15] They found little perturbation of the backbone geometry or electronic properties by the substituent, although this result may not be reliable, since MNDO does not treat torsions in conjugated systems accurately.[17] Highly substituted polyacetylenes were modeled by Leclerc and

Prud'homme using a molecular mechanics approach.[16] The backbone of poly(methylacetylene) was found to be much less twisted than that of poly(*t*-butylacetylene). They concluded that their results, along with the experimental results of Ciardelli et al.,[18] imply that chain geometry is most affected by substitution at the first carbon of a substituent. These polymers differ from the polycyclooctatetraenes in that the more highly substituted polyacetylenes should have appreciable substituent-substituent interactions (Figure 2 and Chapter 1, Figure 2).

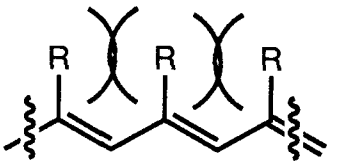

Figure 2. Steric interactions between side groups in a polymer made from a monosubstituted acetylene.[16, 19]

Molecular mechanics calculations have been used in this project to complement and, to some extent, quantify chemical intuition.[20] In particular, a correlation between the solubility properties and the structures of the trans polymers has been sought. An examination of the structure of a polyene chain with widely spaced substituents indicates that the 1,3-interactions between the substituent and adjacent protons should influence the conformation of the backbone. These 1,3-interactions are similar to those experienced by a substituent in the axial position of a monosubstituted cyclohexane (Figure 3). The free energy change associated with moving a substituent from an axial to a less congested equatorial position of a cyclohexane ring, termed an *A*-value,[21] should thus be related to the substituent's size as manifested on a polyene chain. Table 1 divides some substituted polycyclooctatetraenes that have been studied[22-25] into two classes on the basis of their solubility in the trans form.

"Soluble" in this case means that concentrations of at least 1 mg/mL are easily obtained. The *A*-values of the various substituents are also listed. Aside from R = phenyl, those substituents with *A*-values larger than ~2 kcal/mol are soluble. It is not unexpected that the phenyl group is the exception, since in a polyene chain the phenyl ring can rotate out of the plane of the backbone to avoid interactions between the protons in the ortho position and those on the chain. However, in phenylcyclohexane, the phenyl ring and the two axial protons are not colinear, so it is not possible for the phenyl ring to twist out of the way. To explore the connection between substituent size and polyene chain conformation more explicitly, polycyclooctatetraene oligomers were examined computationally.

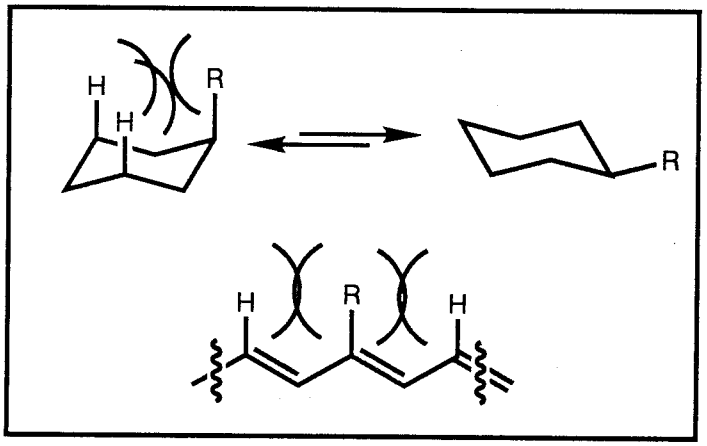

Figure 3. Steric interactions important for determining *A*-values (top), and those found in trans-transoid substituted polyenes.

Table 1. Soluble and insoluble *trans*-poly(RCOT)s and *A*-values of the different substituents.

Soluble		Insoluble	
R	*A*-Value (kcal/mol)	R	*A*-Value
i-Pr[25]	2.1[26]	H	0
t-Bu[23]	>4.5[26]	*n*-Bu[23]	1.8 (Et)[26]
s-Bu[23]	–	MeO[25]	0.6[26]
(1-alkoxy)-2-propyl[27]	–	Me_3Sn	0.94,[28] 1.06[29]
Me_3Si[24]	2.4 - 2.6[30]	phenyl[23]	3.1[26]
		Br[31]	0.48[26]

Results

The substituted polyacetylenes were generally modeled as trimers (Figure 4).[32] Molecular mechanics calculations on molecules of this size do not require inordinate amounts of computer time, and yet the model should be large enough to represent adequately a much longer polymer. The central substituent of the trimer model is assumed to represent a typical substituent in the middle of a long polymer chain, where any effects that might result from being near a chain end are negligible.

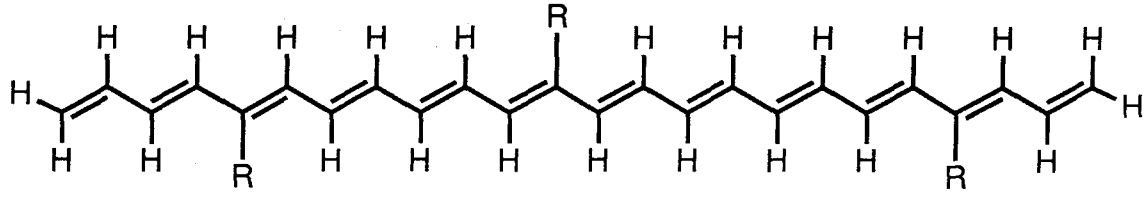

Figure 4. All trans trisubstituted tetracosadodecaene (a polycyclo-octatetraene trimer) used for molecular mechanics simulations.[32]

In pure molecular mechanics programs, such as Batchmin (a batch mode version of Macromodel[33]) with the MM2 force field,[9] effects resulting from extended conjugation are neglected. In a polyene, all double bonds will have the

same equilibrium bond length, and all single bonds located between double bonds will have the same torsional barrier regardless of the length of the extended π-system. (See Figure 1.) It has been found that these approximations are not too grotesque.[10, 34, 35] Some preliminary calculations were done in which these assumptions were not made (see the Experimental Section); however, initial results obtained with this procedure (using PCModel[36]) on substituted polyenes were subsequently found to be qualitatively similar to those obtained with the MM2 force field used in the program Batchmin.[33] Therefore, all subsequent molecular mechanics calculations employed Batchmin, since the other routine was readily available only on prohibitively slow hardware.

Minimized structures of a variety of trimers are shown in Figures 5-10. These were generated with Allinger's MM2 force field,[9] using the Batchmin program. Since complete molecular mechanics parameters are not yet available for tin,[37] the force field was modified to obtain Figure 11. The tin atom was modeled as being identical to silicon but with 0.3 Å longer bonds to carbon. This is certainly an oversimplification, since the bending, stretching and nonbonded parameters should also be different.

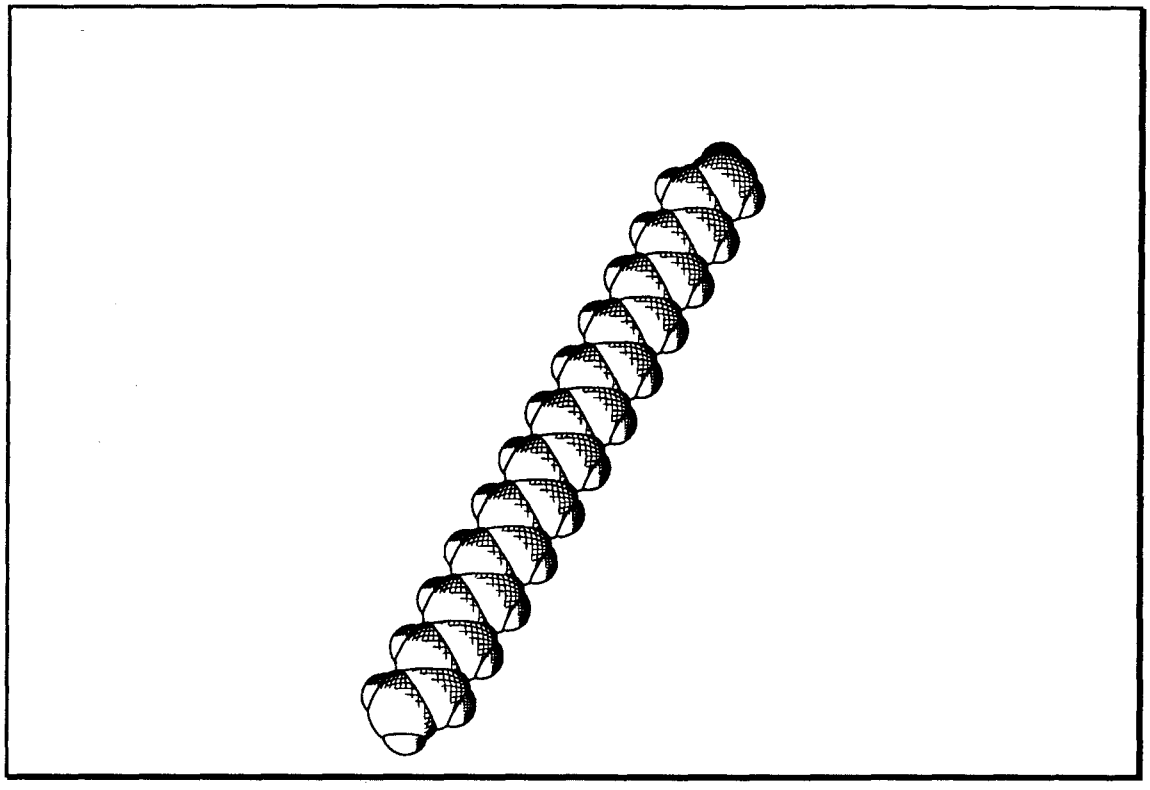

Figure 5. Polyacetylene.

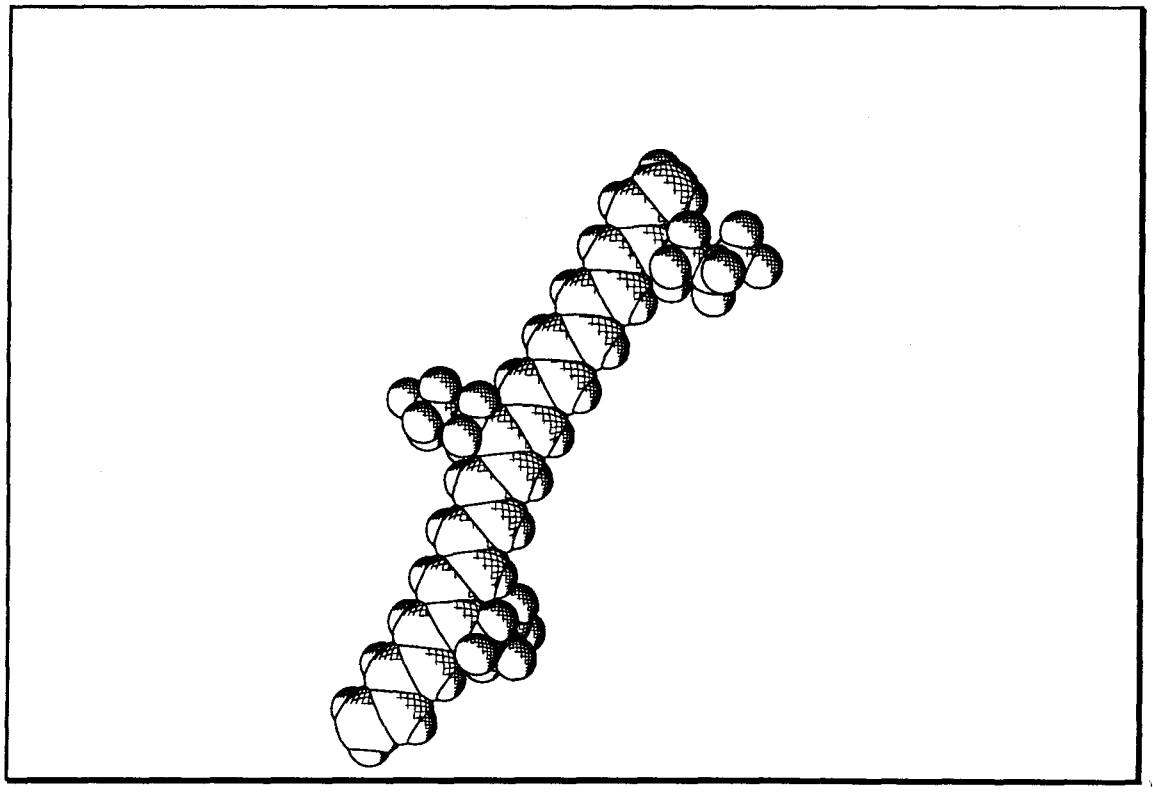

Figure 6. Poly(*n*-butylcyclooctatetraene).

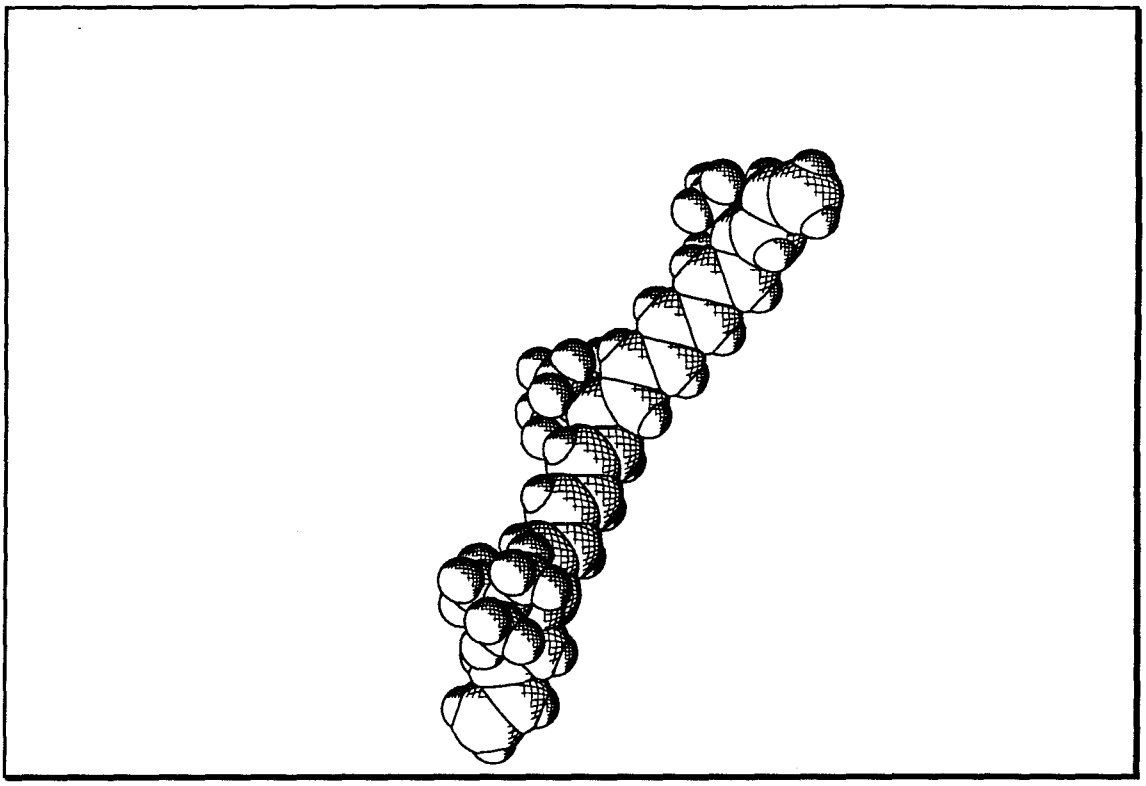

Figure 7. Poly(*t*-butylcyclooctatetraene).

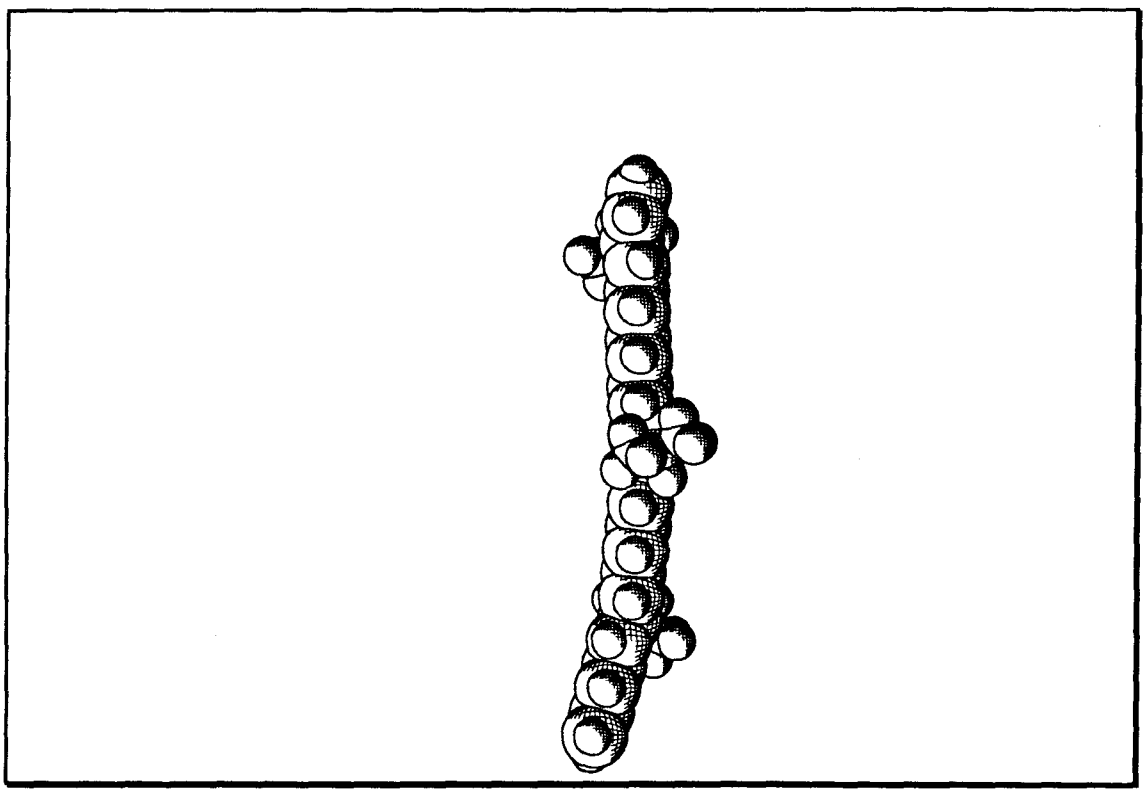

Figure 8. Poly(*i*-propylcyclooctatetraene).

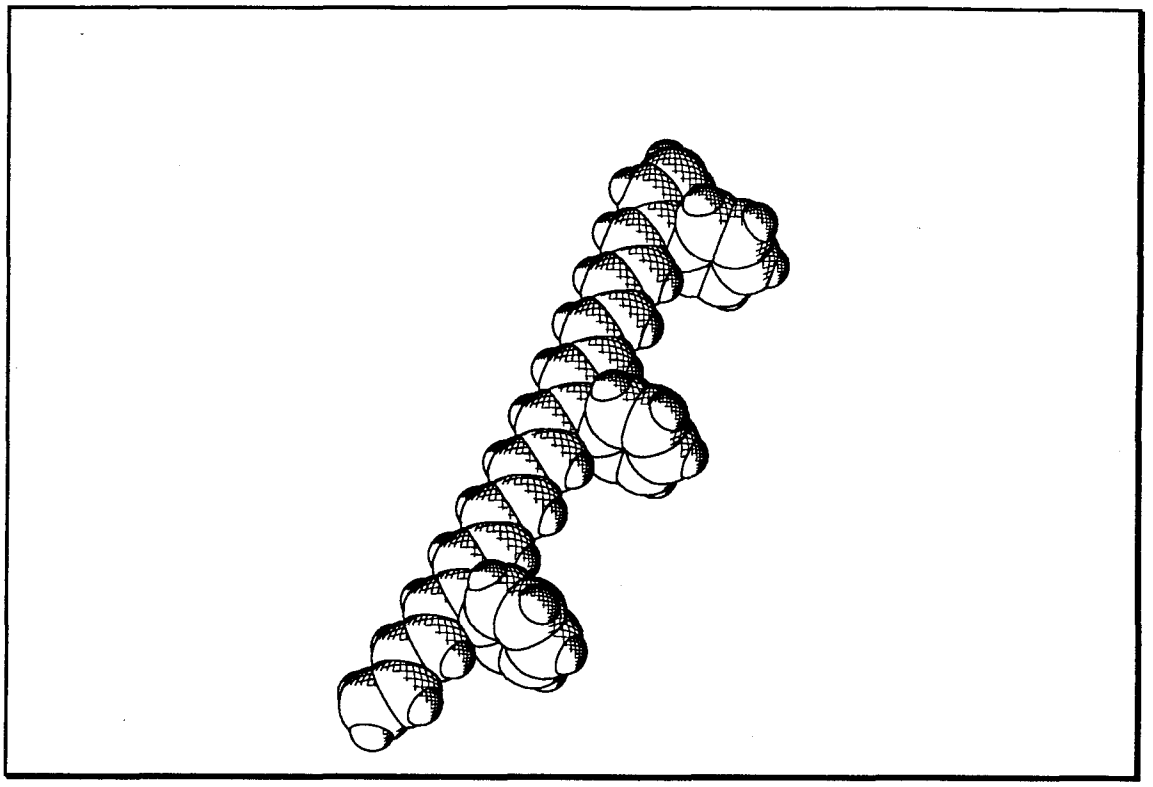

Figure 9. Poly(phenylcyclooctatetraene).

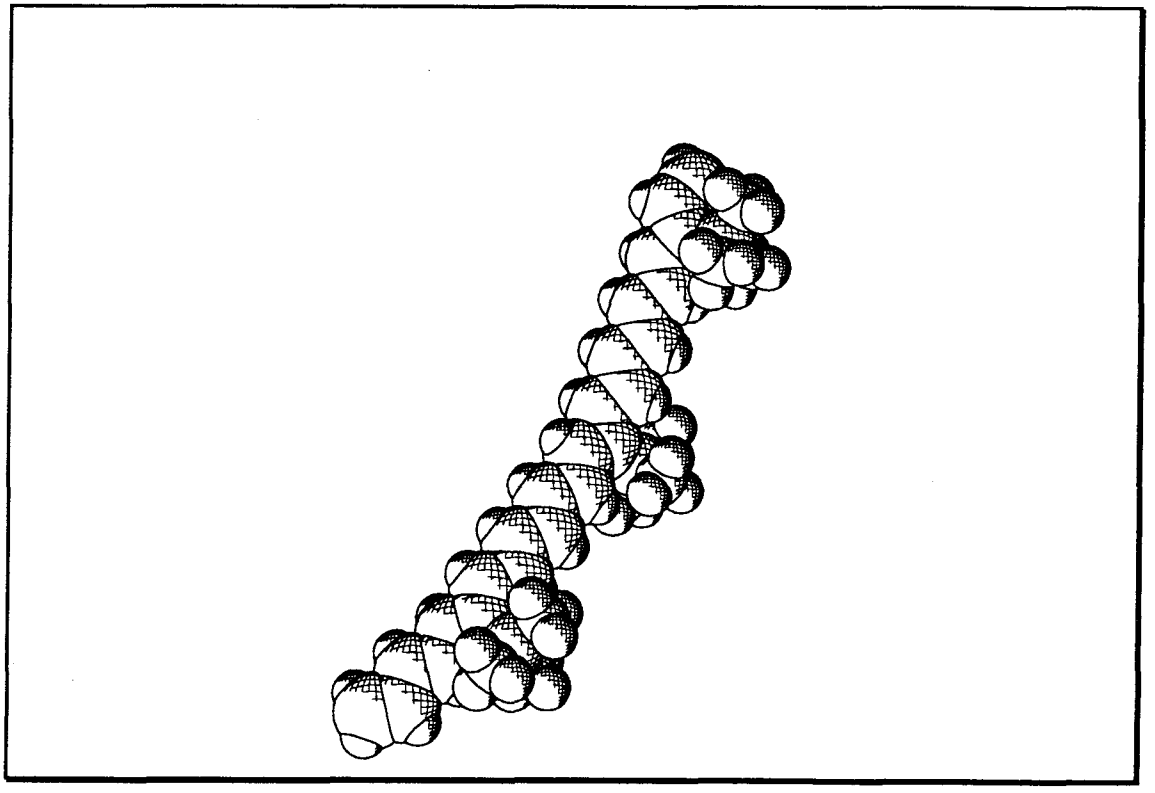

Figure 10. Poly(trimethylsilylcyclooctatetraene).

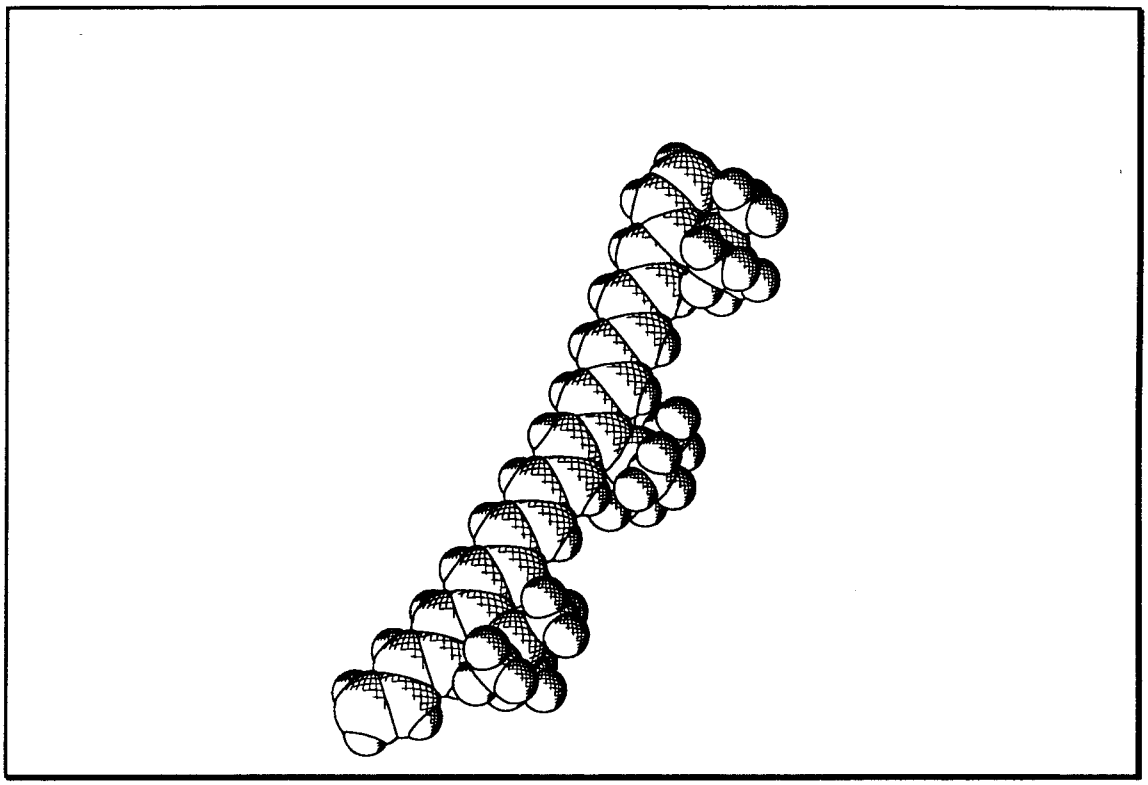

Figure 11. Poly(trimethylstannylcyclooctatetraene) (see text).

The feature of interest in these minimized structures is the varying degree of twist about the single bonds adjacent to the double bond carrying the substituent. The computed dihedral angles (θ_1 and θ_2, Figure 12) (defined to equal 0° at the eclipsed conformation) about these two single bonds are tabulated in Table 2. A comparison with the *A*-values shown in Table 1 indicates that the two parameters do show similar trends. Those polymers with $\theta_1 < 160°$ and $\theta_2 < 170°$ are soluble.

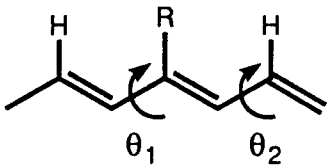

Figure 12. The dihedral angles θ_1 and θ_2.

Table 2. Dihedral angles (defined to equal 0° at the eclipsed conformation) for single bonds about the central substituted double bond for a series of poly(RCOT) trimers computed with MM2 using Batchmin.

R	θ_1	θ_2 (degrees)
H	180	180
n-butyl	174	174
i-propyl[25]	158	167
s-butyl	158	168
t-butyl	127	166
methoxy[20]	180	174
phenyl[a]	173	176
Me_3Si	152	167
Me_3Sn[b]	163	172

(a) The phenyl group is twisted 65° out of the plane of the backbone. (b) Modeled by substituting tin-carbon bond lengths of 2.11 Å for the carbon-silicon bond lengths in the MM2 force field.

It should be emphasized that the precise values found for the twist angles are not intended to be accurate. The approximation of using the same torsional barriers for all the backbone single bonds and the dependence of the angle on a balance between torsional and steric interactions combine to make the exact angle very sensitive to the parameters chosen. Given experimental and computational uncertainty concerning the position of even the minimum energy conformers, much less the full torsional potential, of 1,3-butadiene,[38] the computational results presented here must be thought of as approximations. To get a sense of the dependence of a torsion angle on the particular parameters used, the dihedral angle about the central bond in 2-*t*-butyl-1,3-butadiene was computed with MM2 (Macromodel), using different values for the torsional parameters shown in Equation 2. Equation 2 is simply a general form of

Equation 1. The force field used to calculate the results presented above[33] uses the values $B = 1.25$ and $C = 8.0$; MM2(85) uses –0.93 and 8.0.[39]

$$E = (0.5)[B(1 + \cos\omega) + C(1 - \cos 2\omega)] \qquad (2)$$

Table 3. Computed dihedral angles (defined as 0° at the eclipsed conformation) for the single bond of 2-*t*-butyl-1,3-butadiene for different values of *B*, *C*. (See Equation 2.) The parameters in the third row are the defaults in the MM2 force field of Macromodel;[33] those in the last row are used in MM2(85).[39] The minimizations were performed using Macromodel.[33]

B	*C* (kcal/mol)	θ (degrees)
1.25	7	154.3
1.25	7.5	160.6
1.25	8	167.8
1.25	8.5	178.6
1.25	9	179.6
–0.93	8	167.5

Some geometry optimizations were also performed on the poly(RCOT)s using the semiempirical MOPAC program with AM1 parameters.[8] The data in Table 4 indicate that the semiempirical results are qualitatively similar to those obtained with the molecular mechanics calculations for the series of butyl-substituted polymers. Across the Me_3M series, the trend is less clear. The *t*-butyl oligomer is much more twisted than the silyl-, germyl-, and stannyl-substituted molecules, which are twisted to about the same extent.

Table 4. Dihedral angles (defined to equal 0° at the eclipsed conformation) for single bonds about the central substituted double bond for a series of poly(RCOT) trimers computed with AM1 parameters using AMPAC.

R	θ_1	θ_2 (degrees)
H	180	180
n-butyl	179	179
s-butyl	154	164
t-butyl	115	161
Me_3Si	142	170
Me_3Ge	148	164
Me_3Sn	142	165

Molecular Dynamics. One issue that has not yet been addressed is the extent to which the solubility-inducing kink is a static or a dynamic phenomenon. (See the discussion of solubility in Chapter 1). The question remains: Are the substituted polycyclooctatetraenes rigid, but kinked, molecules or does the attachment of substituents make the backbone flexible by providing hinge points about which the polymer rotates? In the absence of experimental data, molecular dynamics calculations, which are used to explore the evolution of molecular motion over time,[40, 41] can provide some insight. A few molecular dynamics simulations of the same trimers used in the molecular mechanics calculations discussed above have been conducted. The structures were held at 300 K for a simulated 20 picoseconds. The torsion angle, θ_1, was sampled every 20 femtoseconds. Figure 13 shows the total distribution of torsion angles sampled over 20 ps in molecular dynamics simulations at 300 K of three different polycyclooctatetraene trimers. In general, the dihedral angles remain close to transoid planarity (180°) during the run. The *s*-butyl oligomer rocks from side to

side, spending the major part of the time at 150°-160° angles, without dwelling in the planar conformation nearly as long as does the *n*-butyl substituted molecule. The behavior of the *t*-butyl oligomer is different. The bond alternates between a transoid ($|180°| \leq \theta_1 \leq |90°|$) and a cisoid ($|90°| \leq \theta_1 \leq |0°|$) structure. During the run tabulated in Figure 13, the *t*-butyl substituent never flipped over to the opposite side; that is, having been started with a "negative" dihedral angle, it never passed through the planar conformation to the "positive" side. In longer runs or at higher temperatures, the *t*-butyl substituent will eventually move to the other side.

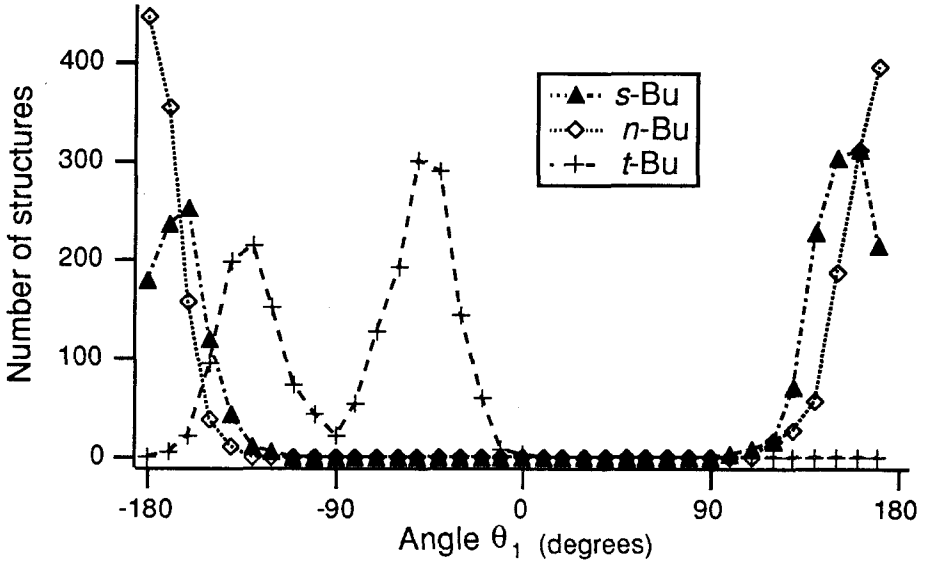

Figure 13. Values of torsion angle θ_1 at 10 fs intervals accumulated during a 20 ps molecular dynamics run at 300 K (Batchmin).[33]

Discussion

A key assumption is incorporated into the models that have been chosen. The R groups are placed far apart, i.e. never in a 1,3-relationship to one another, on the assumption that for steric reasons, the trisubstituted olefin of the monomer can be considered unreactive during the polymerization.[42, 43] The

substituted bond would have to be reactive for the substituents to end up close to one another. (See the ROMP mechanism in Chapter 1, Figure 3.) If this assumption is not warranted, then it is possible that substituent-substituent effects at 1,3-disubstituted points along the chain substantially contribute to polymer properties. Unfortunately, a method for determining the spacing of the substituents along the polycyclooctatetraene backbone has not yet been devised.

In any case, the different computational methods employed, as well as the experimental results presented in Chapter 2, are all consistent with the steric requirements of the side group being the major determinants of the polymer properties. There is a correlation between the computed twist angles, θ_1 and θ_2, and the solubility properties. Only those polymers computed to have a sufficiently kinked π system are totally soluble in the trans form. Polymers with side groups, such as the trimethylstannyl, phenyl, and *n*-alkyl substituents, that do not twist the chain significantly are not totally soluble in the trans form. To date, only polymers with groups that are substituted at the α-atom, such as *iso*-propyl,[25] trimethylsilyl or *sec*-butyl have been found to be soluble. However, α-substitution is not sufficient for solubility as evidenced by the insoluble *trans*-poly(Me_3SnCOT). The trimethylstannyl group, because of the long carbon-tin bond length, is distanced from the chain, reducing its effective size. The correlation between solubility and structure illustrated by the set of poly(RCOT)s is significant, because it implies that a compromise must be made between planarity and solubility. While it is possible that this compromise may be avoided by placing a very flexible substituent on the chain so that the side group's entropy of dissolution carries the rest of the chain into solution, this tactic has not succeeded with poly(*n*-octadecylcyclooctatetraene)[20] and poly[(2-ethylhexyl)cyclooctatetraene],[25] both of which are insoluble in the trans form. These

two polymers indicate that implementation of the "bound solvent" approach[44] is not straightforward for polyenes.

The realization that a kink in the chain is necessary for solubility provides a recipe for synthesizing a soluble polyacetylene. As a general rule, a new polycyclooctatetraene should be soluble if calculations indicate that its twist angles are comparable to those of polymers already known to be soluble. This idea was exploited by Moore et al. in the design and synthesis of chiral polyacetylenes.[27] Other properties, such as water-solubility (Figure 14), could be conveyed to soluble polyacetylenes by attaching the appropriate functional group to a chain-twisting moiety.

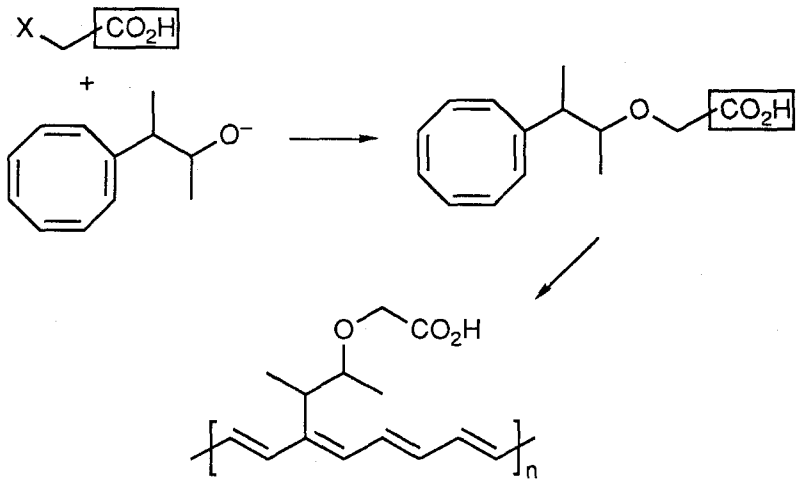

Figure 14. A possible route to a water-soluble polyacetylene, designed on the principle that any polycyclooctatetraene with a *sec*-butyl substituent will be soluble.[27] (The carboxylate must be protected to avoid reaction with the nucleophilic tungsten alkylidene.)

Summary

The calculations presented here support the hypothesis that the polycyclo-octatetraene chains are twisted slightly by the addition of sufficiently large side

groups. Moreover the solubility properties and the effective conjugation length of a given substituted polycyclooctatetraene may be predicted qualitatively from the relative magnitude of the twist found in the structures minimized with molecular mechanics programs. Also, molecular dynamics calculations imply that the polymers are somewhat rigid. The polymer chromophore may thus be thought of as a long run of double bonds containing irregularly spaced kinks. These kinks serve to render the polymer soluble, but also disrupt conjugation somewhat, making the effective conjugation length shorter than the actual number of double bonds in conjugation.

Experimental Section

MM2. MM2 calculations were performed using Batchmin[33] Version 3.1b (on a DEC MicroVax 3500) or Version 2.6 (on a Silicon Graphics Iris 4D/220GTX workstation). Macromodel, Version 3.0,[45] was used for the 2-*t*-butylbutadiene calculations in which the force field was varied. In all other MM2 calculations, the default force field was used, except for the simulation of poly(Me_3SnCOT), in which case the C2-Si and C3-Si equilibrium bond lengths were changed to 2.11 Å. The derivatives convergence criterion was employed, with convergence defined to be when the root mean square of the first derivative reached 0.1. A typical command file, run on the Iris, is shown below.

```
filename.dat
filename.out
DEBG        28      102
#1=mm2 2=charmm 3=amber 5=opls/a
FFLD        1
READ
CONV        2       1
MINI        3       0       1000
```

π-Calculations. Programs are available that do Hückel π calculations in an iterative manner with molecular mechanics geometry optimization.[12] In this technique, bond orders calculated with the π calculation for a given geometry are used to adjust molecular mechanics torsional potentials; the geometry calculated by the molecular mechanics routine is, in turn, used to calculate new bond orders. The calculation shuttles back and forth in this fashion until specified convergence criteria are met. (These routines exist primarily because older molecular mechanics programs were unable to differentiate between the single and double bonds of a conjugated system, so the bond orders had to be calculated first. Newer programs, such as Macromodel, are equipped to read input that explicitly gives bond orders, so the calculation is not necessary.) Some preliminary calculations on substituted polyenes were done with this procedure using PCModel (Serena Software) on an Apple Macintosh II personal computer.

AM1. Semiempirical calculations were done using AM1 version 1.00[8] on a DEC MicroVax 3500. The AM1 Hamiltonian was employed. The minimization output usually included the message: "Gradient test not passed, but further work not justified. SCF field was achieved."

Molecular Dynamics.[40] Molecular mechanics force fields are used, but instead of searching for the lowest energy (0 K) structure, the geometry of the molecule is adjusted to keep the temperature at a specified (nonzero) value. At a finite temperature, the atoms have finite velocities, which are monitored. The kinetic energy that is due to atomic motion and the potential energy that is due to

the constraints of the force field are calculated at specified intervals. Algorithms have been developed to keep the system at a specified temperature, within a certain level of random fluctuation, given constraints such as bond lengths and bond angles.[41]

Molecular dynamics calculations were run at 300 K for 20 ps using Batchmin.[33] A typical command file for molecular dynamics on the Iris computer (Batchmin Version 2.6) is shown below.

```
filename.dat
filename.out
DEBG        28        102
#1=mm2 2=charmm 3=amber 5=opls/a
#OPCD   IIIII     IIIII     IIIII     IIIII     FFFFF.FFFF     FFFFF.FFFF
FFLD        1
READ
MDIT                                                 300.
MDBT                                                 300.
MDMT
MDSA        0         500
MDYN        1                                          1.              20.
WRIT
```

References and Notes

(1) Much of this work was done in close cooperation with Christopher B. Gorman.

(2) Trinajstic, N. *Theochem* **1989**, *59*, 219-224.

(3) Kollman, P. A.; Merz, K. M., Jr. *Acc. Chem. Res.* **1990**, *23*, 246-252.

(4) Schaefer, H. F. *Science* **1986**, *231*, 1100-1107.

(5) Houk, K. N.; Paddon-Row, M. N.; Rondan, N. G.; Wu, Y.; Brown, F. K.; Spellmeyer, D. C.; Metz, J. T.; Li, Y.; Loncharich, R. J. *Science* **1986**, *231*, 1108-1117.

(6) Burkert, U.; Allinger, N. *Molecular Mechanics (ACS Monograph 177)*; American Chemical Society: Washington, DC, 1982.

(7) Allinger, N. L.; Yuh, Y. H.; Lii, J. H. *J. Am. Chem. Soc.* **1989**, *111*, 8551-8566.

(8) Dewar, M. J. S.; Zoebisch, E. G.; Healy, E. F.; Stewart, J. J. P. *J. Am. Chem. Soc.* **1985**, *107*, 3902-3909.

(9) Allinger, N. L. *J. Am. Chem. Soc.* **1977**, *99*, 8127-8134.

(10) Allinger, N. L.; Lii, J. H. *J. Comput. Chem.* **1987**, *8*, 1146-1153.

(11) Engler, E. M.; Andose, J. D.; Schleyer, P. v. R. *J. Am. Chem. Soc.* **1973**, *95*, 8005-8025.

(12) Kao, J.; Allinger, N. L. *J. Am. Chem. Soc.* **1977**, *99*, 975-986.

(13) Dewar, M. J. S.; Thiel, W. *J. Am. Chem. Soc.* **1977**, *99*, 4899-4907.

(14) Cernia, E.; D'Ilario, L. *J. Polym. Sci.: Polym. Chem. Ed.* **1983**, *21*, 2163-2176.

(15) Thémans, B.; André, J. M.; Brédas, J. L. *Synth. Met.* **1987**, *21*, 149-156.

(16) Leclerc, M.; Prud'homme, R. E. *J. Polym. Sci.: Polym. Phys. Ed.* **1985**, *23*, 2021-2030.

(17) Clark, T. *A Handbook of Computational Chemistry*; Wiley: New York, 1985.

(18) Ciardelli, F.; Lanzillo, S.; Pieroni, O. *Macromolecules* **1974**, 174-179.

(19) Masuda, T.; Higashimura, T. *Adv. Polym. Sci.* **1986**, *81*, 121-165.

(20) Gorman, C.; Ginsburg, E.; Marder, S.; Grubbs, R. *Polym. Prepr.* **1990**, *31*, 386-387.

(21) Winstein, S.; Holness, N. J. *J. Am. Chem. Soc.* **1955**, *77*, 5562-5578.

(22) Ginsburg, E. J.; Gorman, C. B.; Grubbs, R. H.; Klavetter, F. L.; Lewis, N. S.; Marder, S. R.; Perry, J. W.; Sailor, M. J. in *Opportunities in Electronics, Optoelectronics, and Molecular Electronics.*; Brédas, J. L. Chance, R. R., Eds. Kluwer: Dordrecht, the Netherlands, 1990; pp 65-81.

(23) Gorman, C. B.; Ginsburg, E. J.; Marder, S. R.; Grubbs, R. H. *Angew. Chem. Adv. Mater.* **1989**, *101*, 1603-1606.

(24) Ginsburg, E. J.; Gorman, C. B.; Marder, S. R.; Grubbs, R. H. *J. Am. Chem. Soc.* **1989**, *111*, 7621-7622.

(25) Gorman, C. B.; Grubbs, R. H. unpublished results.

(26) Carey, F. A.; Sundberg, R. J. *Advanced Organic Chemistry: Part A - Structure and Mechanisms*; Plenum: New York, 1977; Chapter 3.

(27) Moore, J. S.; Gorman, C. B.; Grubbs, R. H. *J. Am. Chem. Soc.* in press.

(28) Moder, T. I.; Hsu, C. C. K.; Jensen, F. R. *J. Org. Chem.* **1979**, *45*, 1008-1010.

(29) Kitching, W.; Doddrell, D.; Grutzner, J. B. *J. Organomet. Chem.* **1976**, *107*, C5-C10.

(30) Kitching, W.; Olszowy, H.; Drew, G. M.; Adcock, W. *J. Org. Chem.* **1982**, *47*, 5133-5156.

(31) Klavetter, F. L.; Grubbs, R. H. *J. Am. Chem. Soc.* **1988**, *110*, 7807-7813.

(32) For a cautionary note on the selection of an all trans structure, see Reference 41 of Chapter 2.

(33) Still, W. C., Columbia University.

(34) Tai, J. C.; Allinger, N. L. *Tetrahedron* **1981**, *37*, 2755-2761.

(35) Goddard, W. A. personal communication.

(36) Gilbert, K. E.; Gajewski, J. J. Serena Software.

(37) Allinger, N. L.; Quinn, M. I.; Chen, K.; Thompson, B.; Frierson, M. R. *J. Mol. Struct.* **1989**, *194*, 1-18.

(38) Fisher, J. J.; Michl, J. *J. Am. Chem. Soc.* **1987**, *109*, 1056-1059 and references therein.

(39) Liljefors, T.; Tai, J. C.; Li, S.; Allinger, N. L. *J. Comp. Chem.* **1987**, *8*, 1051-1056.

(40) Gunsteren, W. F. v.; Berendsen, H. J. C. *Angew. Chem. Int. Ed. Engl.* **1990**, *29*, 992-1023.

(41) Ryckaert, J. P.; Ciccotti, G.; Berendsen, H. J. C. *J. Comp. Phys.* **1977**, *23*, 327-341.

(42) Ivin, K. J. *Olefin Metathesis*; Academic: London, 1983.

(43) Grubbs, R. H. in *Comprehensive Organometallic Chemistry*; Wilkinson, G., Ed.; Pergamon: New York, 1982; pp 499-551.

(44) Ballauff, M. *Angew. Chem. Int. Ed. Engl.* **1989**, *28*, 253-267.

(45) Still, W. C. Columbia University, 1990.

Chapter 4

An Overview of Electrochemical and Optical Investigations of Substituted Polycyclooctatetraene Films

Abstract

In the last two chapters, evidence was presented to show that the steric bulk of the trimethylsilyl side chain in poly(TMSCOT) is sufficient to twist the polymer backbone, rendering it soluble, but is not so large that conjugation along the chain is completely interrupted. The combination of processability and extended conjugation that result from this happy balance makes the polymer well-suited for a number of investigations. This chapter will summarize studies of poly(trimethylsilylcyclooctatetraene) as a material for electronic and nonlinear optical applications. Chemical doping of the polymer will be discussed, as well as preliminary electrochemical data. Also, a brief account of Schottky-type solar cells prepared with the polymer by Dr. Michael J. Sailor et al.[1] and of nonlinear optical properties determined by Dr. Joseph W. Perry[2] will be given.

Electrical Conductivity and Doping

Introduction. Conjugated polymers are most often acclaimed for their ability to conduct electricity upon oxidation or reduction.[3-5] This process is called "doping" in analogy to semiconductor technology, but unlike semiconductors, conjugated polymers undergo substantial chemical changes upon doping.[6] After doping, the polymer contains a substantial weight percentage of dopant, which causes changes in the packing of the chains[7] and in the properties of the material. Bulk electrical conductivity arises from the delocalized mobile negative or positive charges that the addition or removal of electrons creates (Figure 1).[8, 9] These charge carriers travel along and hop between the polymer chains. The hopping process remains poorly understood, but is thought to limit the passage of charge through a film. Doped polyacetylene is oxidatively doped with iodine to conductivities of $\sim 10^2\ \Omega^{-1}$ cm^{-1}, a value similar to that of intrinsic germanium.[10-12] Recently, Naarman has

reported a technique for synthesizing oriented polyacetylene with few defects to obtain doped polymers with conductivities of $10^5\ \Omega^{-1}\ cm^{-1}$, making it twice as conductive as copper on a per-weight basis.[13] The combination of light weight and high conductivity has sparked interest in polyacetylene and other conducting polymers for use in plastic batteries that would rely on the doping process as a means to store charge.[14]

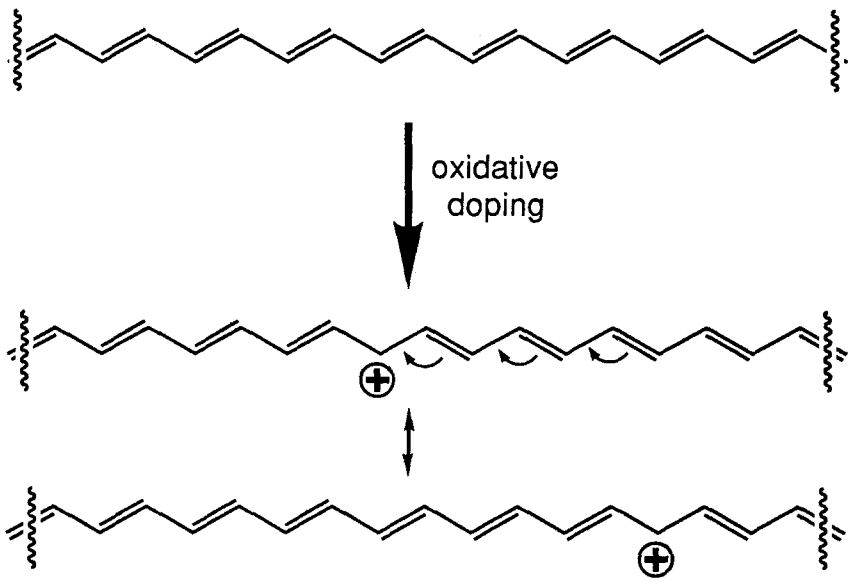

Figure 1. Oxidative doping of polyacetylene to create a mobile cationic center.

Redox Chemistry. The polymer films were doped by exposing them to iodine vapor *in vacuo,* then pumping to remove excess iodine. The polymer was found to be unstable, becoming colorless, when sodium benzophenone ketyl was tested as a potential reductive doping agent. The conductivity of iodine-doped *cis*-poly(TMSCOT) films, measured in a nitrogen atmosphere using a four-point probe,[15] was found to be less than $10^{-5}\ \Omega^{-1}\ cm^{-1}$. In contrast to unsubstituted *cis*-polyacetylene, which is known to isomerize to the trans form upon doping[16] to give conductivities of $10^2\ \Omega^{-1}\ cm^{-1}$, the conductivity of poly(TMSCOT) increased

only after photochemical conversion to the trans isomer.[17] Photoisomerized doped *trans*-poly(TMSCOT) films conduct electricity at 10^{-1} to 1 Ω^{-1} cm^{-1}. Apparently, *cis*-poly(TMSCOT) does not isomerize upon doping. The reasons for this are still unclear. It remains to be determined whether there is a difference in the ability of iodine to diffuse into the polymers, or whether the oxidation potential of *cis*-poly(TMSCOT) is too high for iodine doping. Preliminary electrochemical experiments on *cis*-poly(TMSCOT) films conducted by Dr. Thomas Jozefiak indicate that the latter might be the case.[18] This difference in oxidation potential between poly(TMSCOT) and unsubstituted polyacetylene is not unexpected. Intuitively, the oxidation potential of the trimethylsilyl-substituted polymer is expected to be higher than that of the unsubstituted polymer because it is less highly conjugated, implying that carbocation formation is less favorable. If *cis*-poly(TMSCOT) is simply not oxidized by iodine, it is possible that stronger chemical oxidants could be used to dope and isomerize the *cis* polymer.

The conductivity of I_2 doped *trans*-poly(TMSCOT) (and to date, of all of the substituted polycyclooctatetraenes) is one to three orders of magnitude lower than that generally found for polycyclooctatetraene[10] or Shirakawa polyacetylene (~300 Ω^{-1} cm^{-1}).[12, 19] This difference may be attributable to differences in the microstructure of the polymers. In contrast to highly crystalline *trans*-polyacetylene, the poly(RCOT)s are amorphous. Their amorphous nature is indicated both by powder x-ray diffraction data (obtained for poly(*n*-octylCOT)[2]) and the lack of optical scattering in the near infrared spectrum. The well-ordered, close-packing present in crystalline polyacetylene is presumed to be important for efficient charge transfer between chains. In the bulk of an amorphous polymer, the random arrangement of poorly packed chains might be less conducive to electron transport. Also, there may be a tendency for the charge carriers to

localize at substituted sites along the chains, making them less mobile. Since conductivity measurements of the substituted polycyclooctatetraenes have not indicated a clear correspondence between conjugation length and conductivity,[2] and furthermore, since they seem to be highly sensitive to the past history of the sample (for instance, a decrease in conductivity of approximately one order of magnitude has been observed for *trans*-poly(TMSCOT) samples after rinsing to remove excess monomer and low molecular weight oligomers) more experimental, and perhaps computational, work is needed before a comprehensive understanding of electrical conductivity in these polymers develops.

To learn more about the nature of the doped polymer, it would be useful to observe doped polymer chains in solution. Methods for preparing solutions of doped polymers have been reported. The first conducting polymer solutions were prepared by dissolving AsF_5-doped poly(phenylene sulfide) in AsF_3.[20] Recently, alkyl-substituted polythiophenes doped with $NOBF_4$ have been found to be soluble in more conventional solvents.[21]

Iodine-doped poly(TMSCOT) films are insoluble; organic solvents only leach free iodine from the films. Addition of iodine to a solution of poly(TMSCOT) results in rapid precipitation of the polymer from solution. Preliminary experiments[22] indicate that the use of $NOBF_4$ does dope poly(TMSCOT) in solution. Addition of solid $NOBF_4$ to a dilute *trans*-poly(TMSCOT) CH_2Cl_2 solution resulted in the appearance of a greenish color. A spectrum of this solution is shown in Figure 2. The resulting solution was unstable over time, as indicated by a loss of color within minutes at room temperature, or tens of minutes at –78 °C. Electrochemical experiments described below indicate that poly(TMSCOT) is not very stable at high oxidation potential, and so the use of such a strong oxidant may simply have led to

decomposition of the material. Thus, the viability of solution doping of poly(TMSCOT) has not yet been adequately tested. It is possible that spectroelectrochemical work will produce better results.[18]

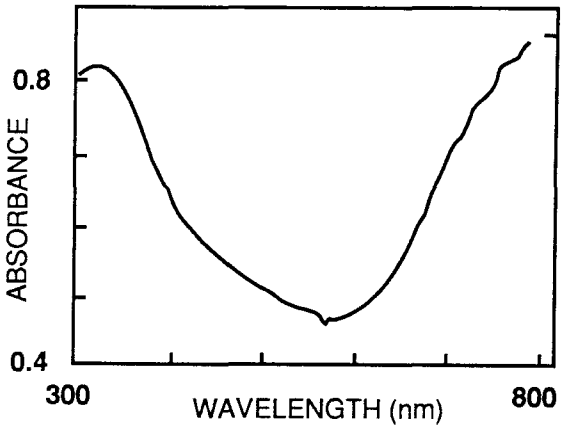

Figure 2. UV/Visible spectrum of $NOBF_4$-doped poly(TMSCOT) in CH_2Cl_2.

Electrochemistry. The electrochemistry of films of conjugated polymers, including polyacetylene, has been extensively studied.[14] Preliminary electrochemical work on films of poly(TMSCOT) was done by the author with Michael Sailor and Nathan Lewis. More extensive electrochemical investigations of poly(TMSCOT) and other poly(RCOT)s are currently being carried out by Dr. Thomas Jozefiak.[18]

Cyclic voltammetry experiments of films of *trans*-poly(TMSCOT) coated onto glassy carbon electrodes were carried out under nitrogen using 0.1 M $NaSO_3CF_3$ or $LiClO_4$ in propylene carbonate as supporting electrolyte. The anodic half of a typical voltammogram is shown in Figure 3. There is an oxidative peak at +0.85 V vs. a Ag/Ag^+ pseudoreference. This is followed by a nonreversible peak at a higher potential associated with decomposition. When polymer is coated on top of an electrode consisting of a conductive layer of indium tin oxide (ITO) on a glass slide, the color of the film can be observed as

the film is cycled through the oxidative peak. Figure 4 shows changes in the visible spectra of a *trans*-poly(TMSCOT) film as it is scanned through the oxidative wave at +0.85 V. The spectrum of the electrochemically doped film is somewhat similar to that observed upon chemical doping (Figure 2). As was found for other conjugated polymers,[9, 21, 23] doping poly(TMSCOT) results in a decrease in absorption in the visible wavelengths and an increase in the near-infrared region. Attempts to find an experimental configuration that would allow the conductivity of the electrochemically oxidized films to be measured were not successful. These experiments are complicated by the necessity to coat the film on an electrode, in order to dope it, and then either move the film to a nonconductive substrate or render the electrode nonconductive to ensure that there are no parallel pathways for passing current. Future work in this direction may require coating the polymer onto lithographically fabricated microelectrode arrays.[24]

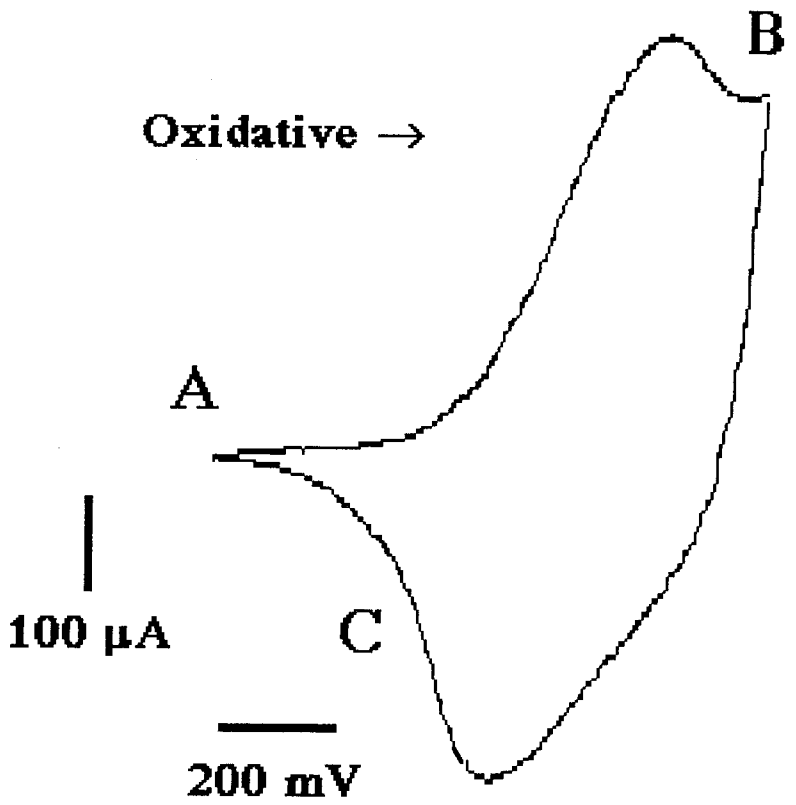

Figure 3. A cyclic voltammogram of a poly(TMSCOT) film on an ITO slide.; The maximum anodic current is at +0.85 V vs. Ag/Ag^{+}. The letters refer to the spectra in Figure 4. The scan speed was 20mV/sec. The electrolyte was 0.1 M $NaSO_3CF_3$ in propylene carbonate.

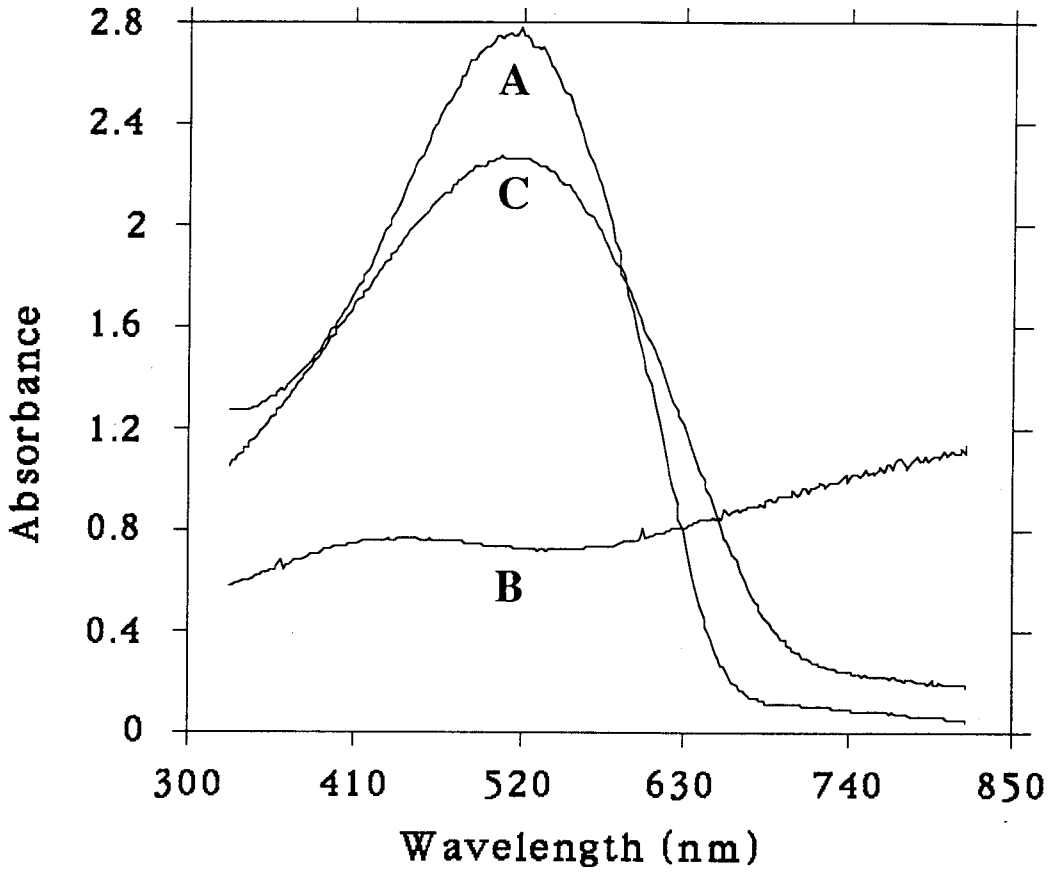

Figure 4. Absorption spectra of films of poly(TMSCOT) on an ITO electrode. The potential was ramped to +0.85 V vs. Ag/Ag+, spectrum B was obtained, then the potential was ramped back to 0.0 V and C was obtained. See Figure 3.

The size of the peak at +0.85 V decreased with repeated cycling. This is not surprising, given the proximity of this peak to the decomposition wave. A nonreversible reductive wave was also observed at ~–1.2 V, if the polymer was first cycled through the oxidative wave, using 0.1 M $LiClO_4$ in propylene carbonate as supporting electrolyte. No reductive wave was observed if the film was scanned in the cathodic direction initially. Jozefiak et al. have since found conditions under which a reversible reductive wave may be observed.[18]

Schottky-type Solar Cells[1]

Background. Schottky diodes and solar cells are electronic devices that rely on the electrostatic barrier that results when a doped semiconductor is brought in contact with a metal.[25] The excess mobile electrons of an n-doped semiconductor will migrate to a metal with an energetically lower electron Fermi level (Figure 5). The presence of excess electrons at the semiconductor-metal interface creates an electrostatic barrier to electron transfer between the semiconductor and the metal. The resulting coulombic repulsion is represented by an upward curvature ("band bending") of the conduction (LUMO) and valence (HOMO) bands near the interface. In solar cells, when light directed through the metal layer is absorbed by the semiconductor, photoexcited electrons are driven away from the interface by the electrostatic barrier. This description is reversed for positive charges, "holes," since they are attracted to the interface. This attraction is represented by an upward curvature of the valence band (HOMO). In a band diagram, electrons "sink"; i.e., decreasing energy (away from vacuum) is down, whereas holes "float"; i.e., decreasing energy is in the upward direction. The photoexcited electrons can return to the ground state in a number of ways (Figure 6).[26] In a solar cell, the goal is to have the electrons reach the back end of the semiconductor, travel through a circuit to do electrical work, then pass through the metal to recombine with a hole at the interface. Any process that leads to electron-hole recombination before the photoexcited electron goes around the circuit represents a loss of efficiency.

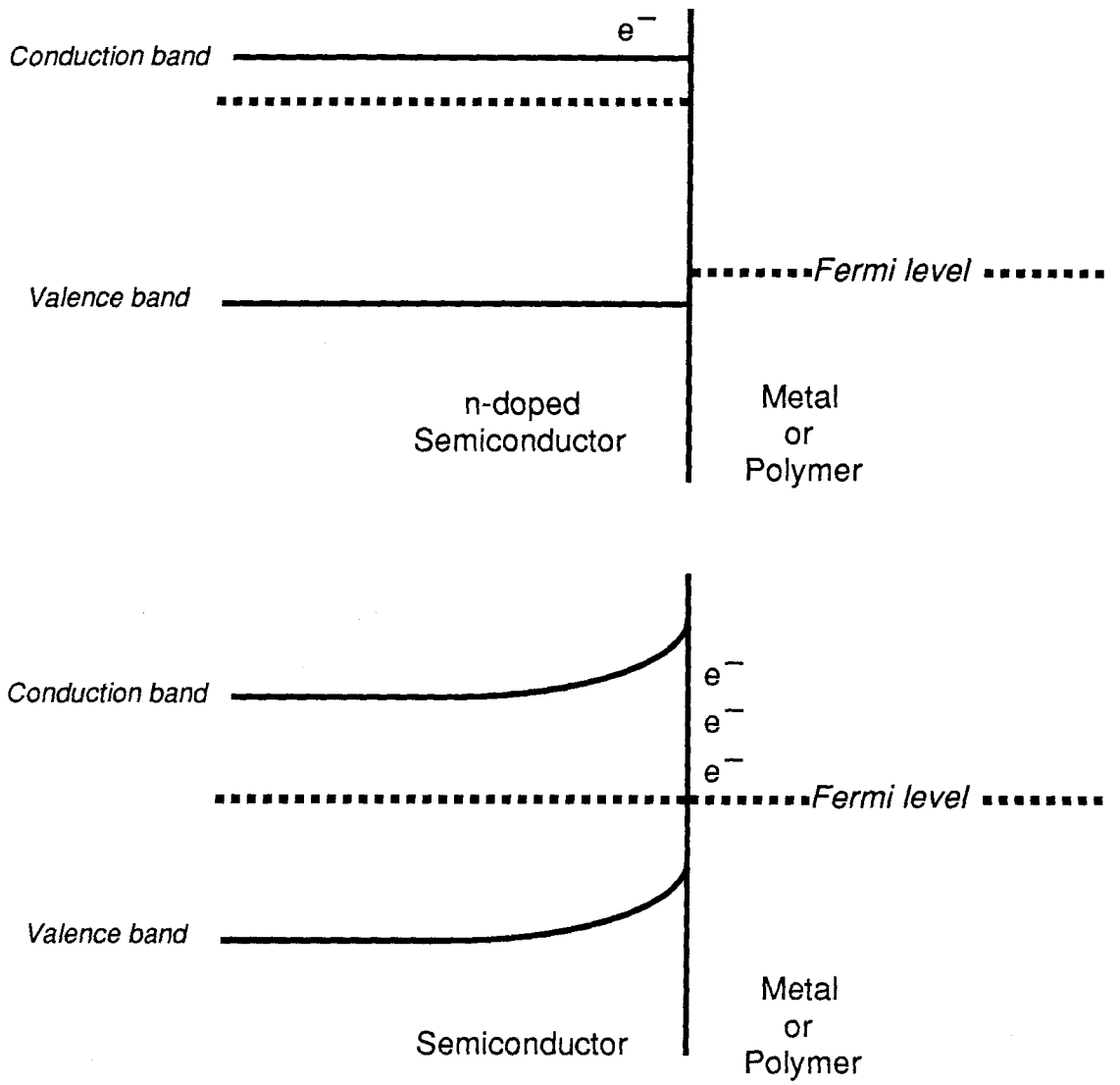

Figure 5. Conduction and valence bands of an n-doped semiconductor before (top) and after (bottom) electron migration to equilibrate Fermi levels ("band-bending").

In a traditional Schottky-type solar cell, the simplest type of photovoltaic device, a thin, transparent metal overlayer is evaporated onto a semiconductor surface. An examination of Figure 6 will indicate that the open circuit voltage, V_{oc}, which is a measure of the driving force for electron-hole recombination, should depend on the Fermi level, or work function, of the particular metal that

is used. In fact, it is found that when silicon, the most widely used semiconducting material, is used in Schottky solar cells, the V_{oc} does not scale with the work function of the metal. All metals give roughly the same open circuit voltage. This phenomenon is termed "Fermi-level pinning" and is thought to be due to the formation of an intermetallic metal silicide layer at the interface.[27] The electronic properties of this layer are responsible for the device properties; pinning occurs because different metal silicides differ little in their work functions. This phenomenon is undesirable for a few reasons. The voltage of the cell cannot be tuned by using different metals, and more significantly, the interface is pinned at a level that causes thermionic emission (Figure 6) to be fast enough to be the limiting factor in the efficiency of the cell.

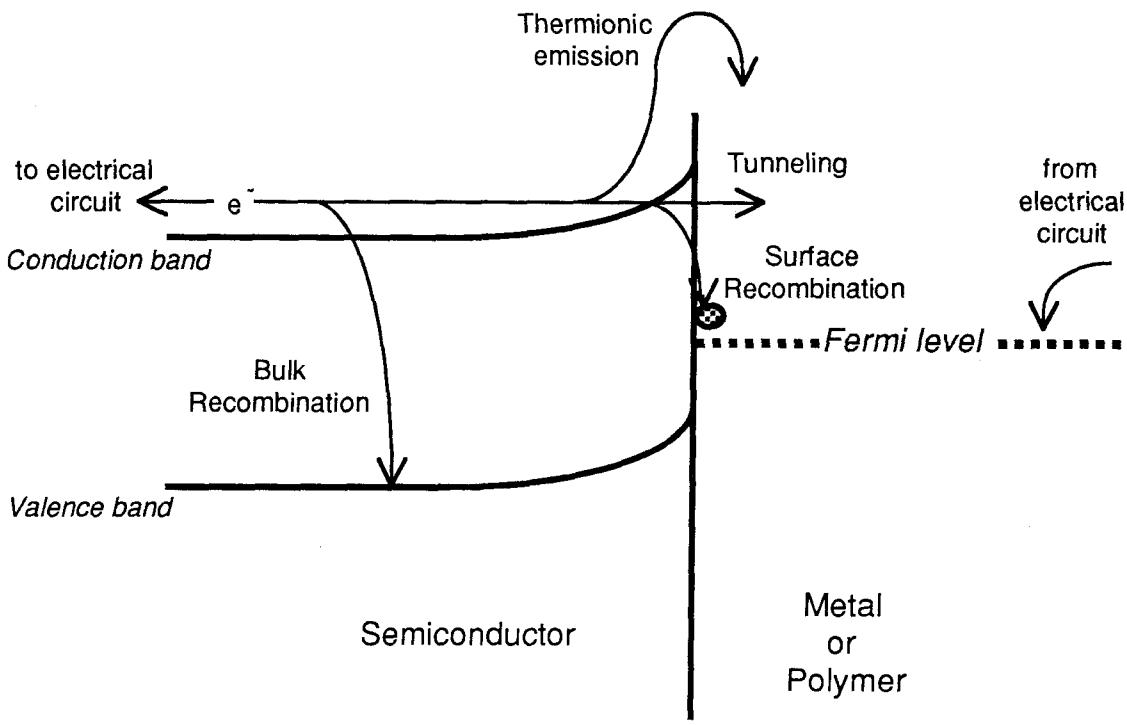

Figure 6. Recombination pathways available to a photoexcited electron in a Schottky-type solar cell.

Results. Drs. Michael Sailor, Nathan Lewis, et al. began an investigation of conducting polymer/semiconductor junctions by studying the properties of

polycyclooctatetraene/silicon junctions.[28] This work indicated that the Fermi level of the polymer could be tuned by changing the polymer dopant, indicating that the resulting devices were not subject to the same pinning constraints that characterize metal/silicon interfaces. Poly(TMSCOT)/silicon interfaces were then examined as Schottky-type solar cells. The silyl polymer was chosen for this work primarily because of its solubility. The ability to recast films from solution is thought to be important for forming smooth, homogeneous contacts to the semiconductor. Figure 7 shows three electron micrographs (taken by Sailor) that indicate the difference in morphology between polyacetylene films prepared in different ways. Shirakawa polyacetylene, made from acetylene, has a very porous structure. Polycyclooctatetraene, which is formed in situ on the desired substrate, has a "brainy" texture, whereas a recast poly(trimethylsilylcyclo-octatetraene) film is very smooth. Moreover, the solubility of poly(TMSCOT) enables the polymer to be deposited with a spin-coater, ensuring even deposition of thin films.

Figure 7. Scanning electron micrographs of (a) Shirakawa polyacetylene[29] (b) polycyclooctatetraene, and (c) a *trans*-poly(TMSCOT) film cast from solution. The scale bar is applicable to all three micrographs.

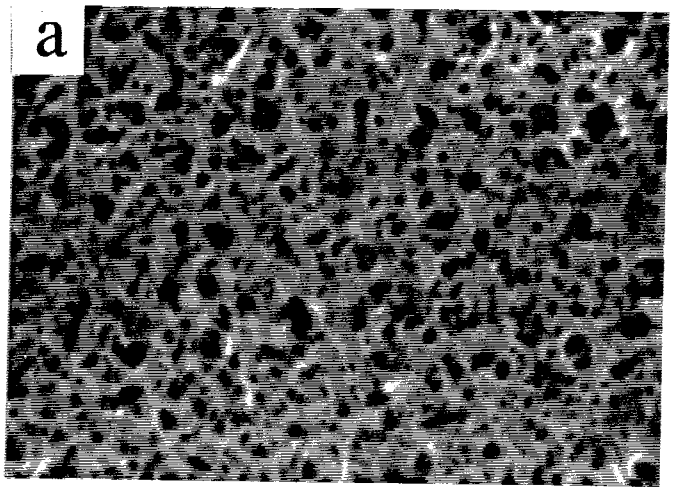
a

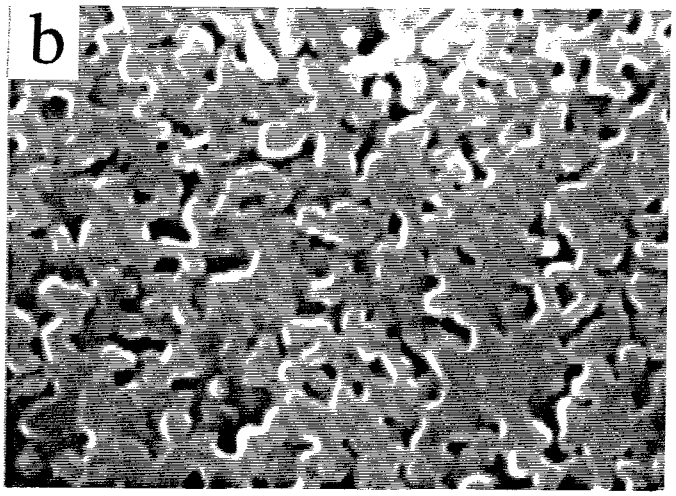
b

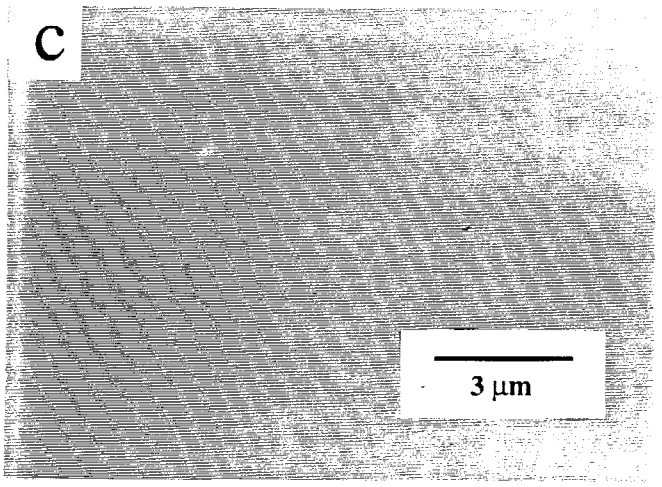
c
3 μm

The major finding of the research on the poly(TMSCOT) solar cells[1] is that the efficiency of the cells is not limited by thermionic emission, as are all known metal-silicon photovoltaic devices. That is, electron recombination at the interface is sufficiently slow that recombination in the bulk silicon, away from the interface, competes with sending electrons around the circuit. This limiting bulk recombination rate is determined only by the properties of the silicon[26] (e.g., dopant density, purity, etc.), not those of the polymer/semiconductor interface.

The significance of this is that a conducting polymer has been shown to be, in a strict sense, better than a metal, in that it forms a nonlimiting interface with silicon. Presumably, since the polymer does not react with the silicon layer as metals do, the properties of the device are not determined by an unwanted intermediate layer of material at the interface.[30] Conducting polymer/silicon semiconductor devices have been made before;[31-36] however, none were examined by systematically varying the silicon used to determine if the interfaces were behaving ideally.[26] Also, many of the devices were made using insoluble films press-contacted onto the semiconductor, or directly electropolymerized into place, presumably resulting in more heterogeneous polymer/semiconductor interfaces. While the air-instability of poly(TMSCOT) might limit its use to research applications, this result should be generalizable to other conducting polymers and perhaps to other semiconductors. In sum, the use of soluble, conductive and readily available poly(TMSCOT) facilitated the investigation of the fundamental properties of conducting polymer/semiconductor junctions, and demonstrated that the limitations of conventional metal contacts can, in principle, be overcome.

Multilayers

As a demonstration of the processing capability that is possible once a variety of soluble poly(RCOT)s are in hand, multilayered polymer films were prepared. Figure 8 is a scanning electron micrograph of a five-layer sandwich of doped poly(TMSCOT) and poly(Me_3SnCOT). The assembly was prepared by casting a thin layer of the silyl polymer onto a glass slide, then doping it with iodine vapor to render it insoluble and casting a solution of the stannyl polymer on top. The doping and coating process was repeated, alternating polymers in each step. The resulting multilayer was then peeled up to form a free-standing film. The SEM of the film indicates that the layers are well-defined. Multilayers are of interest in semiconductor technology for use in "quantum well" devices[37, 38] and in optical waveguiding, and the ease with which soluble conducting polymers may be processed into a variety of forms may make them amenable to investigations in these fields.

Figure 8. Scanning electron micrograph of a poly(TMSCOT)/poly-(Me_3SnCOT) five-layered sandwich.

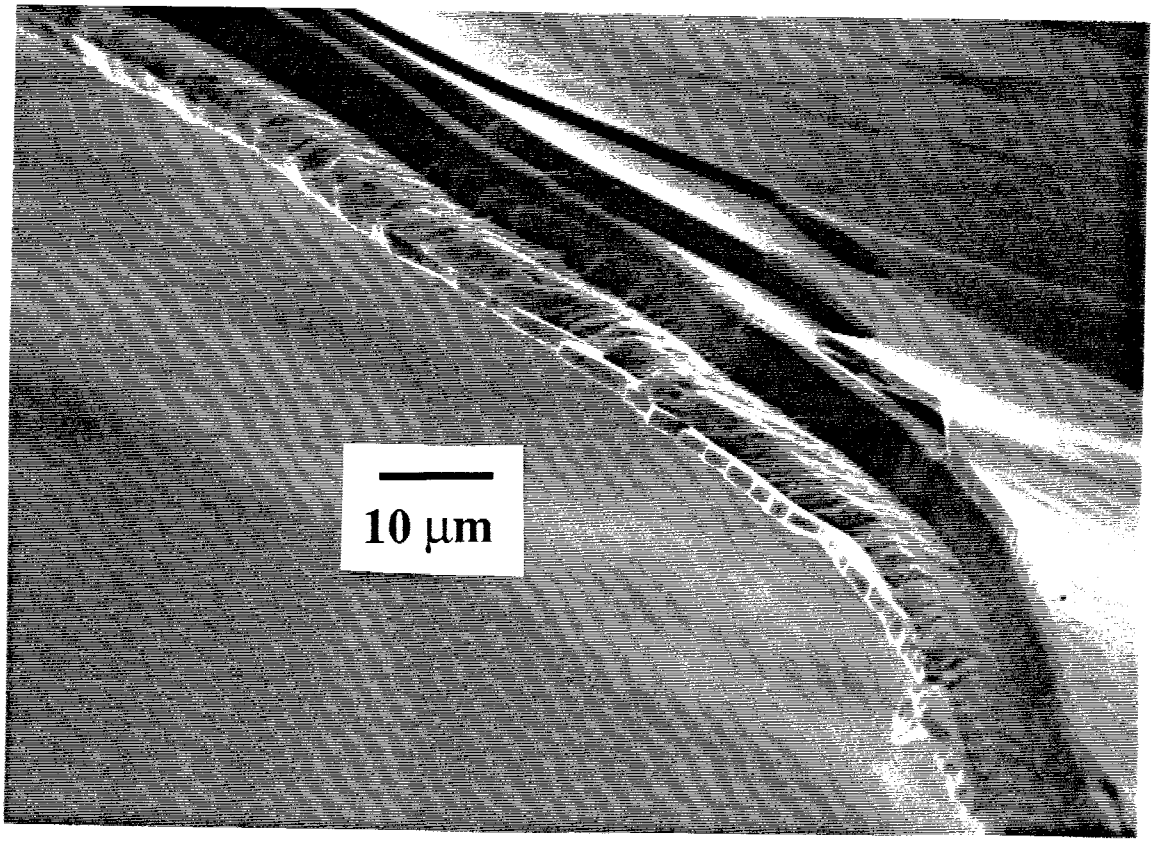
10 μm

Nonlinear Optical Properties.

Chemists, materials scientists and physicists have been actively pursuing materials with high nonlinear optical (NLO) coefficients.[39] Such materials are sought for their ability to change the phase or frequency of light passing through them in a controlled manner. The development of optical computers[40] will require devices capable of switching beams of light as conventional computers switch electronic currents. These devices will be made from materials with an optimum balance of properties: high third-order nonlinear optical coefficients, χ_3; transparency at the appropriate wavelengths; and processability. Conjugated polymers (in their undoped state) have shown promise as materials for nonlinear optical applications. To date, polydiacetylenes have been the most studied organic materials for waveguiding applications.[41] They are of interest for their high nonlinear optical coefficients and because films of crystalline monomer may be polymerized directly into a crystalline polymer. It has been found that polyacetylene[42] has a higher nonlinear optical coefficient than do polydiacetylenes. However, the intractability and crystallinity of polyacetylene limit its usefulness. Crystallinity is a problem because the scattering of light in the near infrared region by micron-sized crystallites leads to high transmission losses through the material at these wavelengths. The soluble, amorphous poly(RCOT)s were thus examined by Drs. Joseph Perry and Seth Marder (JPL) to determine their third-order nonlinear optical properties.[2] The magnitude of the frequency-tripled signal generated when a polymer sample was irradiated with a 1064 nm YAG laser line was compared to that of a standard to obtain χ_3. It was found that the (NLO) properties of the polymers that were tested are dependent on the effective conjugation length of the polymer. Whereas *trans*-poly(TMSCOT) was found to have a third-order NLO coefficient of only $2\pm1 \times 10^{-11}$ esu, *trans*-poly(*n*-butylCOT), $\lambda_{max} \approx 600$ nm,[43] has a third-order nonlinear

optical coefficient of ~10^{-10} esu, similar to that of unsubstituted polyacetylene ($\lambda_{max} \approx 650$ nm, NLO coefficient = 10^{-9} esu[42]). Moreover, poly(RCOT)s, because they are amorphous, transmit more near-infrared light than does polyacetylene. It is expected that future work with other poly(RCOT)s will show that polymers such as soluble *trans*-poly(*sec*-butylCOT)[43] which has an absorption maximum (~550 nm) slightly to the red of poly(TMSCOT), possess the preferred balance of properties for nonlinear optics. These polymers' high conjugation length leads to a high χ_3, and their solubility allows the facile fabrication of waveguides.

Summary

In summary, the characterization of the poly(RCOT)s with a view towards a variety of applications has begun. The conductivity of *trans*-poly(TMSCOT) has been found to be ~10^{-1} Ω^{-1} cm^{-1}, two to three orders of magnitude lower than that of unsubstituted polyacetylene. The predominantly cis isomer of the polymer does not isomerize to a highly conductive state upon iodine doping, and evidence suggests that its oxidation potential is too high. The materials may also be electrochemically doped; research in this area is ongoing.

Although the choice of a particular material for a "real-world" application is an engineering decision, and it is uncertain that the soluble polyacetylenes described here will prove practical for widespread use, their availability to researchers studying a range of phenomena should facilitate a number of studies on the capabilities and fundamental properties of conducting polymers. The ability to tune the polymer properties by selecting a substituent of a certain "size," and the ability to predict those properties using molecular modeling, make the substituted polycyclooctatetraenes a versatile set of compounds. The conductivity of poly(TMSCOT), while sacrificed somewhat to afford solubility, has been demonstrated to be high enough to allow the fabrication of efficient

solar cells. Similarly, an optimum balance between conjugation length and solubility will be found for further explorations of the nonlinear optical capabilities of the polymers. Given the results to date, it is not unlikely that the use of soluble conducting polymers in other areas of physics and chemistry will yield more unexpected discoveries.

Experimental Section

Iodine doping. Doping was accomplished by exposing the polymer films to iodine vapor for 3 to 6 hours in a previously evacuated chamber, followed by pumping (< 0.01 torr) for approximately one hour or longer to remove any excess iodine. Films immediately become blue-black in color but remained flexible. Conductivities were measured using a four-point probe in a nitrogen drybox or a four-wire probe attached to a Schlenk line.[15] Similar conductivities were seen using both methods. Film thicknesses were measured either with Fowler Digitrix II digital calipers or a Dektak 3030a profilometer.

Multilayers. THF solutions of isomerized poly(TMSCOT) and as-synthesized poly(Me_3SnCOT) were spin-coated onto glass slides, using a Headway Instruments spin coater. After depositing a layer, the slide was placed in a chamber connected to a pump and an evacuated iodine chamber. Each layer was exposed to iodine in vacuo for one minute, then pumped on for one minute. Edge-on views of films were obtained by freeze-fracturing them. This was accomplished by breaking them in half with tweezers while they were immersed in liquid nitrogen. Scanning electron micrographs were obtained with the Caltech Geology Department's Camscan scanning electron microscope.

Cyclic voltammetry. Cyclic voltammetry was done using 0.1 M $NaSO_3CF_3$ or $LiClO_4$ in propylene carbonate on glassy carbon electrodes. The

working electrode was in a fritted compartment, and a silver wire that had been dipped in 1 M HCl was used as a pseudoreference.

The solar cell fabrication and nonlinear optical studies are discussed in References 2 and 1, respectively.

References and Notes

(1) Sailor, M. J.; Ginsburg, E. J.; Gorman, C. B.; Kumar, A.; Grubbs, R. H.; Lewis, N. S. *Science* **1990**, *249*, 1146-1149.

(2) Ginsburg, E. J.; Gorman, C. B.; Grubbs, R. H.; Klavetter, F. L.; Lewis, N. S.; Marder, S. R.; Perry, J. W.; Sailor, M. J. in *Opportunities in Electronics, Optoelectronics, and Molecular Electronics.*; Brédas, J. L., Chance, R. R., Eds.; Kluwer: Dordrecht, the Netherlands, 1990; pp 65-81.

(3) Brandstetter, F. *ECN Speciality Chemicals Supp.* **1988**, *Jan.*, 32-36.

(4) Freundlich, N. *Business Week* **1989**, *Dec. 11*, 114-115.

(5) Frommer, J. E.; Chance, R. R. in *Encyclopedia of Polymer Science and Engineering*; Kroschwitz, J. I., Ed.; Wiley & Sons: New York, 1986; pp 462-507.

(6) Pekker, S.; Jánossy, A. in *Handbook of Conducting Polymers, Vol. 1*; Skotheim, T. A., Ed.; Marcel Dekker: New York, 1986; pp 45-79.

(7) Baughman, R. H.; Murthy, N. S.; Miller, G. G.; Shacklette, L. W. *J. Chem. Phys.* **1983**, *79*, 1065-1074.

(8) *Handbook of Conducting Polymers, Vol. 2*; Skotheim, T. A., Ed.; Marcel Dekker: New York, 1986; Chaps, 1-6.

(9) Spangler, C. W.; Rathunde, R. A. *J. Chem. Soc. Chem. Commun.* **1989**, 26-27.

(10) Klavetter, F. L.; Grubbs, R. H. *J. Am. Chem. Soc.* **1988**, *110*, 7807-7813.

(11) Bott, D. C.; Brown, C. S.; Chai, C. K.; Walker, N. S.; Feast, W. J.; Foot, P. J. S.; Calvert, P. D.; Billingham, N. C.; Friend, R. H. *Synth. Met.* **1986**, *14*, 245-269.

(12) Shirakawa, H.; Louis, E. J.; MacDiarmid, A. G.; Chiang, C. K.; Heeger, A. J. *J. Chem. Soc. Chem. Comm.* **1977**, 578-580.

(13) Basescu, N.; Liu, Z. X.; Moses, D.; Heeger, A. J.; Naarman, H.; Theophilou, N. *Nature* **1987**, *327*, 403-405.

(14) MacDiarmid, A. G.; Kaner, R. B. in *Handbook of Conducting Polymers, Vol. 1*; Skotheim, T. A., Ed.; Marcel Dekker: New York, 1986; pp 689-727.

(15) Sze, S. M. *Physics of Semiconductor Devices*; Wiley & Sons: New York, 1981; p 30.

(16) Chien, J. C. W. *Polyacetylene: Chemistry, Physics, and Material Science*; Academic: Orlando, FL, 1984; p 160.

(17) Experiments to examine the properties of thermally isomerized poly(RCOT)s are in progress (Gorman, C. B.; Ginsburg, E. J.; Jozefiak, T. H. Grubbs, R. H. unpublished results).

(18) Jozefiak, T. H.; Lewis, N. S.; Grubbs, R. H. manuscript in preparation.

(19) Chiang, C. K.; Fincher, C. R., Jr.; Park, Y. W.; Heeger, A. J.; Shirakawa, H.; Louis, E. J.; Gau, S. C.; MacDiarmid, A. G. *Phys. Rev. Lett.* **1977**, *39*, 1098-1101.

(20) Frommer, J. E. *Acc. Chem. Res.* **1986**, *19*, 2-9.

(21) Hotta, S.; Rughooputh, S. D. D. V.; Heeger, A. J.; Wudl, F. *Macromolecules* **1987**, *20*, 212-215.

(22) Ginsburg, E. J.; Gorman, C. B.; Jozefiak, T. H. Grubbs, R. H. unpublished results.

(23) Reference 16, pp 404-410.

(24) Kittlesen, G. P.; White, H. S.; Wrighton, M. S. *J. Am. Chem. Soc.* **1984**, *106*, 7389-7396.

(25) See Chapter 5 of Reference 15.

(26) Lewis, N. S. *J. Electrochem. Soc.* **1984**, *131*, 2496-2503.

(27) Bachrach in *Metal-Semiconductor Schottky Barrier Junctions and Their Applications*; Sharma, B. L., Ed.; Plenum: New York, 1984; pp 61-112.

(28) Sailor, M. J.; Klavetter, F. L.; Grubbs, R. H.; Lewis, N. S. *Nature (London)* **1990**, *346*, 155-157.

(29) Ito, T.; Shirakawa, H.; Ikeda, S. *J. Polym. Sci.: Polym. Chem. Ed.* **1974**, *12*, 11-20.

(30) This result is analogous to that found by Lewis and coworkers for semiconductor/liquid junctions. See Reference 26 and Lewis, N. S. *Acc. Chem. Res* **1990**, *23*, 176-183.

(31) Cohen, M. J.; Harris, J. S. *Appl. Phys. Lett.* **1978**, *33*, 812-814.

(32) Frank, A. J.; Glenis, S.; Nelson, A. J. *J. Phys. Chem.* **1989**, *93*, 3818-3825.

(33) Garnier, F.; Horowitz, G. *Synth. Met.* **1987**, *18*, 693-698.

(34) Ozaki, M.; Peebles, D.; Weinberger, B. R.; Heeger, A. J.; MacDiarmid, A. G. *J. Appl. Phys* **1980**, *51*, 4252-4256.

(35) Skotheim, T.; Lundstroem, I. *J. Electrochem. Soc.* **1982**, *129*, 894-896.

(36) Tsukamoto, J.; Ohigashi, H.; Matsumura, K.; Takahashi, A. *Synth. Met.* **1982**, *4*, 177-186.

(37) Jaros, M. *Physics and Applications of Semiconductor Microstructures*; Oxford University: Oxford, 1989.

(38) Herman, M. A. *Semiconductor Superlattices*; Akademie-Verlag: Berlin, 1986.

(39) Chemla, D. S.; Zyss, J. *Nonlinear Optical Properties of Organic Materials and Crystals, Vol. 2*; Academic: Orlando, FL, 1987.

(40) Wilson, J.; Hawkes, J. F. B. *Optoelectronics: An introduction, 2nd ed.*; Prentice Hall: New York, 1989; Section 9.4.

(41) Bloor, D.; Ando, D. J.; Norman, P. A.; Drake, A. F.; Mann, S.; Oldroyd, A. R.; Wherrett, B. S.; Kar, A. K.; Ji, W.; Harvey, T. in *Opportunities in Electronics, Optoelectronics, and Molecular Electronics*; Brédas, J. L. Chance, R. R., Eds.; Kluwer: Dordrecht, the Netherlands, 1990; pp 377-386.

(42) Kajzar, F.; Etemad, S.; Baker, G. L.; Messier, J. *Synth. Met.* **1987**, *17*, 563-7.

(43) Gorman, C. B.; Ginsburg, E. J.; Marder, S. R.; Grubbs, R. H. *Angew. Chem. Adv. Mater.* **1989**, *101*, 1603-1606.

Chapter 5

A Preliminary Investigation of Substituted Polyacetylenes by Scanning Tunneling Microscopy

Abstract

Preliminary results of an investigation by scanning tunneling microscopy (STM) of substituted polyacetylenes deposited on highly oriented pyrolytic graphite (HOPG) will be presented. This project was initiated by Dr. Reginald Penner and Prof. Nathan Lewis, and was carried on jointly by Dr. Pui Tong Ho and the author. This chapter is somewhat of a progress report: The techniques for reproducibly acquiring meaningful data on this system by STM have not yet been perfected, although some intriguing images have been obtained.

Introduction

Background. A scanning tunneling microscope[1] consists typically of a sharp tip mounted on a piezoelectric crystal in such a way that its movement can be controlled in three dimensions with subangstrom resolution. To obtain an STM image, a conductive tip is held at a constant electrical potential relative to the surface while it is scanned laterally over a conductive substrate. The sample-to-tip separation may be modulated such that the current that is due to electron tunneling across the ambient medium is kept constant ("constant-current" mode). The voltage sent to the piezoelectric tip mount in order to maintain this constant current is plotted versus the tip's lateral position to form a topographic image of the sample. The microscope is capable of subnanometer resolution both parallel and perpendicular to the surface. The achievement of such high resolution might have been unexpected, given the relatively large macroscopic radii of the tips used, but has been accounted for theoretically.[2]

Because the STM is capable of resolving atoms, and because the mechanics of the instrument are experimentally straightforward, the technique has the potential to revolutionize the way scientists visualize surfaces and molecules.[3] To date, the majority of STM research has been directed towards clean metal and

semiconductor surfaces in ultrahigh vacuum. Increasingly though, the microscope is being used to image adsorbates on surfaces not only in vacuum, but also in air and under liquids. Conducting polymers have received some attention, in part, because some may be electropolymerized directly onto the substrate from solution,[4-6] but also because of a sense that in order to image a species by STM, it must be conductive. However, recent images of DNA,[3, 7, 8] viral protein coats,[9] Langmuir-Blodgett multilayers,[10-12] "liquid crystals,"[13-19] nonconducting polymers,[20, 21] and, most dramatically, 1000 Å-thick alkane crystals,[22] belie the latter idea.

In general, theoretical descriptions of electron tunneling through organic materials are lagging behind experiment. The images of alkane crystals[22] are inexplicable, given current theories of tunneling. The tunneling current and bias used imply that the crystals are orders of magnitude more conductive than bulk paraffin is found to be. Similarly, images of ordered, liquid-crystal-forming biphenyls have been subject to different interpretations,[17, 19] with uncertainty surrounding the relative importance of electronic and steric contributions to the topography observed.

Nonetheless, a number of exciting images have been obtained. The images of the "liquid crystals"[13] on graphite provide evidence that it is possible to resolve the shapes of organic molecules.[14-19] Ordered arrays of shapes are observed, and in more than one case, a rough correspondence may be made between the size and shape expected for the deposited molecule and those observed in the image. Recently, an exceptional image of DNA on graphite was obtained in UHV by Driscoll, Youngquist and Baldeschwieler.[8] The double helix may be clearly resolved, and a plot of the height of the image across a section of the molecule corresponds almost atom-for-atom to that expected based on molecular models of DNA.

The state of the art of STM is such, however, that resolution this high cannot yet be obtained reproducibly. There are STM images of DNA in the literature of lower resolution,[7] and Driscoll et al. do not obtain at will images of the quality reported.[23] Methods for controlling the experimental variables, including sample and tip quality, that determine the quality of the image have not yet been perfected. A report by Caple and coworkers[6] is a good example of both the possible achievements of STM and the inherent difficulties. They examined electropolymerized polythiophene, poly(3-methylthiophene) and poly(3-bromothiophene) on platinum. Among the images they observed were included: regular arrays of zigzagging lines (i.e., a "herring-bone" pattern) on part of a substrate covered with poly(3-methylthiophene), with 90° kinks approximately every 100 Å; long straight ridges about 60 Å in diameter, which are suggested to be poly(3-bromothiophene) superhelical coils; and at higher magnification, bumps 1-2 Å apart that "might be interpreted as tunneling from about where the sulfur atoms might be found" in poly(3-bromothiophene). Certainly, one reason for the variety of images they observed is the inherent problem of reproducibility in such a high-powered microscope. A technique that is capable of imaging single molecules will produce images representing structures or adsorption sites that span the range allowed by the Boltzmann distribution (assuming thermal equilibrium). Still, these images raise many questions. For instance, if the bumps observed at high magnification are really sulfur atoms along the chain, why are only the sulfur atoms observed? Given the images of liquid crystals mentioned above, it seems that the rest of the monomer units could be visualized as well. Furthermore, the zigzagging lines they attribute to ordered polymer bear some resemblance to moiré patterns observed by Albrecht et al. on clean graphite.[24] In the Albrecht paper, these patterns are shown to be an interference effect that results from two "minitips" on the end of the STM tip, simultaneously imaging

two sides of a grain boundary that separates two slightly dislocated graphite crystallites. Caple's results could be an example of a related phenomenon occurring on platinum.

An Investigation of Substituted Polyacetylenes by STM. There are several motivations for studying substituted polyacetylenes by STM, some more ambitious than others. At a fundamental level, successfully imaging any easily varied system, such as the set of poly(RCOT)s, should aid in understanding the mechanism of STM. The RCOT/ROMP methodology (see Chapter 2) allows a variety of side groups to be placed on the polyacetylene chain. By imaging an array of polymers that differ only in their side group, it should be possible to formulate an empirical relationship between the structure of a molecule and its appearance in an STM image. This is desirable, because, as outlined above, it is currently not possible, theoretically or empirically, to predict a priori how a given molecule will be visualized by STM. At a more applied level, the STM could yield information about the poly(RCOT) structure. It might be possible, for instance, to obtain information about the conformations of the polymer chains. In this respect, it would be interesting to observe differences between the cis and trans isomers of the polymer. Furthermore, if the side groups could be resolved in an STM image, their spacing along the chain, still an unknown (see Chapter 2), could be measured directly. Moreover, once a protocol is developed for visualizing the polymers and side chains, it should be possible to determine the overall sequence of poly(RCOT) copolymers, including the degree of blockiness. Methods for determining copolymer structures would be of general use in polymer science.

The electrochemical properties of the substituted polyacetylenes add another dimension to this project. Since the conductivity of the polymer should depend on its oxidation state, its STM image might change as it is

electrochemically cycled (see Chapter 4). STM offers the potential for observing these electrochemical events on the scale of a single strand.

The HOPG[25] (0001) surface was used as a substrate because it is relatively inert, and thus is well-suited for work in air, and because, unlike most metals, its atomic structure can be resolved by STM. The ability to image the graphite substrate serves as a built-in control by indicating whether the microscope is functioning properly, and as a scale, since the atomic spacings of the graphite image are known. A disadvantage associated with using graphite is that although it is atomically smooth over large areas, there are known to be many grain boundaries and defects in the crystal.[25] Since STM images of these features can be somewhat varied, it is not always possible to determine readily whether an image is due to a molecule adsorbed onto graphite or to the graphite itself. Such ambiguities have been a concern in this project, as demonstrated below.

Experimental Section

Preparation of Samples. Highly ordered pyrolytic graphite was a gift from Arthur Moore of Union Carbide. Approximately 1 cm^2 graphite squares were attached to the microscope stage in such a way that layers of the graphite crystal could be removed with Scotch tape to expose a fresh surface. Solutions of *trans*-poly(TMSCOT) were diluted in distilled benzene under nitrogen to known concentrations of approximately 10^{-7} to 10^{-9} g/mL Typically, 10 μL of the polymer solution was placed on the horizontal graphite surface and the solvent was allowed to evaporate. Alternatively, solutions were sprayed onto the graphite, using a TLC sprayer equipped with a rubber bulb. The stage was then placed in vacuo and exposed to iodine vapor for one minute, then pumped on for an additional minute. The sample was kept under nitrogen or vacuum until it

was loaded into the microscope. New samples and tips were prepared for each daily imaging session.

Data Collection.[26] The images were obtained in air, using a home-built analogue, scanning tunneling microscope.[27] Images were obtained in constant current mode using electrochemically etched tungsten tips.[27] The images were displayed and recorded in a differential mode in which the voltage controlling the motion of the piezoelectric tip holder in the z direction (normal to the surface) was sent through a low-pass filter, and the raw signal was then subtracted from the filter output using a differential amplifier. The differential output from scans in the right-to-left direction (along the x-axis) was displayed versus the x-y raster of the tip, using an Arlunya video processor, and was stored on videotape. In an image obtained in the differential mode, a white region indicates an upward motion of the tip (along the z-axis, perpendicular to the horizontal surface), while dark regions indicate a downward motion. Scanning speeds were typically 5 or 10 Hz in the x direction and 0.015 or 0.03 Hz in the y direction. At these rates, a full screen was acquired in 30 or 60 seconds. The sample-to-tip bias was +100 mV (tip positive), and the tunneling current was usually 100 pA. Changes in the sign and magnitude of the bias did not cause significant changes in the images. Tip oscillations, which caused a loss of the image and damage to the tip, were frequently encountered at higher tunneling currents.

The typical imaging protocol was as follows. After landing the tip on the surface, it was determined whether atomically resolved graphite could be observed at high magnification on an ostensibly clean region. If not, a new tip was put in. If nothing of interest (i.e., nothing but flat graphite) was visible at first, the window size was increased to 1200×1200 Å^2 on a side, and the total viewing area (~1 μm^2) was manually reconnoitered in 1200×1200 Å^2 increments. If nothing of interest was observed in the total accessible viewing area, the tip

was retracted and the sample holder turned slightly to allow examination of a fresh area.

Results

Figure 1. Highly ordered pyrolytic graphite under water. (Image recorded by Reginald Penner.) Scan parameters: 116 mV bias, 0.4 nA tunneling current, ~40×40 Å^2.

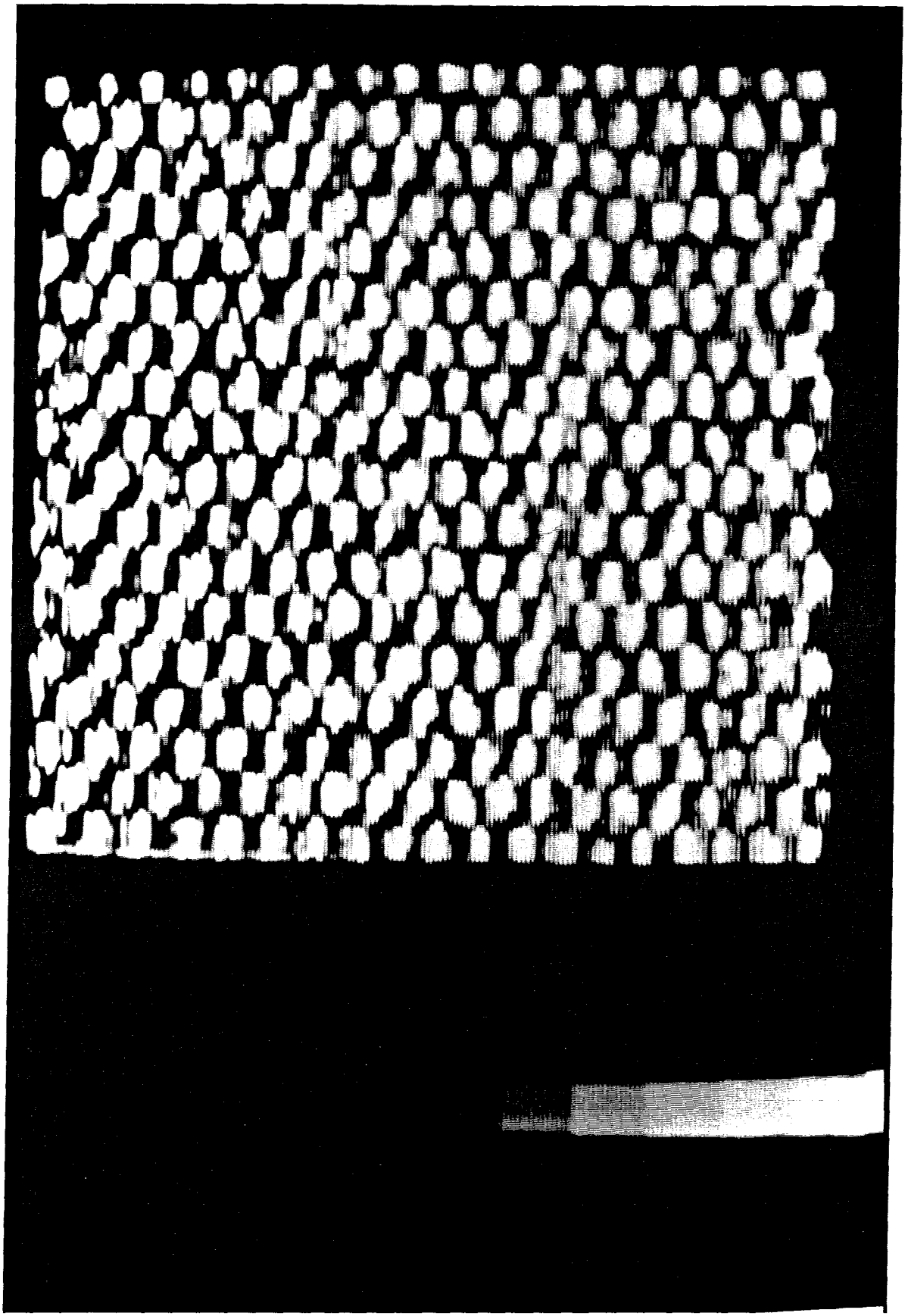

Figure 2. Straight line on graphite. Scan parameters: 150 mV bias, 0.2 nA tunneling current, 1200 × 1200 $Å^2$. Poly[(ferrocenylmethoxy)COT][29] on graphite.

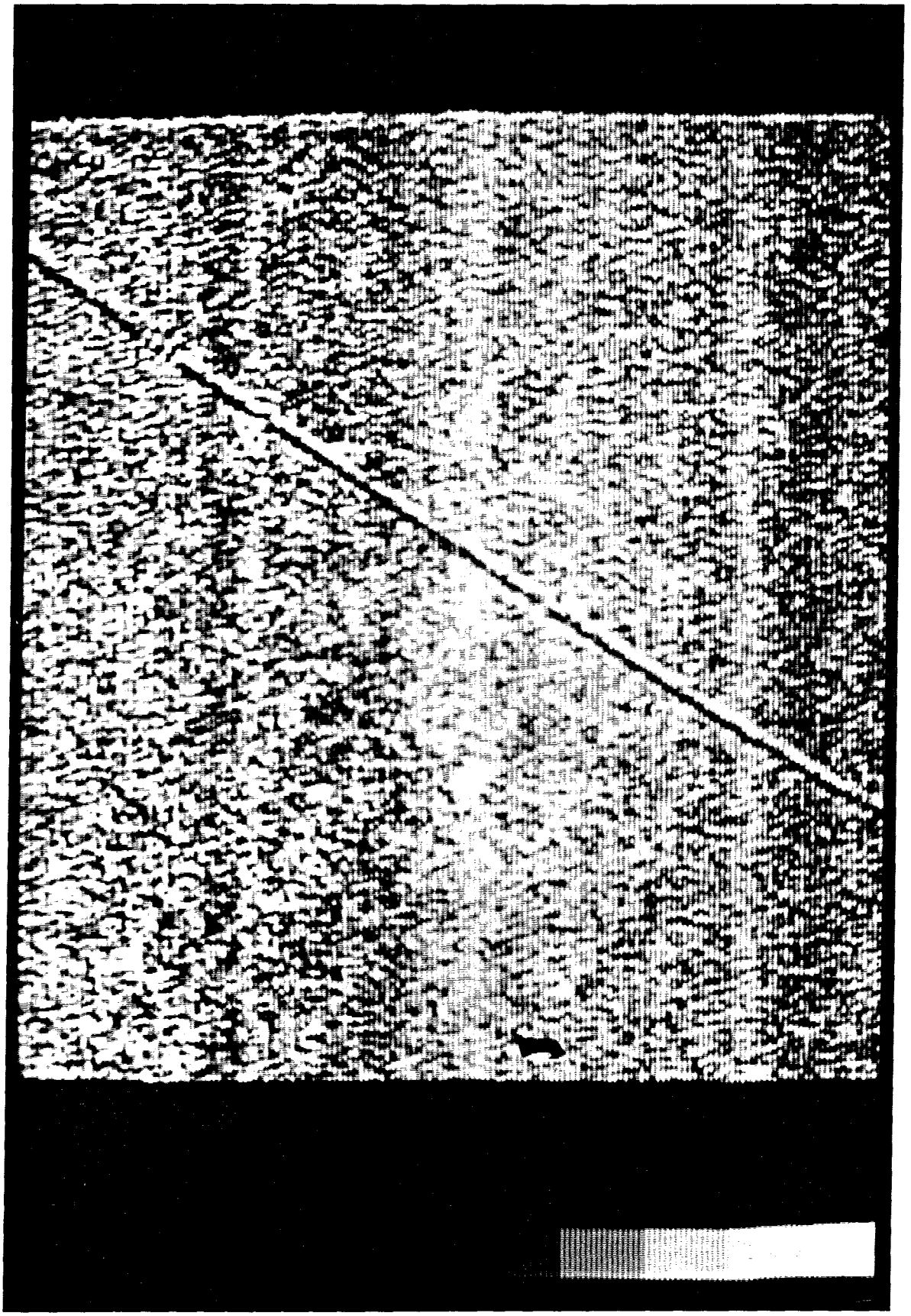

Figure 3. Scan parameters; 100 mV bias, 30 pA tunneling current, 540×540 Å^2. Poly(TMSCOT) on graphite.

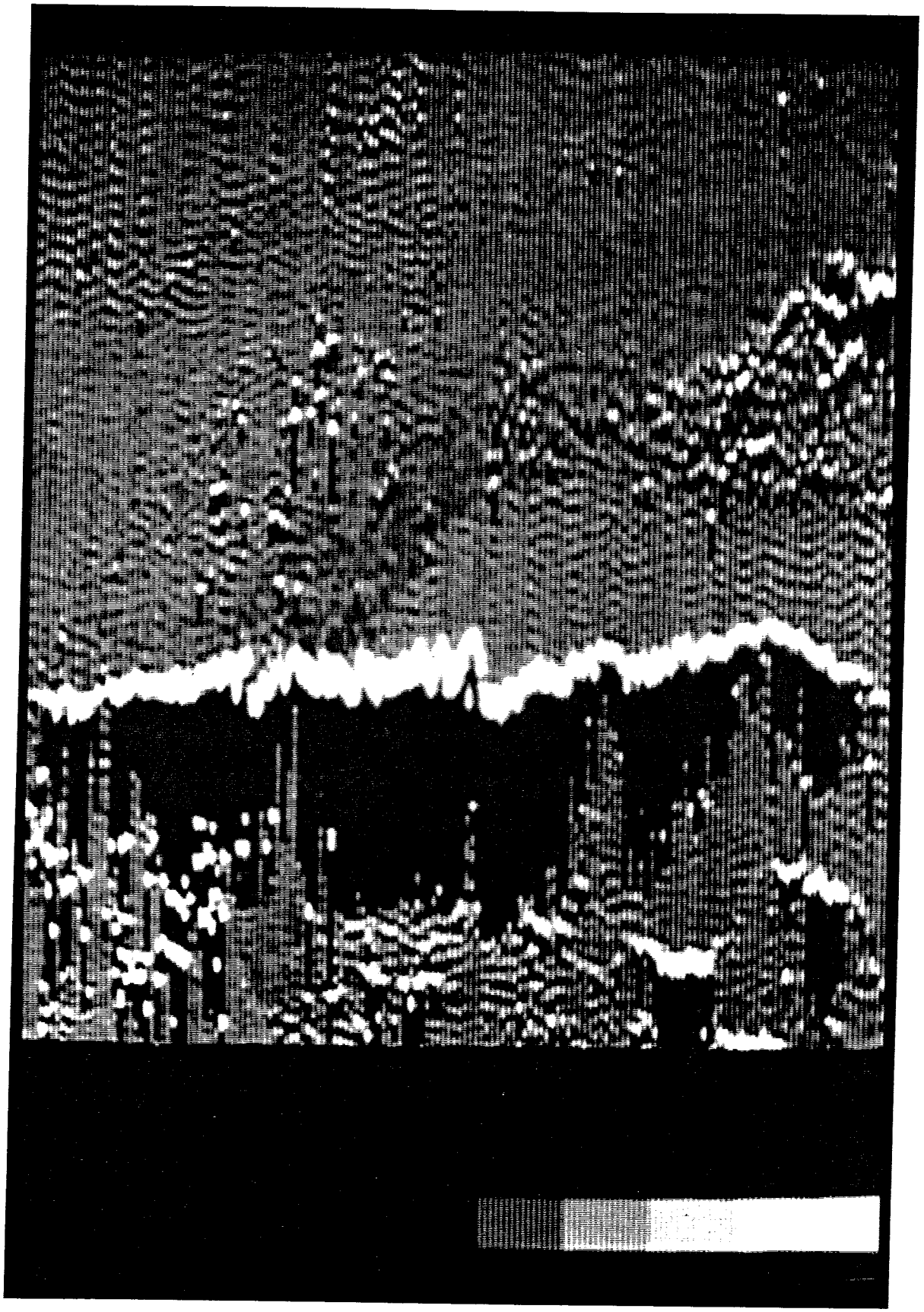

Figure 4. Figure 1 of Reference 24. The STM image of a tilt boundary between two crystallites in HOPG. The caption reads, in part: "The depression seen to the left of the boundary is artificial and is caused by the response of the feedback in the fast scan current imaging mode." (Reprinted with permission of the author.)

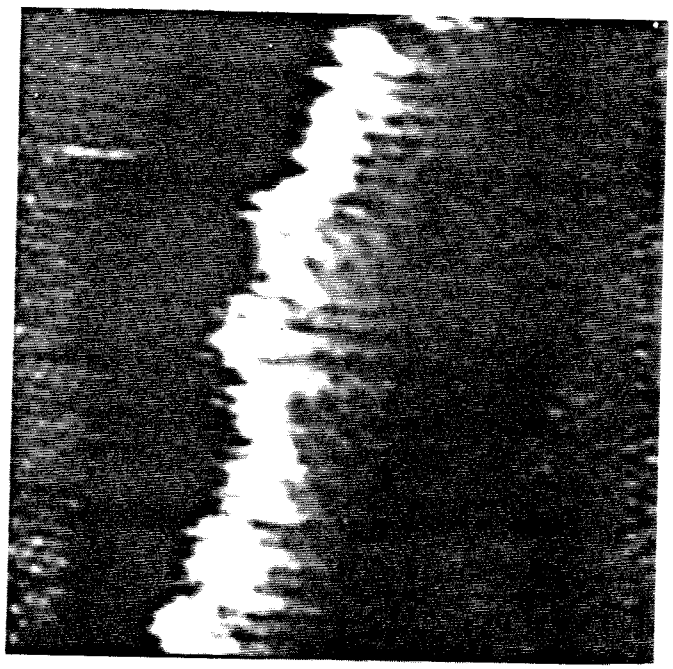
60 Å

Figure 5. Image of graphite covered with a polymer plaque. Scan parameters: 100 mV bias, 0.2 nA tunneling current, ~500 × 500 Å^2. Poly(TMSCOT) sprayed onto graphite.

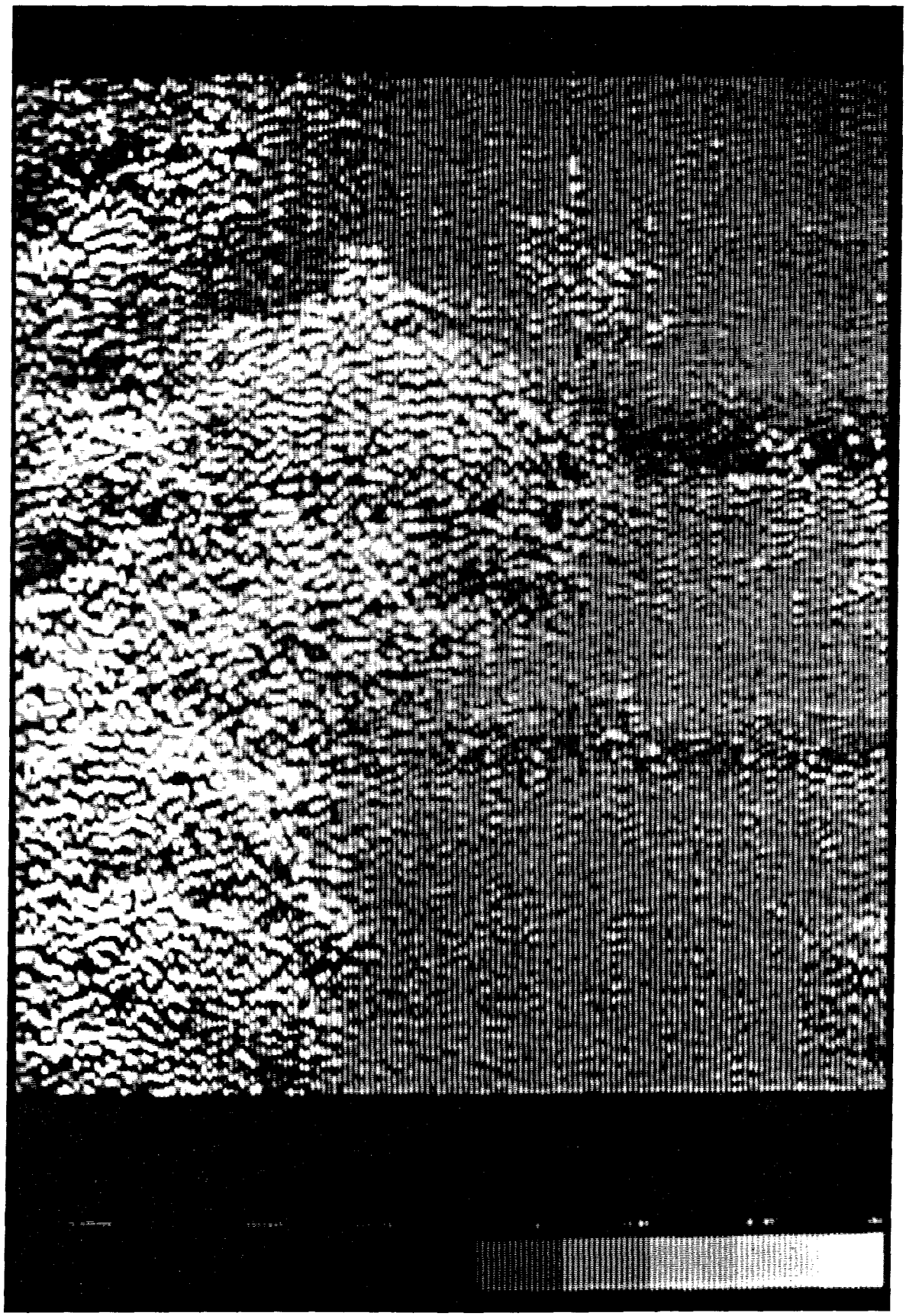

Figure 6. Scan parameters: 100 mV bias, 0.2 nA tunneling current, 1000×1000 Å^2. Poly(TMSCOT) on graphite.

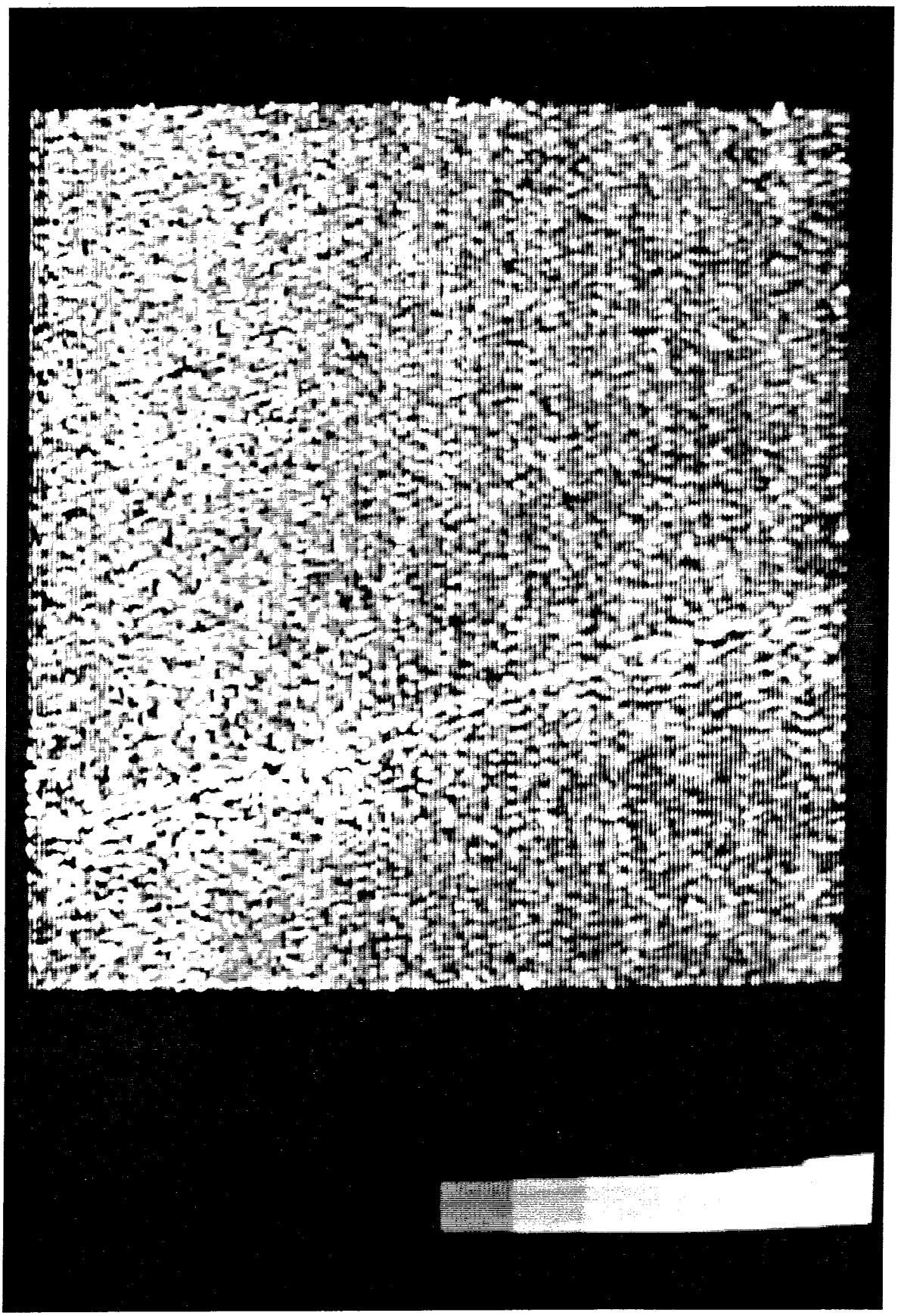

Figure 7. The image corresponding to the amplitude traces in Figure 8. Scan parameters, 100 mV bias, 0.3 nA, 60 × 60 $Å^2$. Poly(TMSCOT) on graphite.

Figure 8. Three z vs. x slices of Figure 7. The three profiles were obtained minutes apart at the same value of y, near the left edge of the image in Figure 7 (as viewed from a normal orientation). As viewed from the side of the page, these profiles are arranged from top to bottom in the order they were obtained.

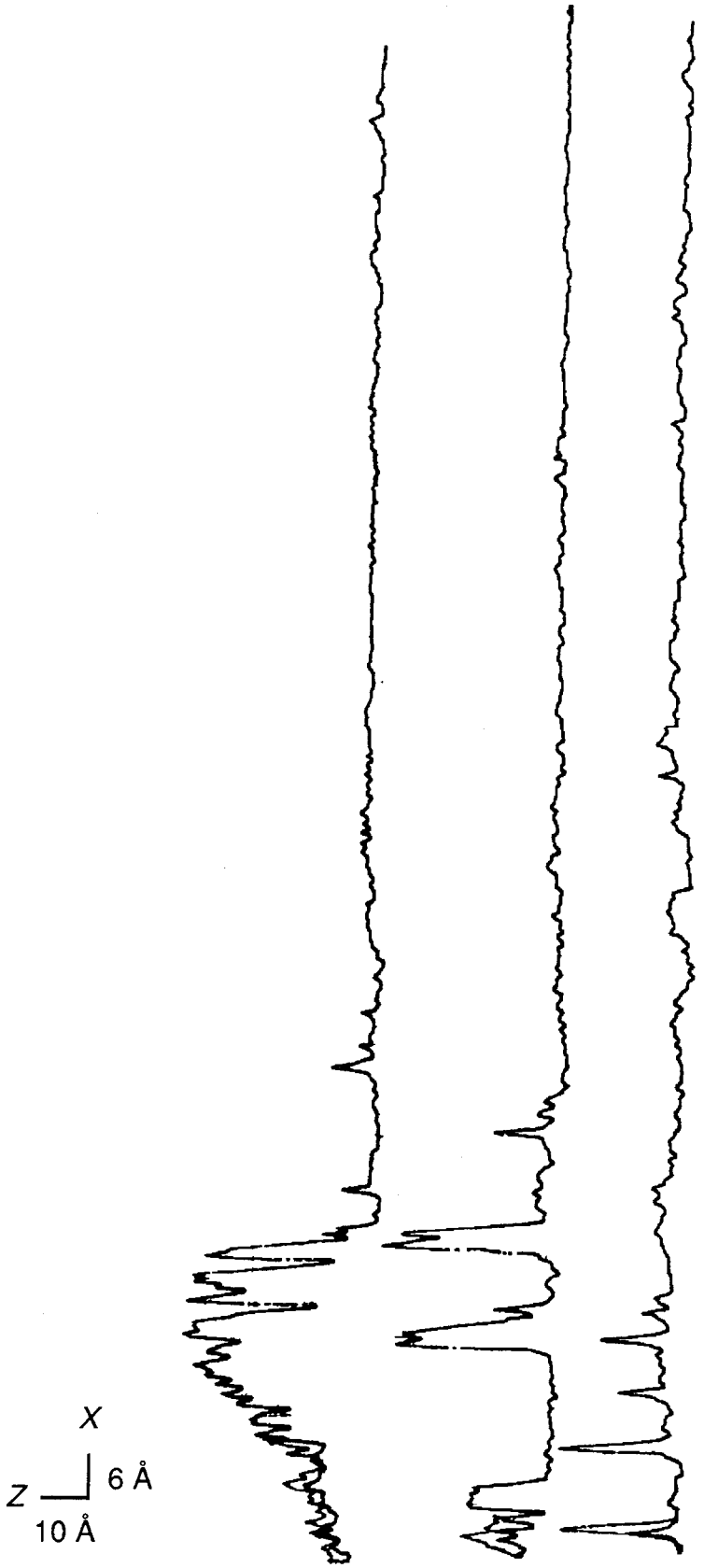
X
Z
6 Å
10 Å

Figure 9. A fork. Scan parameters: 100 mV bias, 0.5 nA tunneling current, 240×240 Å^2. Poly(TMSCOT) on graphite.

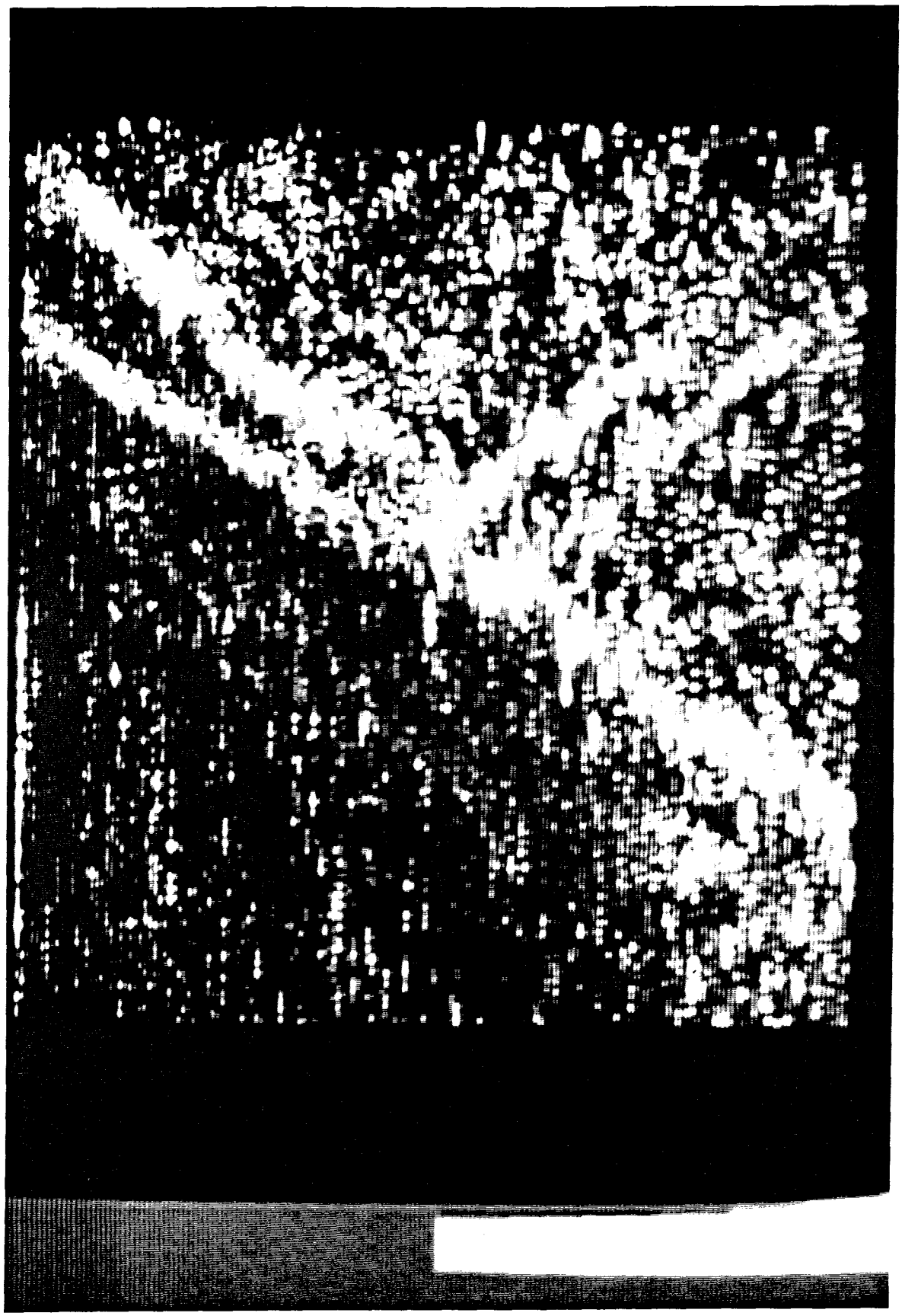

Figure 10. A view of an intriguing feature. Scan parameters: 100 mV bias, 0.5 nA tunneling current, 1200×1200 Å^2. Poly(TMSCOT) on graphite.

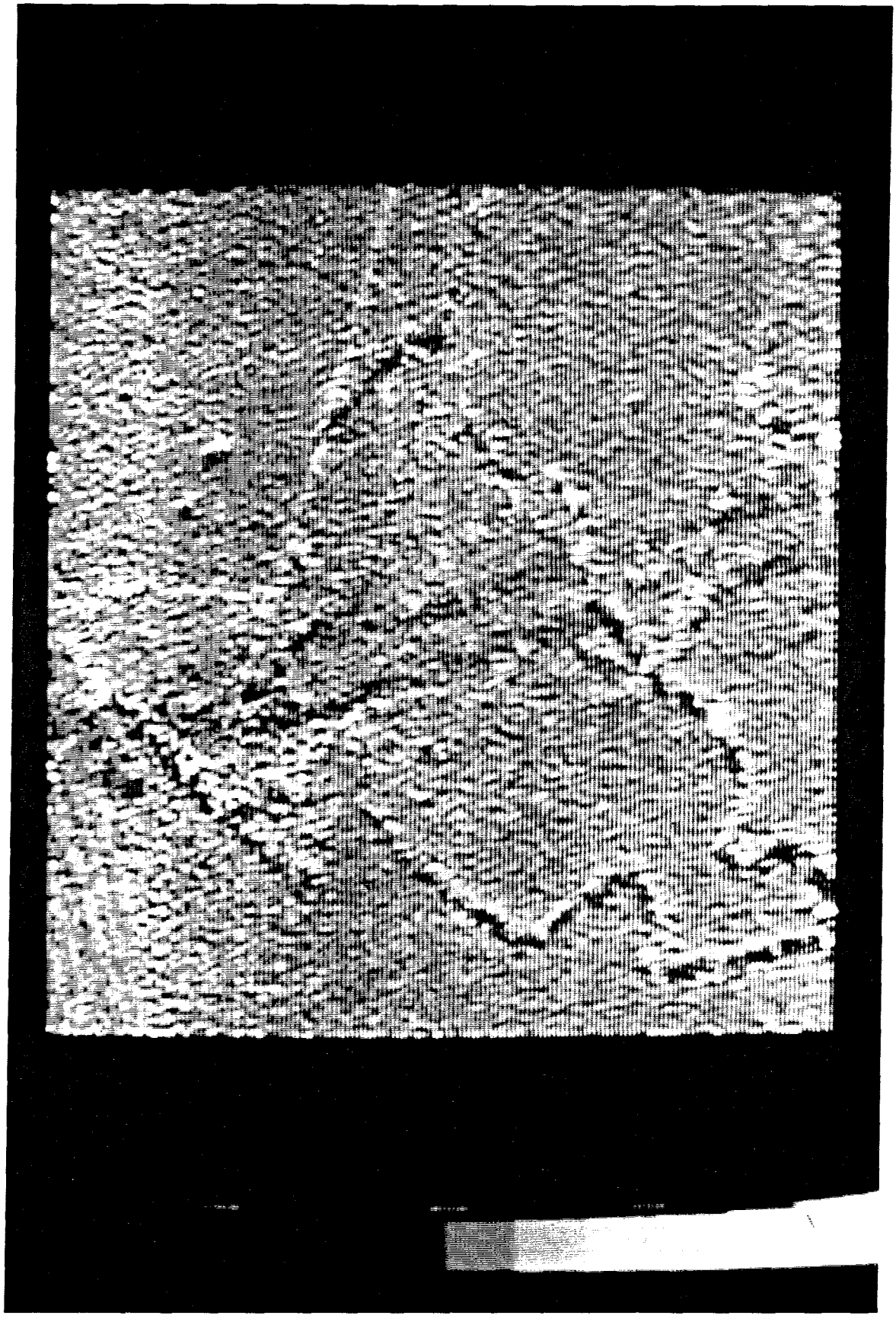

The STM images are presented as photographs of the video screen. They represent what were considered to be some of the more interesting views culled from many hours of scanning. In the set of figures, unless specified, the x direction is top-to-bottom on the page, and y was recorded from left to right as the page is held in a normal orientation.

Figure 1 - Graphite. Figure 1 shows a freshly cleaved, highly ordered, pyrolytic graphite[25] (HOPG) surface. The bright spots correspond to *every other* atom of the graphite surface. The atoms of the top graphite layer are divided into two sets, distinguished by whether or not there is an atom of the second layer directly beneath. Only one set is visualized.[29-31] The ability to image clean graphite is used as a test of the working order of the instrument and of tip quality. Note that because of the resolution of the data-collection apparatus, atomically resolved graphite is not observed at large scan dimensions ($\gtrsim 300 \times 300$ Å^2). Also, the level of resolution in z prevents the observation of atomic corrugation when the data collection apparatus is set to a scale suitable for imaging objects that span a large distance in z.

Figure 2-4. Long, straight features such as that shown in Figure 2 were observed repeatedly. Typically, these features are many thousands of Ångstroms long and very straight. Since it is extremely unlikely that a long polymer chain would assume a conformation in which it was stretched to its full length,[32] they are considered to be a part of the graphite. At least one long, straight feature observed on a polymer-coated surface (not depicted here) had two approximately 120° kinks in it. This is unlike those features commonly found on clean graphite. This does not necessarily imply that it is due to polymer, because unfortunately, there is not yet a published (or in-house, for that matter) compendium of various forms of HOPG grain boundaries and defects observed by STM. Also, it may be that some defects in the HOPG crystal are visible by

STM only when polymer accumulates at the defect site. It has been observed previously that contamination can accumulate at defect sites associated with grain boundaries.[24, 33] Further, while it would be tempting to call the feature seen in Figure 3 a polymer chain, the image of a HOPG tilt boundary obtained by Albrecht et al.[24] shown in Figure 4 indicates otherwise.

Figure 5. The area in the middle left section of Figure 5 (as viewed with the page oriented normally) is assumed to be a polymer "plaque" on clean graphite. The two dark lines to the right are thought to be steps in the underlying HOPG substrate because they are linear and wide. Optimal conditions for depositing the polymers onto the graphite have not yet been found, and plaques such as this were frequently seen if higher concentrations of polymer ($\approx 10^{-8}$ to 10^{-7} g/mL) were used. If the polymer solutions were too dilute, then nothing but graphite was observed. A few experiments were conducted in which the polymer solution was sprayed onto the graphite as a mist; however, this did not give any better results. One variable that has not yet been dealt with is the effects of polymer decomposition. Many of the solutions used in these studies were stored for weeks before use, since no decomposition has been observed in more concentrated solutions that are stored similarly. It is possible that at low concentrations the polymer is susceptible to impurities that could induce crosslinking. Even if interchain crosslinking is slow at low concentrations, intrachain crosslinking might cause the polymers to appear more as amorphous shapes than as single strands.

Figure 6-8. Figures 6 and 7 are two views of the same long, straight object. Figure 8 shows four plots of z vs. x that represent cross sections taken near the top of Figure 7. The different profiles were obtained within a few minutes of each other. The tip was held at a constant value of y as it was slowly (10 to 30 s per sweep) scanned in the x-direction. The profiles differ somewhat from scan to

scan, but all are approximately 30 Å high. Aside from the bumps in the third profile, which have a rather high aspect ratio (~10 Å wide by ~30 Å tall), the image approximates the shape expected for a bundle of polymer chains.

Figure 9-10. The images in Figures 9 and 10 could represent polymer strands. The lines in Figure 9 are approximately 10 to 15 Å wide. The shape in the lower right of Figure 10 is intriguing. The lines in this image, which is at a magnification 5 times lower than that of Figure 9, are about 30 Å in width. These lines have straight sections approximately 100 to 200 Å long. Attempts to view either of these two scenes at higher magnification did not yield any recognizable features, so it was not possible to ascertain whether the width of the observed lines was dependent on the magnification. The observed width of an object will be a function of both its actual width and the ability of the tip to track it. A single, planar strand of poly(TMSCOT) should have a width of about 3 to 9 Å. Figure 10 also contains two faint straight lines running horizontally across the center. These appear to be ramps in the HOPG, and are similar to those seen in Figure 5.

Discussion

The data presented here are preliminary. An examination of the images will show that reproducibility has not yet been achieved. While some of the images, specifically those in Figures 9 and 10, might be consistent with what would be expected for polymer strands, as a set the pictures are too varied to make conclusions as to which are more representative than others. There are many directions to be pursued in future work. New instrumentation that is currently being added to the microscope, including a device to rotate the tip *x-y* raster pattern continuously, will help in any future investigations with this system. This particular device will make discriminating bumps from steps

easier, since the tip may be scanned across the questionable feature in any direction.

Since one goal of the project is to view individual polymer strands, the repeated observation of polymer plaques has been unwanted. A different method for coating polymer on the substrate might result in other forms of polymer deposits. Recent work by T. H. Jozefiak,[34] indicating that poly(s-butylCOT) may be deposited on an electrode from solution electrochemically, might offer a more controlled method of preparing samples for STM. In addition, the investigation of other polymers, besides the substituted polyacetylenes, would be of interest. Given the difficulties encountered in obtaining reproducible images, the instability of the substituted polyacetylenes should be taken into consideration. The selective nature of ring-opening metathesis polymerization allows the synthesis of polymers that vary greatly in their structures.[35] It might be profitable to study more stable polymers with a variety of side chains, as well as block and random copolymers.

In addition, there are clear difficulties associated with using HOPG as a substrate. Assuming that other materials with the same combination of properties, including a readily visualized structure and large atomically flat regions, are not found, it would be worthwhile to obtain a large base of observations on clean graphite. Certainly this base already exists as unpublished data. Its publication would be of assistance in separating those images that are due to adsorbates from those that are due to the underlying substrate.

Scanning tunneling microscopy is not yet a decade old, and is rapidly becoming an established technique in surface science. As more systematic investigations of adsorbates are carried out, and as theorists work to provide an explanation of tunneling through organic molecules, the use of the instrument to observe molecules will become less of an empirical exercise. It is hoped that

studies such as the one described here will eventually lead to the development of STM as a powerful analytical tool in molecular chemistry.

References and Notes

(1) Binnig, G.; Rohrer, H.; Gerber, C.; Weibel, E. *Phys. Rev. Lett.* **1982**, *49*, 57-61.

(2) Tersoff, J.; Hamann, D. R. *Phys. Rev. B* **1985**, *31*, 805-813.

(3) *Scanning Microscopy Technologies and Applications;* SPIE-International Society for Optical Engineering: Bellingham, WA, 1988.

(4) Yang, R.; Dalsin, K. M.; Evans, D. F.; Christensen, L.; Hendrickson, W. A. *J. Phys. Chem.* **1989**, *93*, 511-512.

(5) Yang, R.; Evans, D. F.; Christensen, L.; Hendrickson, W. A. *J. Phys. Chem.* **1990**, *94*, 6117-6122.

(6) Caple, G.; Wheeler, B. L.; Swift, R.; Porter, T. L.; Jeffers, S. *J. Phys. Chem.* **1990**, *94*, 5639-5641.

(7) Lindsay, S. M.; Thundat, T.; Nagahara, L.; Knipping, U.; Rill, R. L. *Science* **1989**, *244*, 1063-1064.

(8) Driscoll, R. J.; Youngquist, M. G.; Baldeschwieler, J. D. *Nature* **1990**, *346*, 294-296.

(9) Barò, A. M.; Miranda, R.; Alamàn, J.; Garcìa, N.; Binnig, G.; Rohrer, H.; Gerber, C.; Carrascosa, J. L. *Nature* **1985**, *315*, 253-254.

(10) Fuchs, H. *Physica Scripta* **1988**, *38*, 264-268.

(11) Swalen, J. D. *Colloids Surf* **1989**, *38*, 71-77.

(12) Loo, B. H.; Liu, Z. F.; Fujishima, A. *Surf. Sci.* **1990**, *227*, 1-6.

(13) These STM images of molecules, which are found to form liquid-crystalline phases in the bulk, appear as two-dimensional ordered arrays of shapes, which roughly correspond to that expected for the molecule.

Strictly, it is not "liquid crystals" that are being imaged, however. See Reference 17.

(14) Shigeno, M.; Mizutani, W.; Suginoya, M.; Ohmi, M.; Kajimura, K.; Ono, M. *Jpn. J. Appl. Phys., Part* **1990**, *29*, L119-L122.

(15) Spong, J. K.; LaComb, L. J., Jr.; Dovek, M. M.; Frommer, J. E.; Foster, J. S. *J. Phys. (Paris)* **1989**, *50*, 2139-2146.

(16) McMaster, T. J.; Carr, H.; Miles, M. J.; Cairns, P.; Morris, V. J. *J. Vac. Sci. Technol., A* **1990**, *8*, 672-674.

(17) Smith, D. P. E.; Hoerber, H.; Gerber, C.; Binnig, G. *Science* **1989**, *245*, 43-45.

(18) Suzuki, M.; Maruno, T.; Yamamoto, F.; Nagai, K. *J. Vac. Sci. Technol., A* **1990**, *8*, 631-634.

(19) Spong, J. K.; Mizes, H. A.; LaComb, L. J., Jr.; Dovek, M. M.; Frommer, J. E.; Foster, J. S. *Nature* **1989**, *338*, 137-139.

(20) Yang, R.; Yang, X. R.; Evans, D. F.; Hendrickson, W. A.; Baker, J. *J. Phys. Chem.* **1990**, *94*, 6123-6125.

(21) Snyder, S. R.; White, H. S.; Lopez, S.; Abruna, H. D. *J. Am. Chem. Soc.* **1990**, *112*, 1333-1337.

(22) Michel, B.; Travaglini, G.; Rohrer, H.; Joachim, C.; Amrein, M. Z. *Phys. B: Condens. Matter* **1989**, *76*, 99-105.

(23) Youngquist, M. G., California Institute of Technology, personal communication.

(24) Albrecht, T. R.; Mizes, H. A.; Nogami, J.; Park, S.; Quate, C. F. *Appl. Phys. Lett.* **1988**, *52*, 362-364.

(25) Moore, A. W. in *Chemistry and Physics of Carbon, Vol. 11*; Walker, P. L., Jr. Thrower, P. A., Eds.; Dekker: New York, 1973; pp 69-176.

(26) The first images of graphite coated with poly(TMSCOT) (the samples were coated by Michael Sailor and imaged by Reginald Penner) were taken in a

"fast-scan," constant-current mode. Typically, the *x* direction was scanned at 300 Hz, and the *y* direction was scanned at 18 Hz. Some of the images obtained (not shown here) had features of dimensions consistent with that expected for a single polymer strand. There was no evidence that side chains were resolved. The features observed in this mode appeared as - striped objects at one bias with the inside of the stripe black, and the outside white. At the opposite bias, the contrast was reversed. This phenomenon has not yet been fully explained.

(27) Heben, M. J.; Ph. D. Dissertation; California Institute of Technology: 1990.

(28) Tiemann, B. G.; Marder, S. R.; Grubbs, R. H. unpublished results.

(29) Tomanek, D.; Louie, S. G.; Mamin, H. J.; Abraham, D. W.; Thomson, R. E.; Ganz, E.; Clarke, J. *Phys. Rev. B: Condens. Matter* **1987**, *35*, 7790-7793.

(30) Tsukada, M.; Kobayashi, K.; Ohnishi, S. *J. Vac. Sci. Technol., A* **1990**, *8*, 160-165.

(31) Batra, I. P.; García, N.; Rohrer, H.; Salemink, H.; Stoll, E.; Ciraci, S. *Surf. Sci.* **1987**, *181*, 126-138.

(32) It has also been suggested that the polymer chains are stretched to an extended conformation upon evaporation of the polymer solution.

(33) Reihl, B.; Gimzewski, J. K.; Nicholls, J. M.; Tosatti, E. *Phys. Rev. B* **1986**, *33*, 5770-5773.

(34) Jozefiak, T. S.; Lewis, N. S.; Grubbs, R. H. manuscript in preparation.

(35) Grubbs, R. H.; Tumas, W. *Science* **1989**, *243*, 907-915.